

SANDIA REPORT

SAND2006-3424

Unlimited Release

Printed June 2006

Neutron Scattering Effects on Fusion Ion Temperature Measurements

Jason R. Starner, Gary W. Cooper, Carlos L. Ruiz, James K. Franklin,
Daniel T. Casey, and Lee Ziegler

Prepared by
Sandia National Laboratories
Albuquerque, New Mexico 87185 and Livermore, California 94550

Sandia is a multiprogram laboratory operated by Sandia Corporation,
a Lockheed Martin Company, for the United States Department of Energy's
National Nuclear Security Administration under Contract DE-AC04-94AL85000.

Approved for public release; further dissemination unlimited.



Sandia National Laboratories

Issued by Sandia National Laboratories, operated for the United States Department of Energy by Sandia Corporation.

NOTICE: This report was prepared as an account of work sponsored by an agency of the United States Government. Neither the United States Government, nor any agency thereof, nor any of their employees, nor any of their contractors, subcontractors, or their employees, make any warranty, express or implied, or assume any legal liability or responsibility for the accuracy, completeness, or usefulness of any information, apparatus, product, or process disclosed, or represent that its use would not infringe privately owned rights. Reference herein to any specific commercial product, process, or service by trade name, trademark, manufacturer, or otherwise, does not necessarily constitute or imply its endorsement, recommendation, or favoring by the United States Government, any agency thereof, or any of their contractors or subcontractors. The views and opinions expressed herein do not necessarily state or reflect those of the United States Government, any agency thereof, or any of their contractors.

Printed in the United States of America. This report has been reproduced directly from the best available copy.

Available to DOE and DOE contractors from
U.S. Department of Energy
Office of Scientific and Technical Information
P.O. Box 62
Oak Ridge, TN 37831

Telephone: (865) 576-8401
Facsimile: (865) 576-5728
E-Mail: reports@adonis.osti.gov
Online ordering: <http://www.osti.gov/bridge>

Available to the public from
U.S. Department of Commerce
National Technical Information Service
5285 Port Royal Rd.
Springfield, VA 22161

Telephone: (800) 553-6847
Facsimile: (703) 605-6900
E-Mail: orders@ntis.fedworld.gov
Online order: <http://www.ntis.gov/help/ordermethods.asp?loc=7-4-0#online>



SAND2006-3424
Unlimited Release
Printed June 2006

NEUTRON SCATTERING EFFECTS ON FUSION ION TEMPERATURE MEASUREMENTS

Jason R. Starner
HEDP Theory/ICF Target Design
Sandia National Laboratories
P.O. Box 5800
Albuquerque, NM 87185-1186

Gary W. Cooper, Carlos L. Ruiz and Daniel T. Casey
Diagnostics and Target Physics
Sandia National Laboratories
Albuquerque, NM 87185-1196

James K. Franklin
Ktech Corporation
Albuquerque, NM 87185

Lee Ziegler
Bechtel/Nevada
Las Vegas, NV 89030

ABSTRACT

To support the nuclear fusion program at Sandia National Laboratories (SNL), a consistent and verifiable method to determine fusion ion temperatures needs to be developed. Since the fusion temperature directly affects the width in the spread of neutron energies produced, a measurement of the neutron energy width can yield the fusion temperature. Traditionally, the spread in neutron energies is measured by using time-of-flight to convert a spread in neutron energies at the source to a spread in time at detector. One potential obstacle to using this technique at the Z facility at SNL is the need to shield the neutron detectors from the intense bremsstrahlung produced. The shielding consists of eight inches of lead and the concern

is that neutrons will scatter in the lead, artificially broaden the neutron pulse width and lead to an erroneous measurement. To address this issue, experiments were performed at the University of Rochester's Laboratory for Laser Energetics, which demonstrated that a reliable ion temperature measurement can be achieved behind eight inches of lead shielding.

To further expand upon this finding, Monte Carlo N-Particle eXtended (MCNPX) was used to simulate the experimental geometric conditions and perform the neutron transport. MCNPX was able to confidently estimate results observed at the University of Rochester.

ACKNOWLEDGMENTS

This work was originally done by Jason Starner as a thesis in partial fulfillment of the requirements for the Degree of Master of Science in Nuclear Engineering at the University of New Mexico. It was prepared under the direction of Dr. Gary Cooper, faculty advisor, and Dr. Carlos Ruiz of Sandia National Laboratories. The authors would like to acknowledge Dr. Thomas Mehlhorn and Dr. Ramon Leeper for providing Sandia National Laboratories' support and funding. Appreciation goes out to Jim Franklin. Without his technical expertise, hours would have been spent trying to determine which scintillator we had. Special thanks go to Vladimir Glebov and everyone at the University of Rochester's Laboratory for Laser Energetics. Their help and support made this experiment possible. Finally, we'd like to thank Lee Ziegler for the construction and calibration of our detectors.

TABLE OF CONTENTS

LIST OF FIGURES10

LIST OF TABLES10

CHAPTER 113

 Introduction..... 13

CHAPTER 215

 Background..... 15

 Ion Temperature Theory 15

 Previous Work 17

CHAPTER 321

 Experimental Method 21

 Detector Description 21

 OMEGA Description 24

 Equipment Setup..... 24

 Experiments Performed 26

CHAPTER 429

 Analysis 29

 Analytical Method 29

 Material Broadening 29

 Detector System Broadening 36

 Ion Temperature Determination..... 40

 Shot 34964 40

 Shot 35003 44

Shots 35004, 35005 and 35006	47
Shot 36721	51
Shot 36723	52
Shot 36730	54
Shot 36731	56
Shot 36732	57
CHAPTER 5.....	61
Results.....	61
CHAPTER 6.....	67
Conclusion	67
Future Work.....	68
REFERENCES.....	69
APPENDICES	71
APPENDIX A.....	73
MCNPX Description.....	73
APPENDIX B	75
Nuclear Physics.....	75
APPENDIX C	79
Bicron 418/422Q Specification Sheets.....	79
Bicron 418 Specification Sheet.....	80
Bicron 422Q Specification Sheet.....	82
APPENDIX D	85
Basic Error Analysis	85

APPENDIX E	87
Truncated MCNPX Output Files	87
MCNPX Output File – Aluminum Housing	88
MCNPX Output File – Light Guide.....	96
MCNPX Output File – Pb Disk (W, Al, Fe, Poly and C Files Similar)	107
MCNPX Output File – 5” Pb Cylinder (10” and ½” Cylinder Files Similar)	115
MCNPX Output File – Shot 35003 DPM (Representative February 2004 Series File).....	123
MCNPX Output File – Shot 36732 SPM (Representative July 2004 Series File).....	132
APPENDIX F	143
BROAD Logic and FORTRAN Code	143
Gaussian Time Convolution	143
BROAD FORTRAN Code	148

LIST OF FIGURES

Figure 1. Ion Temperature Related to Δt	17
Figure 2. SPM Detector Configuration.....	21
Figure 3. DP Detector Configuration.....	22
Figure 4. Cannon Geometry.....	23
Figure 5. Artists rendition of the OMEGA System	24
Figure 6. Electronic Block Diagram.....	25
Figure 7. First Configuration for February Shot Series	26
Figure 8. Second Configuration for February Shot Series.....	27
Figure 9. Configuration for July Shot Series	28
Figure 10. SNL/OMEGA Detector Comparison	30
Figure 11. Geometric Model of Aluminum Housing and Scintillator	31
Figure 12. MCNPX Comparison With and Without Aluminum Housing.....	32
Figure 13. MCNPX Comparison of Scintillator and Light Guide.....	33
Figure 14. MCNPX Pb, W and Fe Comparison.....	34
Figure 15. MCNPX Al, Poly and C Comparison.....	35
Figure 16. MCNPX Lead Cylinder Geometry	35
Figure 17. MCNPX Lead Cylinder Model	36
Figure 18. Process Flowchart to Determine Detector Response.....	37
Figure 19. MCNPX Signal Compared to Raw Shot Data.....	38
Figure 20. MCNPX Comparison to Raw Data with 7.2 ns Gaussian Folding Function	39
Figure 21. OMEGA Shot 34964 Geometry	41
Figure 22. SPM Detector Signal for OMEGA Shot 34964	42

Figure 23. DPM Detector Signal for OMEGA Shot 34964.....	43
Figure 24. SPM Detector Signal for OMEGA Shot 35003	45
Figure 25. DPM Detector Signal for OMEGA Shot 35003.....	46
Figure 26. DPM Detector Signal for OMEGA Shot 35004.....	47
Figure 27. DPM Detector Signal for OMEGA Shot 35005.....	48
Figure 28. DPM (Channel 1) Detector Signal for OMEGA Shot 35005.....	49
Figure 29. DPM Detector Signal for OMEGA Shot 35006.....	50
Figure 30. July Shot Series Geometry	51
Figure 31. SPM Detector Configuration with 4” Pb Shielding	51
Figure 32. SPM Detector Signal for OMEGA Shot 36721	52
Figure 33. SPM Detector Configuration with 2” Pb Shielding	53
Figure 34. SPM Detector Signal for OMEGA Shot 36723	53
Figure 35. SPM (Channel 2) Detector for OMEGA Shot 36723.....	54
Figure 36. SPM Detector Configuration with ½” Pb Shielding (Front and Back).....	55
Figure 37. SPM Detector Signal for OMEGA Shot 36730	55
Figure 38. SPM Detector Configuration with 7.5” Pb Shielding	56
Figure 39. SPM Detector Signal for OMEGA Shot 36731	57
Figure 40. SPM Detector Configuration with 4” Pb Shielding	57
Figure 41. SPM (Channel 2) Detector Signal for OMEGA Shot 36732	58
Figure 42. SNL/OMEGA Detector Comparison	61
Figure 43. SNL/OMEGA Ion Temperature Comparison	64
Figure 44. SNL/OMEGA Ion Temperature Ratio Comparison.....	65

LIST OF TABLES

Table I. MCNPX-Determined Detector Response Times.....	40
Table II. MCNPX-Determined Detector Response Times	62
Table III. SNL/OMEGA Ion Temperature Comparison.....	63

CHAPTER 1

Introduction

To support the nuclear fusion program at Sandia National Laboratories (SNL), a consistent and verifiable method to determine fusion neutron ion temperatures needs to be developed. Since the fusion temperature directly affects the width in the spread of neutron energies produced in DD or DT fusion reactions, a measurement of the neutron energy width can yield the fusion temperature. Traditionally, the spread in neutron energies is measured by using time-of-flight to convert a spread in neutron energies at the source to a spread in time at the detector. One potential obstacle to using this technique at the Z facility at SNL is the need to shield the neutron detectors from the intense bremsstrahlung produced. This shield consists of eight inches of lead and the concern is that neutrons will scatter in the lead, artificially broaden the neutron pulse width and result in an erroneous measurement.

One approach to assessing the viability of making an ion temperature measurement on Z would be to model the neutron transport and detector response with computational tools such as MCNPX™ (See Appendix A for further discussion). Such a calculation could, in theory, predict the effect of the lead on the neutron pulse width at the detector and subsequently allow for this effect, if any, to be accounted for in the analysis of the data. Unfortunately, the Z machine has such a complex geometry, and the source to detector distances are so great (7 to 9 meters), that it is not credible to model this situation with the necessary confidence and accuracy to rely solely on this numerical approach for validating this diagnostic. A more desirable approach would be to devise an experiment that simulates the essentials of the situation on Z, but is simple enough that the ability to make an ion temperature measurement behind eight inches of lead can be both

experimentally and computationally verified. A description of such an experiment and the analysis of the results of the experiment are reported in this thesis.

Specifically, the OMEGA facility at the University of Rochester's Laboratory for Laser Energetics was used as a test bed. OMEGA has a much less complex geometry than Z and, therefore, has less possible neutron scattering issues to consider. The detector(s) can be placed at a variety of locations and source to detector distances to optimize data collection and subsequent modeling of the experiment. In addition, the ion temperature is routinely measured on OMEGA, so the results that we obtain for a temperature measurement in which the detector is situated behind eight inches of lead can be compared directly with the "accepted" temperature measurement.

Two shot series were performed at the OMEGA facility. During the February 2004 series, two current-mode, plastic scintillation neutron detectors were fielded. One was a single paddle neutron time-of-flight (nTOF) detector, which used a mesh type photomultiplier tube, and will be referred to as the SPM detector. The other detector was a dual paddle (DP) detector, which used both a mesh photomultiplier tube (DPM) and a microchannel plate (MCP) to observe the scintillation light. MCPs have proven difficult to field on Z, however, so the data from the MCP were not considered in this thesis. The second series of shots occurred in July 2004. During this shot series, the single paddle detector (SPM) was the only detector fielded.

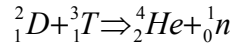
The next chapter presents the physics of ion temperature measurements and discusses previous work that has been done. Chapter 3 describes the experiments that were performed. Chapter 4 describes the techniques employed to analyze the data. Chapter 5 presents the results. Finally, Chapter 6 gives the conclusions and suggestions for future work.

CHAPTER 2

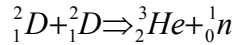
Background

Ion Temperature Theory

There are two fusion reactions that are generally considered for fusion experiments. One is the DT reaction (See Appendix B for further discussion):



The neutron released in this reaction has an energy of 14.1 MeV. The other is the DD reaction:



The neutron released in this reaction has an energy of 2.45 MeV. In addition to the energy contribution from the binding energy released in the reaction, the neutron will carry an energy contribution from the initial kinetic energy carried by the reacting ions. This will result in a spread in energies given to the neutrons, and this spread is related to the ion temperature. The spread in energy can be used to determine the ion temperature as discussed below.

The method used to calculate the ion temperature, T_i in keV, is well defined. The ion temperature is defined (Brysk 1973) as

$$T_i = \left(\frac{\Delta E}{82.5} \right)^2,$$

where ΔE is the FWHM of the neutron energy spectrum in keV. To calculate ΔE , the following formula can be used:

$$\Delta E = \left(\frac{2 \times 10^{-9} * \Delta t * E_n * v_n}{d} \right)$$

E_n is the incident neutron energy in keV, v_n is the incident neutron velocity, in m/s and d is the distance from the source to the detector in meters. As shown in Appendix B, E_n is known to be 2450 keV for DD neutrons. The incident neutron velocity, v_n , can be calculated using

$$v_n = \sqrt{\frac{2E_n c^2}{M}}.$$

E_n is the incident neutron energy in MeV and M is the neutron rest mass. The neutron rest mass (GE and KAPL 1996) is 939.56563 MeV/c². The speed of light, c^2 , has units of meters/second.

Combining constant values will give

$$\Delta E = \frac{106.084\Delta t}{d}.$$

Finally, the ΔE and T_i equations can be combined into the equation

$$T_i = \left(\frac{1.286\Delta t}{d} \right)^2,$$

where Δt is now the time width of the neutron time spectrum. Figure 1 shows the relationship of the ion temperature and the time width for a distance of 5.6 m.

Thus, to make an accurate ion temperature measurement, one uses a fast, current-mode, neutron detector located at a known distance from the source to measure the neutron pulse width. Within the raw data signals recorded, all effects, from the signal attenuation to the detector response times and neutron scattering, are included. Each effect needs to be accounted for individually. MCNPX is used to determine if any neutron scattering is present and what effect it has on the neutron time signal. The detector response time has to be verified and removed, along with any scattering effects, to determine the response solely due to neutron energy broadening. Once the neutron pulse width is extracted from the detector signal, the ion temperature can be calculated by use of the equations above.

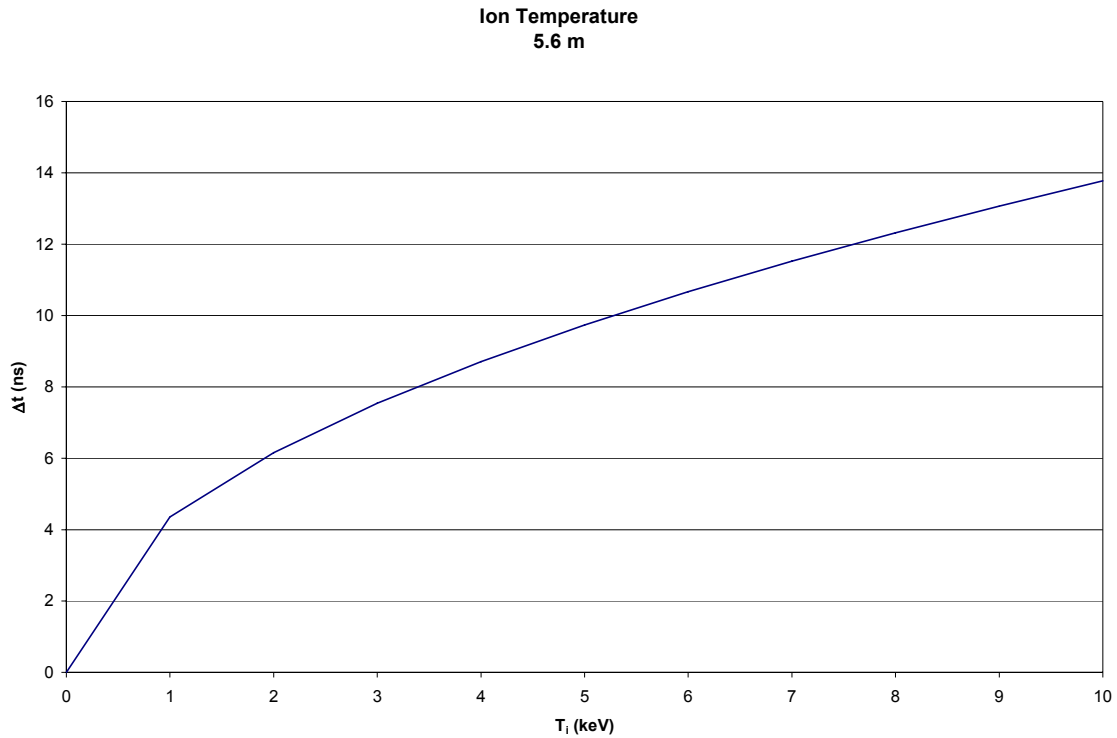


Figure 1. Ion Temperature Related to Δt

Previous Work

Past neutron time-of-flight experiments have been performed to determine fusion ion temperatures. In 1977, the Argus laser-irradiation facility at Lawrence Livermore Laboratory (LLL) attained yields in excess of 10^8 neutrons from DT filled targets and ion temperatures were measured using the time-of-flight method (Lerche et al. 1977). The neutron time-of-flight (nTOF) spectrometer had two separate neutron flight paths from the source to the nTOF. Each path passed through 1.5 mm thick aluminum windows, 3 meters of air and 41 meters of pipe evacuated to $20 \mu\text{m}$. Each detector consisted of an 18 cm diameter by 10 cm thick Pilot U fast plastic scintillator. A typical detector response time for this system was 3.5 ns. No indication of scattered neutrons reaching the detector was observed. The raw data was corrected for the detector response time (3.5 ns) to determine the DT energy widths. Monte Carlo simulations of

the nTOF experiments were done to study the statistics associated with an individual shot. This work demonstrates that for yields lower than those of Z, energy widths and associated ion temperatures could be measured and calculated. However, unlike Z, there was minimal attenuation of the neutrons in this experiment and the nTOF passed through a large water tank to minimize any neutron scattering.

Experiments at the OMEGA and NOVA laser facilities have used MCP tubes for most of the experiments. MCP tubes have sub-nanosecond response times, which make them ideal for use because they minimize the error introduced by the detector response. To date, most, if not all, experiments have used a relatively small amount of lead to shield the detector from x-rays. With this small amount of lead, neutron signals have defined temporal signals that can be easily fit by convoluting a Gaussian to an exponential decay. Currently, multi-staged scintillator decay times are convoluted (Murphy et al. 1995) into the Gaussian response. Data is fit with

$$F(t) = C \sum_n A_n \frac{\exp(-t/\tau_n) \exp(\sigma^2 / 2\tau_n^2)}{2\tau_n} \left[1 + \operatorname{erf} \left(\frac{t - \sigma^2 / \tau_n}{\sqrt{2\sigma^2}} \right) \right],$$

where τ_n is the decay time for a relative value A_n . One can sum multiple decay times to produce a better-than-Gaussian fit to the data. This method has become commonly used in neutron signal analysis for ion temperature determination using neutron time-of-flight.

More recently, a paper investigating neutron time-of-flight diagnostics for the National Ignition Facility (Murphy et al. 2001) prepared a conceptual design for neutron TOF diagnostics. Detectors were designed for both DD and DT fusion sources ranging from yields of 10^6 to 10^{19} neutrons. These detectors are similar to SNL's detector and utilize a microchannel plate. Data was fit using a Gaussian curve with a two-stage exponential scintillator decay time convoluted in.

This method will fit the neutron signals well for geometries that present minimal neutron scattering, but may not be valid for an environment with high scattering. The scattered neutrons would be expected to introduce long tails to the signals that are not part of the normal scintillator and tube response. Unlike the tails from the detector response, the tails due to scattering will change with changes in scattering geometries. To date, we have not been able to model these tails with the necessary accuracy to predict the experimental tails. In addition, the use of MCPs, which are preferred because they minimize the detector response correction, has proved problematic at Z. Unfortunately, MCPs are charge-limited devices that do not function reliably in the Z environment. The intense bremsstrahlung signal, even when shielded with eight inches of lead, is so intense that it depletes the charge in the MCP and the MCP cannot recover in time to respond to the neutron signal with assured accuracy. As a result, mesh photomultiplier tubes, which have longer time responses, must be employed instead. Thus, even though ion temperature measurements have been successfully made at many facilities since 1977, the situation at Z is clearly different and it is not obvious that such a measurement can be accurately made. Since ion temperature measurements are quite important to the Z fusion research program, it is essential that we determine if such measurements can successfully be made at Z. To this end, this work proposes a method of using Gaussian fits to the data that uses only the leading edge of the signals. This approach is then validated using the results of experiments conducted on OMEGA.

CHAPTER 3

Experimental Method

Detector Description

During the experiments at OMEGA, two types of scintillator were used: Bicron 418 and 422Q (See Appendix C for scintillator specification sheets). Detectors were designed at Sandia National Laboratories specifically for use on the Z machine. The single paddle detector shown in Figure 2 includes a 3 inch diameter by either one-half inch thick disk of 418 or one-eighth inch thick disk of 422Q scintillator housed in an eighth inch thick aluminum housing.

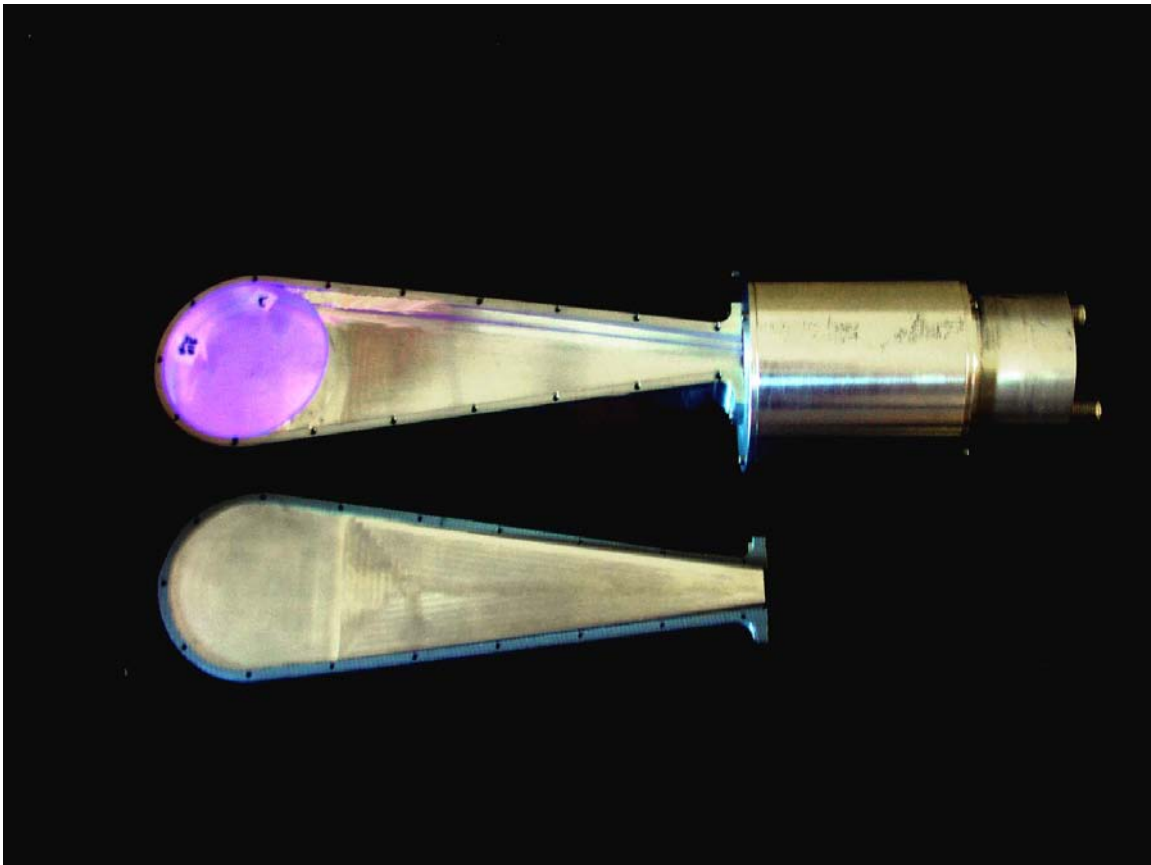


Figure 2. SPM Detector Configuration

This detector used a mesh type photomultiplier tube. Throughout this report, the single paddle detector will simply be referred to as the single paddle mesh (SPM) detector. The space between

the scintillator and the photomultiplier tube is filled with a plastic Lucite light guide, shown in Figure 2. The photomultiplier tube used in the SPM detector is manufactured by Hamamatsu (Model R5500). The SPM detector photomultiplier tube is biased with a high voltage power supply set between 1000 and 2600 volts (negative bias), depending on the expected yield for the shot.

The dual paddle detector utilizes a single shared 3 inch by 1 inch thick scintillator located centrally between two photomultiplier tubes; a mesh type and a microchannel plate. Figure 3 shows the dual paddle detector geometry.



Figure 3. DP Detector Configuration

For this report, the mesh photomultiplier tube side of the detector will be referred to as simply DPM. The microchannel plate was not used in this work. When referring to the double paddle

detector in general, DP will be used. Similar to the SPM detector, the DP detector also utilizes plastic Lucite light guides, located between the scintillator and the two photomultiplier tubes. As with the SPM detector, Bicron 418 or 422Q plastic scintillator can easily be switched based on assumed shot performance. The DP detector is also powered with a high voltage power supply, ranging from 1000 to 2600 volts (negative bias), depending on shot specifications.

To attempt to correctly incorporate a similar geometry to Z at the OMEGA facility, a stainless steel apparatus, or “cannon”, was fabricated. The cannon was designed to secure either or both detectors and accommodate various thicknesses of lead during an OMEGA shot. The lead can be placed at various distances from the detectors in an attempt to determine what, if any, scattering effect is present from the lead. The cannon is 36 inches in length and has an inside diameter of 6 inches. The wall thickness is one-quarter inch. The cannon is bisected and hinged to allow for ease of adding or removing lead disks. Figure 4 depicts the cannon (not to scale). This geometry simulates the geometry of the shield housing on the side detectors on Z.

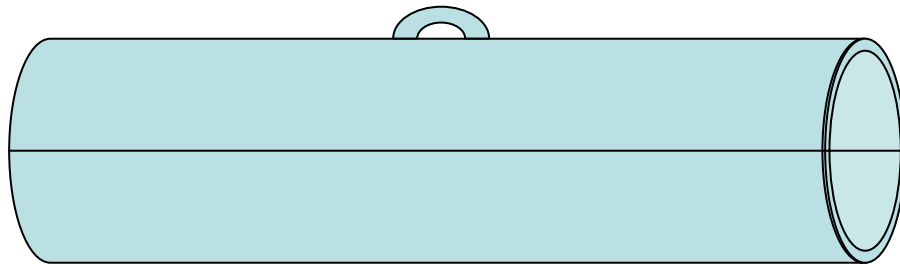


Figure 4. Cannon Geometry

The detectors on Z are located in a stainless steel pipe of essentially the same dimensions as used in the OMEGA experiment. In addition, on Z a total of eight inches of lead plugs are placed in the pipe to shield the detectors, which is also directly simulated in the experiments on OMEGA. The main difference is that on Z, the pipe is surrounded by additional shielding materials

(including lead, borated polyethylene and paraffin) which are not present in the OMEGA experimental set-up.

OMEGA Description

For both sets of experiments performed, the University of Rochester's Laboratory for Laser Energetics (www.lle.rochester.edu/05_omega/05_omega.html) supplied the pulsed DD neutron source. The OMEGA laser system consists of 60 laser beams that can focus up to 40,000 joules of energy to a target smaller than 1 millimeter in diameter. This energy deposition occurs in approximately one billionth of a second. The OMEGA facility measures 10 meters tall and 100 meters in length. Figure 5 shows an artists depiction of OMEGA. The target bay is smaller and considered a "clean" room. The target bay is where the neutron detectors were located during the experiments.



Figure 5. Artists rendition of the OMEGA System

Equipment Setup

During the experiments at the University of Rochester, we utilized their in-house power supplies and signal digitizing equipment. Figure 6 depicts the electronic configuration. For both shot series, the amount of attenuation used to inhibit the signal varied. The raw data analyzed in this report includes corrected attenuation of the signal. The exact amount of attenuation for each

shot is not precisely known and not important, so it is assumed that the attenuated data, although not absolute in amplitude, had no effect on the time response of the signal. For each shot, the signal was split into two channels.

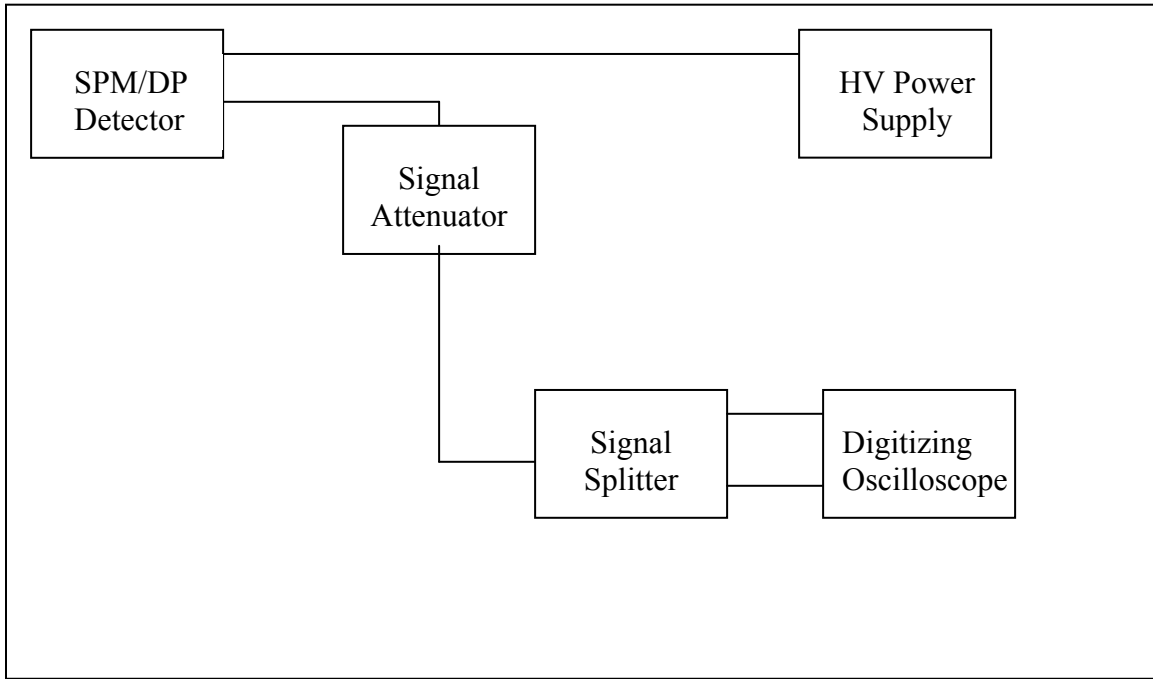


Figure 6. Electronic Block Diagram

Each channel had a different sensitivity setting in an attempt to expand the range of signal amplitudes for each shot. This helps maximize data collection and facilitates future sensitivity setting approximations based on expected neutron yield. The signal splitter was manufactured by Mini-Circuits (www.minicircuits.com). It is a resistive power splitter, model ZFRSC-42. The splitter is valid from 0 to 4.3 GHz. A 1 GHz Techtronix Oscilloscope (Model TDS684) was used to capture the shot signals. Negatively biased high voltage was provided by a LLE built power supply, based on a Bertan PMT-50C-N model (www.bertan.com/pmt.html). The LLE model features a LCD monitor and multi-turn potentiometer. LMR-400 signal cable was used to connect all equipment.

Experiments Performed

Two series of experiments were performed at the OMEGA facility. During the February 2004 series, there were two main geometric configurations. The cannon and detectors were configured at a distance of 10 meters from the source.

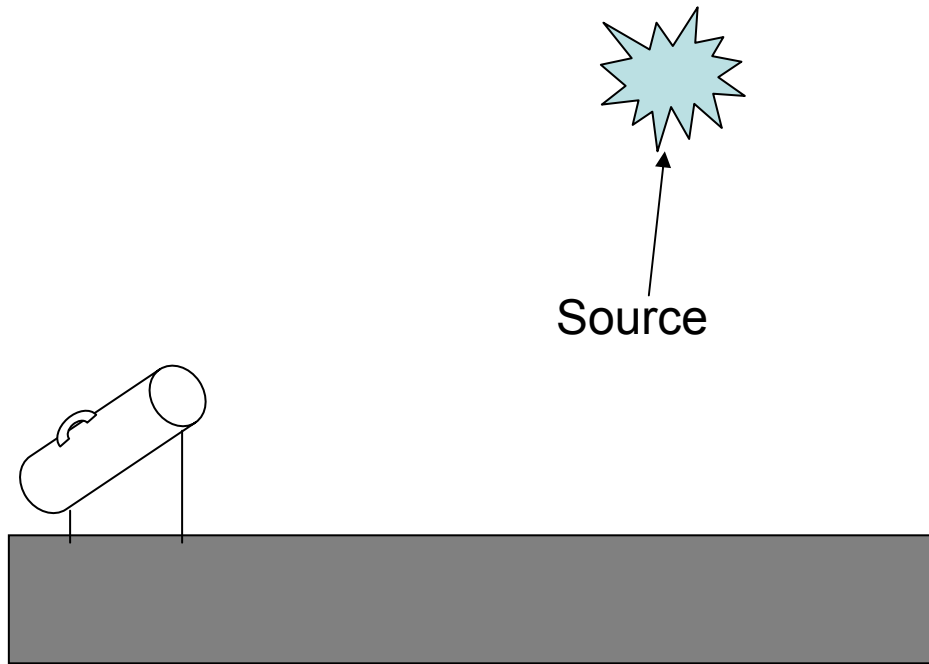


Figure 7. First Configuration for February Shot Series

The cannon had the ability to hold one detector at 10 meters and the other at 9.2 meters. The cannon was set at an angle of 26.57° above horizontal. This corresponds to the angle of the line of sight necessary to observe the source. In this configuration, one-half inch of lead was used to shield the detectors from x-rays produced from the shot. Figure 7 represents this configuration. In this configuration, the detector in the 10 meter position was located approximately 6 inches from the concrete floor of the target chamber.

The second geometry (Figure 8) located the SPM detector at a distance of 10 meters. The SPM detector was placed in the cannon and 8 inches of lead, located in front of the detector, was included to simulate the shield used in experiments at Z. The DP detector was placed at a

location 5.4 meters from the source. The DP detector was placed near one of OMEGA's detectors. There was a thin (one-half inch) lead disk used to shield the double paddle detector. The DP was used as a "calibration" detector to verify that SNL's and OMEGA's signals were similar.

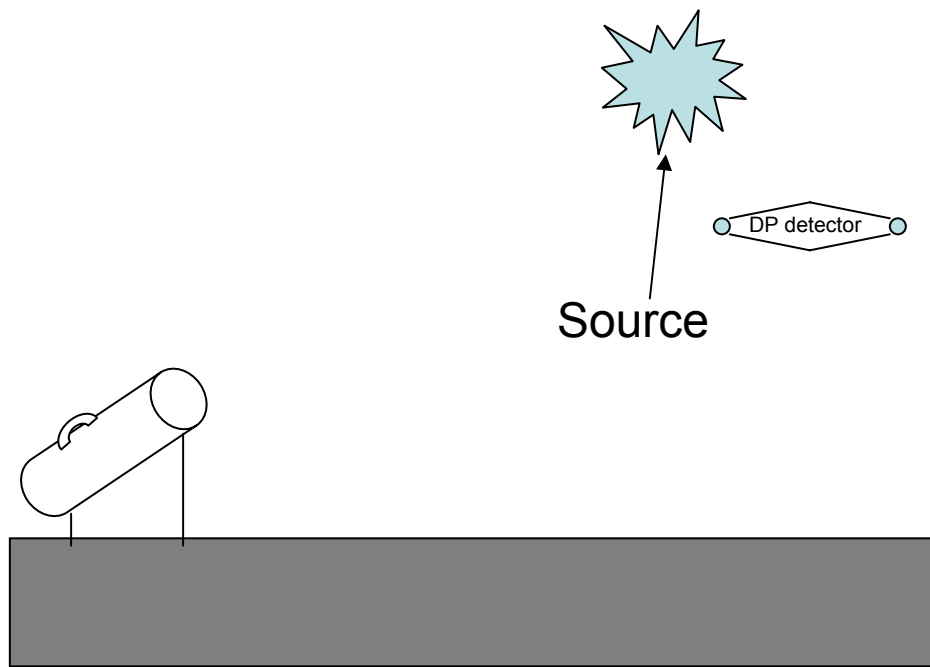


Figure 8. Second Configuration for February Shot Series

During the July 2004 series only one location was used. The cannon was suspended from a catwalk in the target bay. The distance from the source was approximately 5.4 meters. The SPM detector was the only SNL detector available during this shot series. The SPM detector was located in the rear position of the cannon. Various thicknesses of lead were placed either 8 or 30 inches in front of the detector. There was the ability to place one-half inch of lead directly behind the detector to shield it from any backscattered neutrons or photons. Figure 9 depicts this configuration. It should be noted that all experiments were performed as add-on experiments. Our experiments were secondary; the shot schedule was based on the primary experimenter's needs. Because of this, the data collected were constrained and the number of shots containing

useful data was limited. Some target configurations used by the primary experimenter had low neutron yields that were below our detection limits.

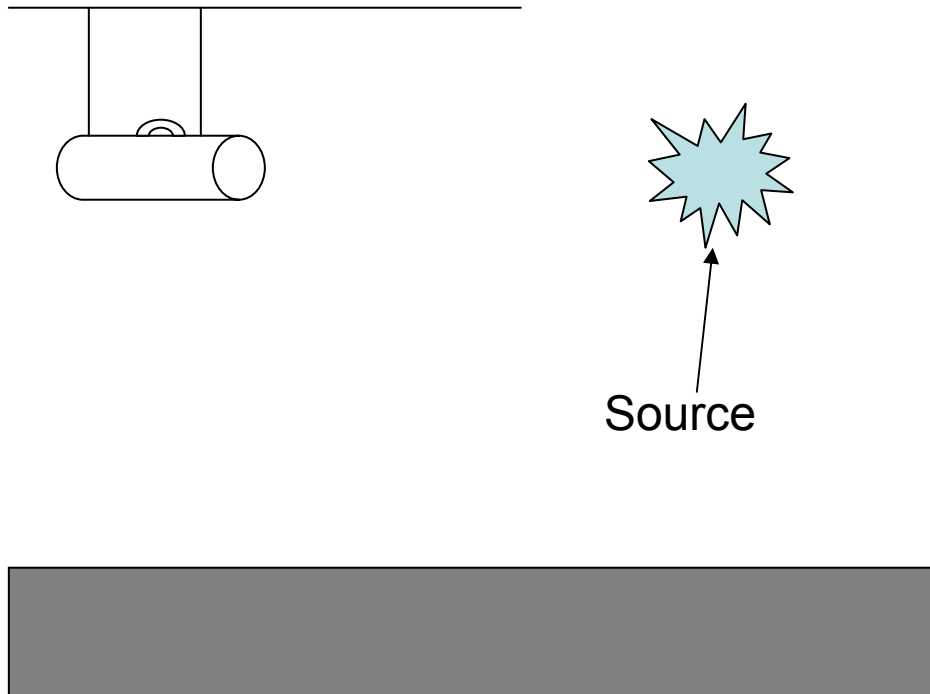


Figure 9. Configuration for July Shot Series

As mentioned previously, each experimental shot gave two signals per detector. One channel was usually set to be more sensitive than the other. Unless specified, the data presented is from the channel that had the best signal to noise ratio.

CHAPTER 4

Analysis

Analytical Method

To analyze the raw neutron signals from the SPM and DPM detectors, basic curve fitting methods were applied. For each signal, a simple Gaussian curve was fit to the signal. Because most signals were asymmetric, the rise time portion of the signal was considered a more important fit. The tails seen during the OMEGA experiments could be an effect from various things, including lead scattering, concrete scattering, photon emission from the lead, etc. Since the tails (beyond the scintillator exponential decay times) are not fully understood, a first order fit utilizing the rise time of the neutron signal was used. When analyzing the data, a 5% error was assumed on the distance measurement and on the raw full width at half max (FWHM) fit. The constant from the simplified ion temperature equation was assumed to have a 1% error.

To make a valid comparison, the basic concepts of error analysis (Taylor 1997) must be included. MCNPX calculates numbers with an associated relative error. Appendix D contains further discussion regarding basic error analysis.

Material Broadening

To attempt to accurately estimate the fusion ion temperature, neutron signals from OMEGA and SNL detectors were compared. As seen in Figure 10, the DPM detector shows a significantly broader temporal signal than the OMEGA detector.

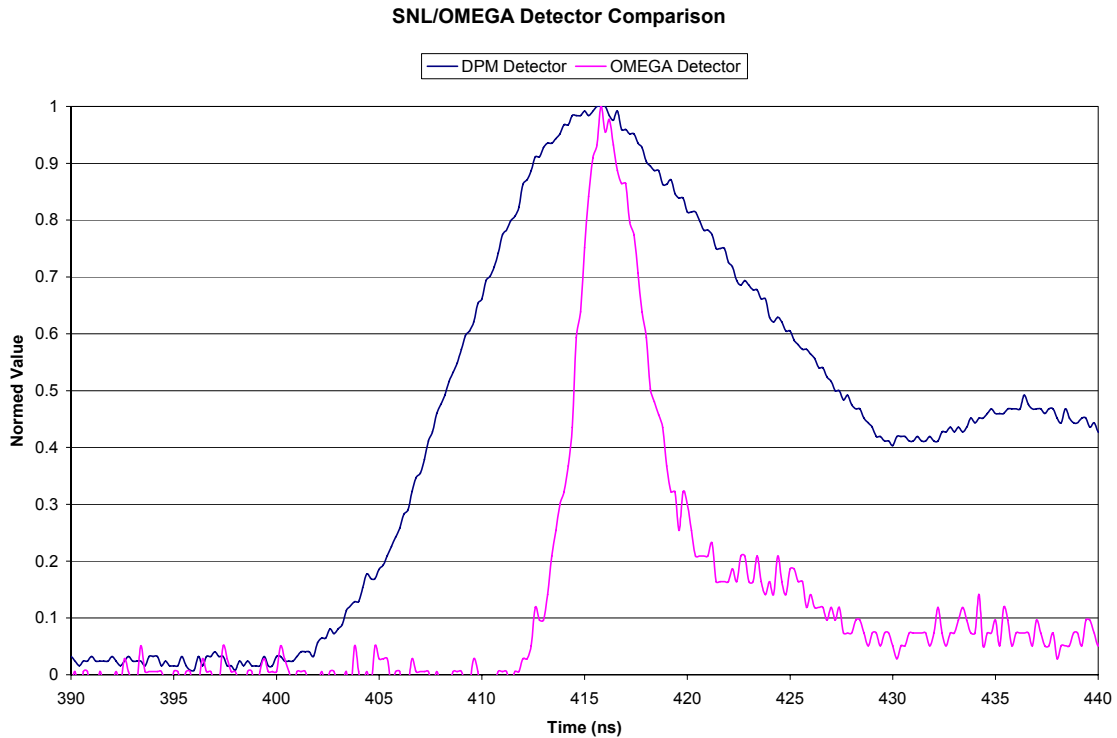


Figure 10. SNL/OMEGA Detector Comparison

The cause of the difference in signals must be investigated before an accurate ion temperature measurement can be calculated. The signal broadening seen in Figure 10 can be caused by a number of things. The broadening can be an effect of the detector system (scintillator and photomultiplier included), the materials surrounding the detector, detection hardware issues, etc. This report will investigate the detector system and material effects on the signal using MCNPX.

In an attempt to determine if there was any effect from local material configurations on the SPM detector neutron signal, different material geometries were simulated with MCNPX. Both detectors (SPM and DP) are housed in one-eighth inch thick aluminum. Simulations were performed to determine any effects from the detector housing. If major effects exist, a determination needs to be made regarding how to address such effects. In the MCNPX model (See Appendix E for truncated MCNPX output files), a one-eighth inch aluminum housing was

placed around the scintillator. Figure 11 shows the radial and axial geometry. This geometry was run to determine if there was significant broadening to the neutron signal from the aluminum housing.

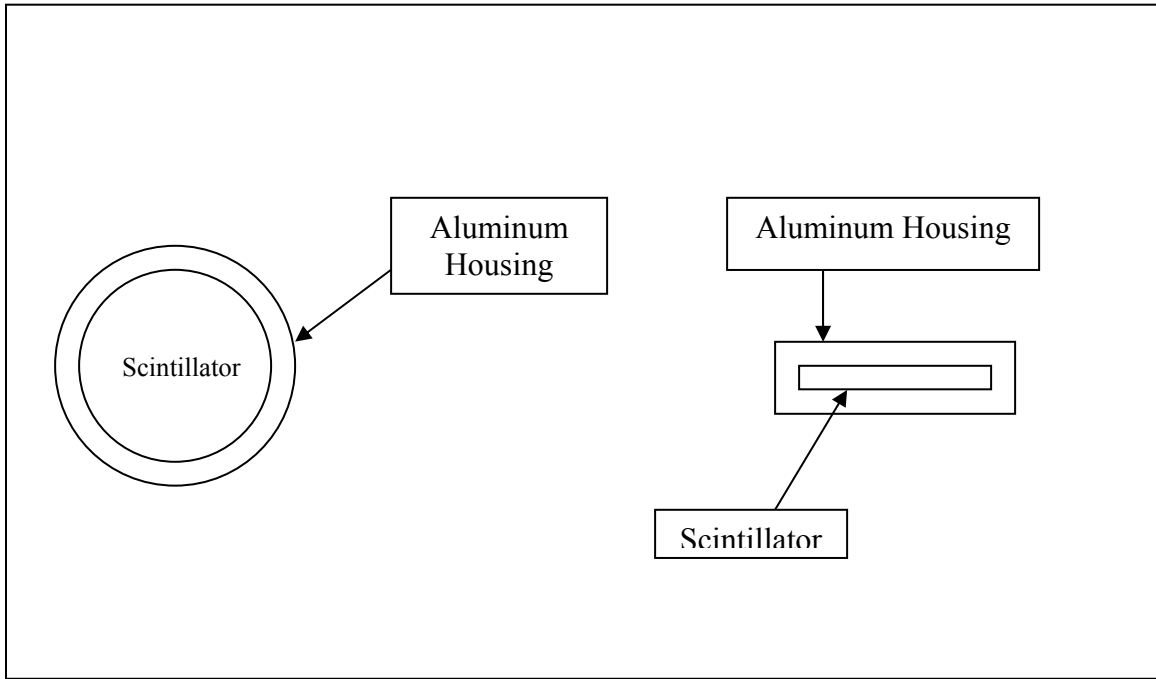


Figure 11. Geometric Model of Aluminum Housing and Scintillator

Figure 12 shows that there are no noticeable effects from the aluminum housing. This is reasonable. The mean free path for 2.45 MeV neutrons in aluminum is ~ 7.3 cm. This shows that, on average, a neutron travels 7.3 cm between interactions. Because the aluminum housing is thin compared to the mean free path of the neutrons, there should be no noticeable effect from the aluminum housing. The only apparent difference seen in Figure 12 is a slight timing difference of 0.2 ns. This difference is caused by the time it takes 2.45 MeV neutrons to travel an extra one-eighth inch. The actual travel time is much lower than 0.2 ns, but due to the digitizing timing resolution and MCNPX time binning (0.2 ns), it is tallied in the next time bin.

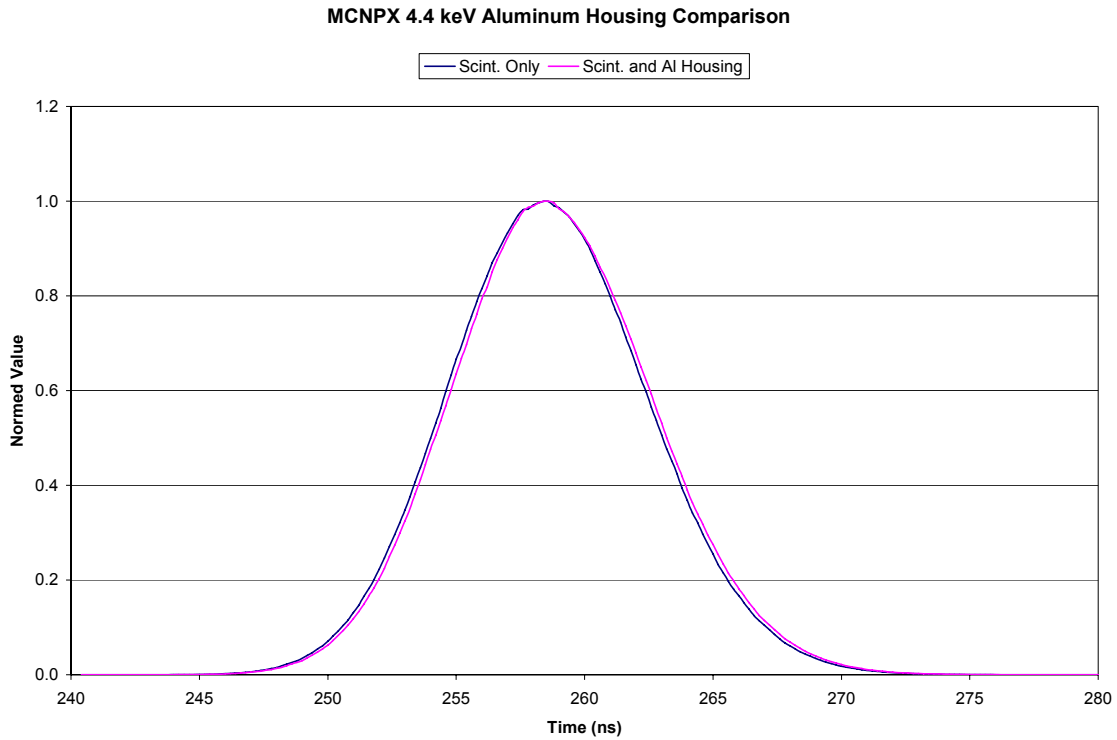


Figure 12. MCNPX Comparison With and Without Aluminum Housing

Another material used in the experiments that is close to the scintillator and could contribute to the temporal broadening is the scattering of neutrons in the Lucite light guides. A conservative model of the light guides was implemented into a MCNPX model. A 4.5” cylindrical annulus of plastic was added around the scintillator. Again, as Figure 13 shows, there is not a noticeable broadening to the spectrum. This is again reasonable. Neutrons would have to undergo a very acute scatter in the light guide to scatter back into the scintillator. For those neutrons that do scatter into the scintillator from the light guide, their energy would be significantly less than 2.45 MeV, where detection sensitivity is much less.

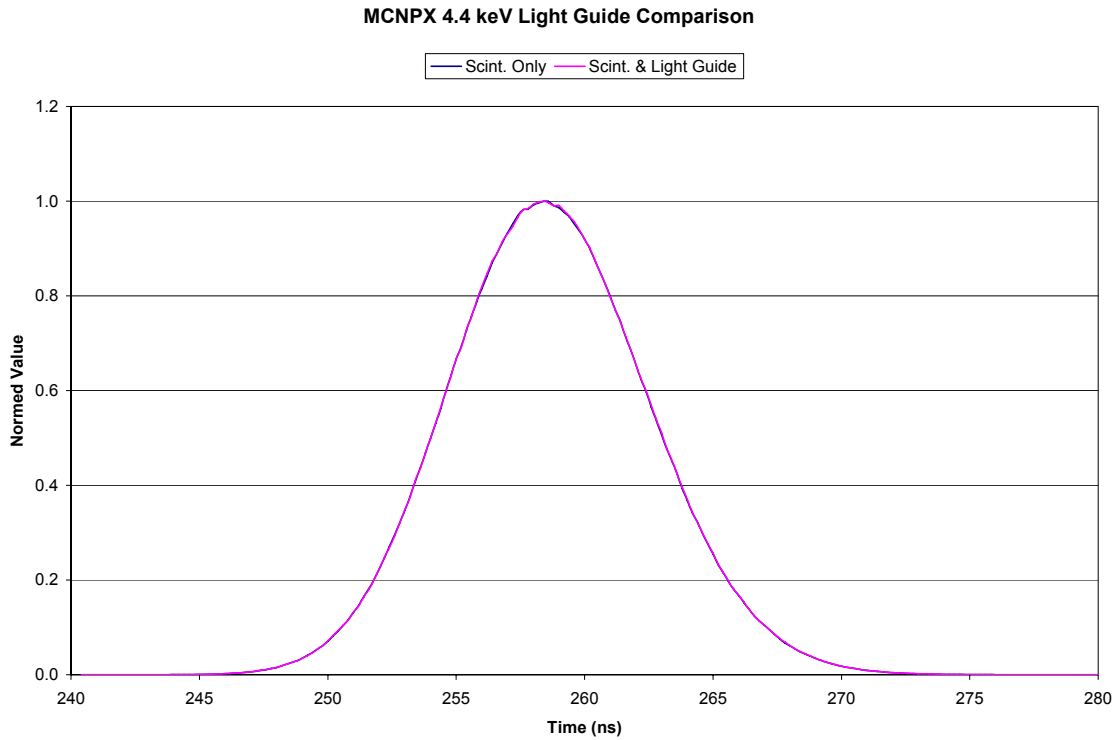


Figure 13. MCNPX Comparison of Scintillator and Light Guide

To determine if any materials in the detector's line of sight have an effect on the signal broadening, simulations were done with lead, tungsten, aluminum, iron, polyethylene and carbon. These models include a 6 inch diameter by one-half inch thickness right circular cylinder (disk) of material. Figures 14 and 15 show the effects from each material. Again, other than structure in the peak, none of the materials modeled caused a noticeable change in the broadening of the spectrum.

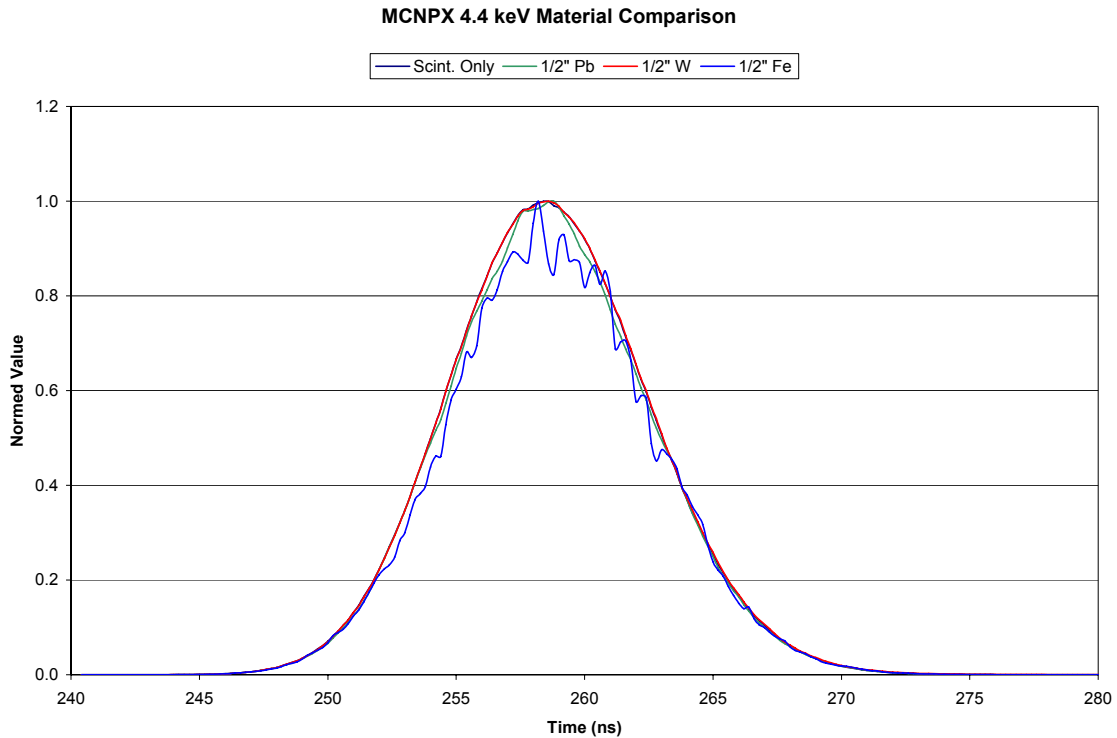


Figure 14. MCNPX Pb, W and Fe Comparison

The materials of interest are iron and aluminum. The structure in peak of the iron curve is not fully understood. The error in the peak is on the order of 0.3%. The aluminum peak error is ~0.2%. It is reasonable to assume that these errors may be physical, but may not play an important role in the temperature determination. The average neutron energy in the scintillator was 2.39 MeV with or without the aluminum in the model. The same is true for the iron. This shows that it is safe to assume that the energy spectrum undergoes no significant change when one-half inch of iron or aluminum is in the problem. The lack of change in the energy spectrum directly suggests no change in the temperature.

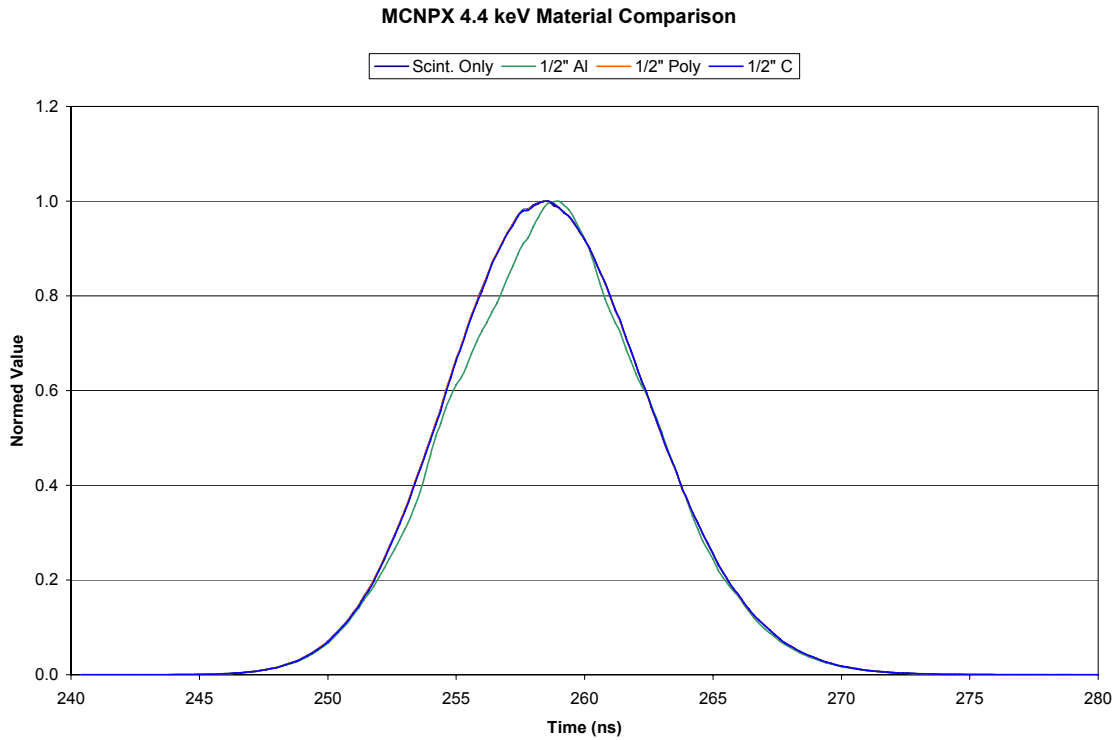


Figure 15. MCNPX Al, Poly and C Comparison

Because there are significant amounts of lead used in the experiments, simulations need to be performed to be sure to understand the effect on the neutron signal. A cylindrical shell (Figure 16) of lead was placed 6 inches from the scintillator out to 8 inches in front.

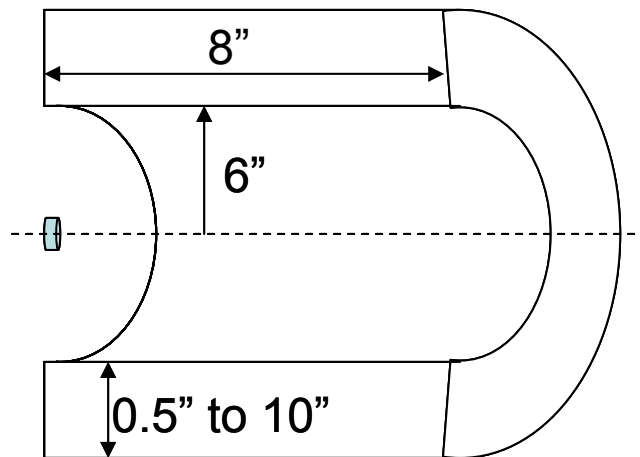


Figure 16. MCNPX Lead Cylinder Geometry

The wall thickness of the lead cylinder varied for each simulation from one-half inch to 10 inches. As Figure 17 shows, there was no appreciable change in the spectrum. Since the MCNPX simulations suggest that there is no signal broadening, the cause of the broadening may be inherent to the detector system.

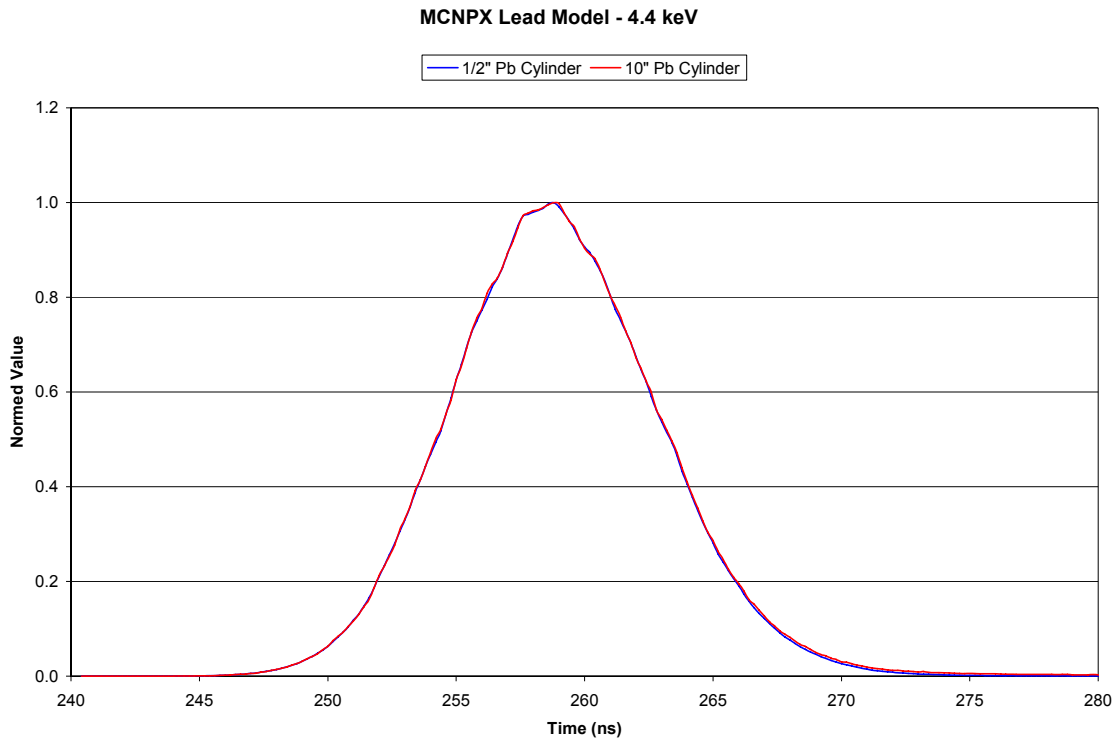


Figure 17. MCNPX Lead Cylinder Model

Detector System Broadening

From the early stages of these experiments, there was available a measured detector “response time”. The response time of ~4 ns was thought to be tentatively accurate for both mesh photomultiplier tube detectors. A recent experiment was performed on the SNL detectors at the Idaho State University (ISU). This experiment was performed to determine if the 4 ns response time was valid. MCNPX was also used to investigate the response time. Data from the ISU experiments suggests that the average response time for the SPM detector was 7.2 ns rather than

4 ns. The response time for the DPM detector was approximately 7.0 ns. Figure 18 indicates the process flowchart used to evaluate the detector response time with MCNPX.

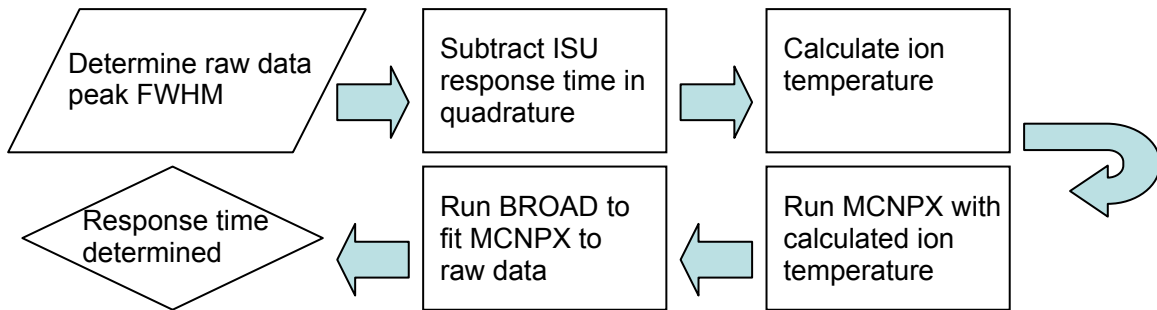


Figure 18. Process Flowchart to Determine Detector Response

The raw OMEGA data was analyzed to determine a time pulse width. Using this measured width, the ISU determined pulse width (7.2 ns for the SPM detector and 7.0 ns for the DPM detector) was subtracted from the raw width, in quadrature. This corrected width was used to determine the fusion ion temperature for the particular shot. The ion temperature was used as the neutron source definition in a basic MCNPX model for the shot geometry (The source distribution used was a Gaussian distribution within the MCNPX program, using the ion temperature as a variable). The MCNPX-produced temporal signal was compared with the raw detector signal. In all cases for the SPM and DPM detectors, the MCNPX-produced signal had a narrower width than the raw data. Figure 19 shows the MCNPX-generated signal compared with the raw signal.

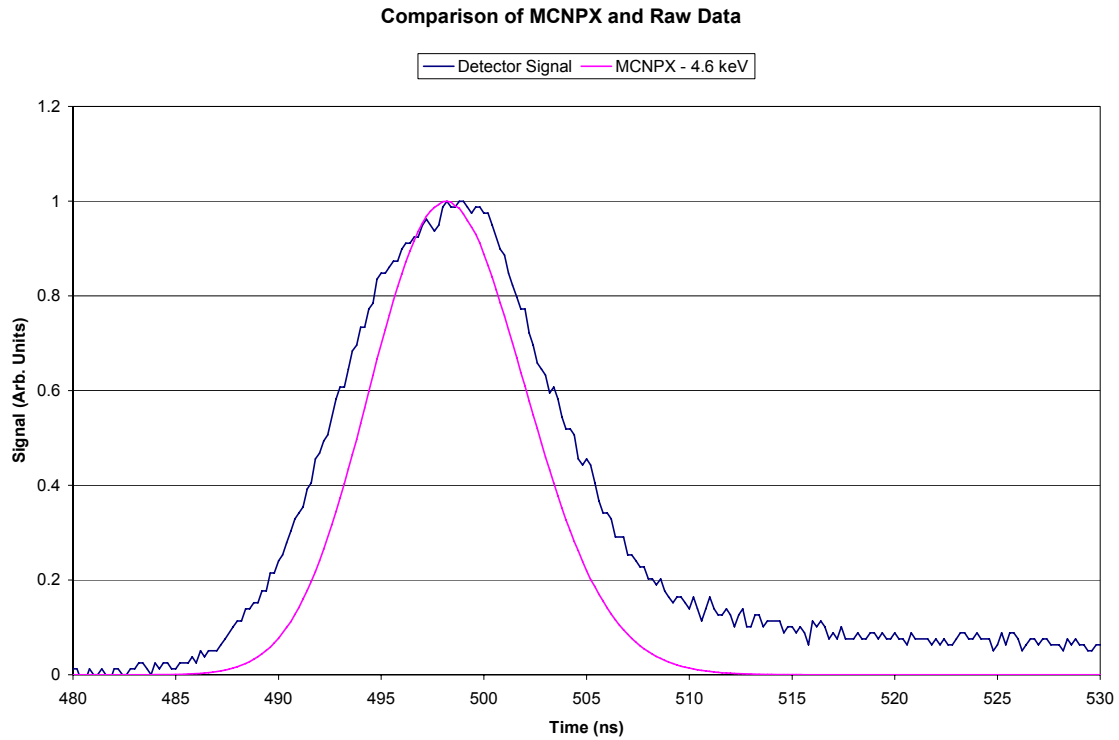


Figure 19. MCNPX Signal Compared to Raw Shot Data

Since it was determined that the materials near the detector system played no effect on the signal's width, a small FORTRAN code, BROAD (Appendix F), was written to broaden the MCNPX signal until its width is close to the raw data signal. BROAD is a basic FORTRAN code that takes the histogram output from MCNPX and broadens the entire signal by folding in a Gaussian curve to each 0.2 ns histogram bin. BROAD also calculates the area of each individual bin and the area of the entire curve to preserve the curve integral. For this example shot, a Gaussian that had a width of 7.2 ns broadened the signal enough to match the raw data (Figure 20).

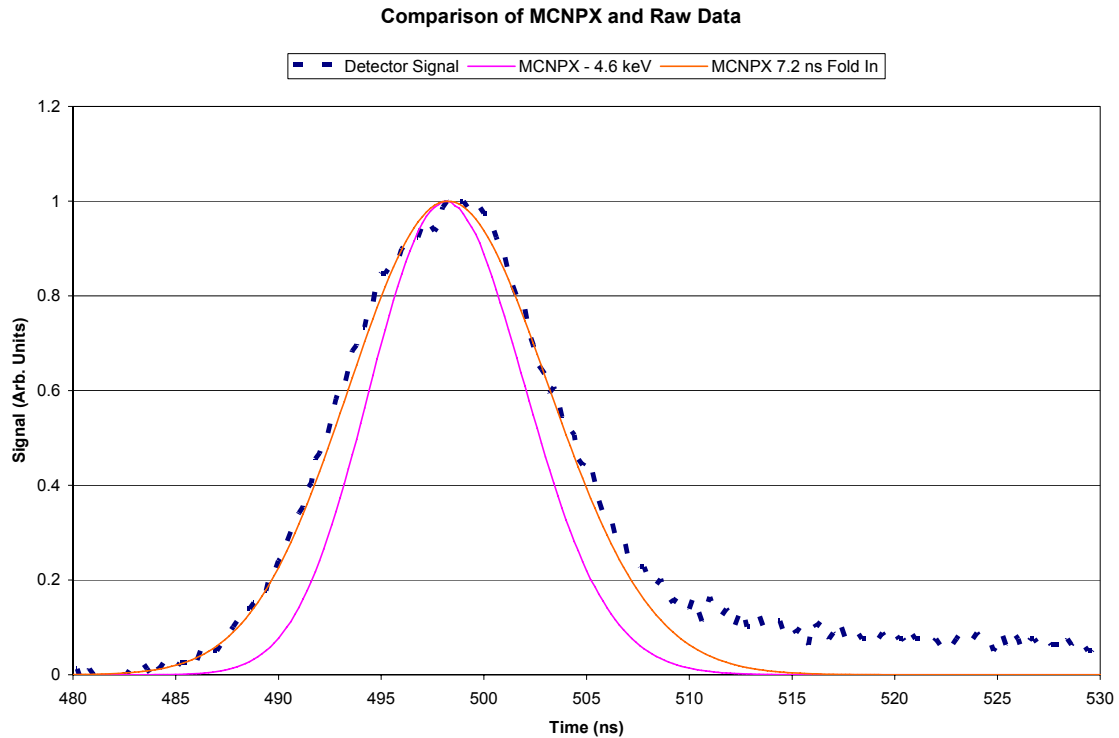


Figure 20. MCNPX Comparison to Raw Data with 7.2 ns Gaussian Folding Function

As shown, the newly folded MCNPX data closely matches the raw detector data, especially the rising portion of the curve. By unfolding the new width from the original MCNPX width, the MCNPX response time can be determined. For this shot, the MCNPX response time was 6.9 ± 0.4 ns. This process was performed on all shots with good data to determine the individual shot response times. The average detector response time was also calculated. Table I shows the individual shot response time calculated using MCNPX. Dashes for the response time indicate that the detector was not evaluated because of the absence of good signals. It should be noted that the MCNPX-determined response factor was very close to the experimentally-determined time response from ISU. For the SPM detector, MCNPX determined a response time of 7.3 ± 0.1 ns while the experimentally-determined response time was ~ 7.2 ns. The DPM detector was experimentally determined to be ~ 7.0 ns while MCNPX calculated 7.2 ± 0.2 ns.

Table I. MCNPX-Determined Detector Response Times

Shot	Rear Lead Thickness (in)	Front Lead Thickness (in)	SPM Detector (ns)	DPM Detector (ns)
34964	0.0	0.5	7.2 +/- 0.5	7.5 +/- 0.4
35003	0.0	0.5	6.1 +/- 0.5	7.0 +/- 0.3
35004	0.0	0.5	-	6.8 +/- 0.4
35005	0.0	0.5	-	7.4 +/- 0.4
35006	0.0	0.5	-	7.3 +/- 0.4
36719	0.0	8.0	7.6 +/- 0.4	-
36721	0.0	4.0	7.0 +/- 0.3	-
36723	0.0	2.0	7.5 +/- 0.4	-
36730	0.5	0.5	6.9 +/- 0.4	-
36731	0.5	7.5	8.2 +/- 0.4	-
36732	0.5	4.0	7.6 +/- 0.3	-
Shot Average	-	-	7.3 +/- 0.1	7.2 +/- 0.2

Ion Temperature Determination

Since a more accurate detector response time has been calculated and experimentally verified, the ion temperatures determined can be compared with the OMEGA ion temperature determination from their detectors.

Shot 34964

This shot was performed with the cannon in the target bay. The SPM detector was located at a distance of 9.2 meters from the neutron source. The DPM detector was in a position 10

meters from the source. Both detectors used one-half inch Bicron 418 plastic scintillator, 3 inches in diameter. Both detectors were biased with -2600 volts and there was one-half inch lead shielding both detectors. Figure 21 depicts the geometry for this shot.

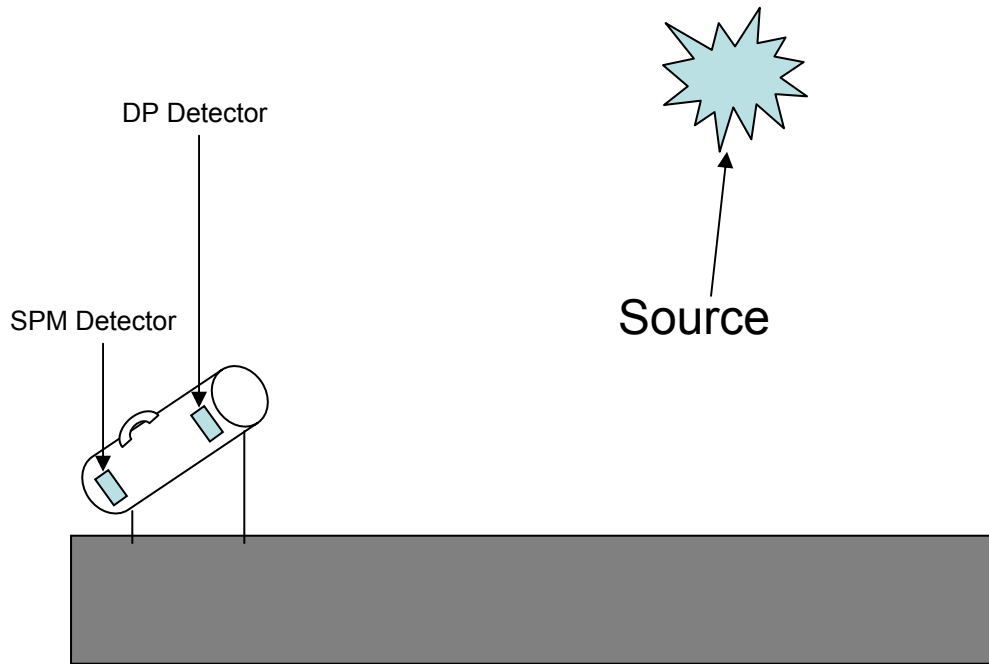


Figure 21. OMEGA Shot 34964 Geometry

One-half inch of lead was used to attenuate the small amount of prompt x-rays that may interfere with the neutron signal. The reported yield for this shot was $2.84E9 \pm 9.39E7$ neutrons. Figure 22 shows the SPM detector signal.

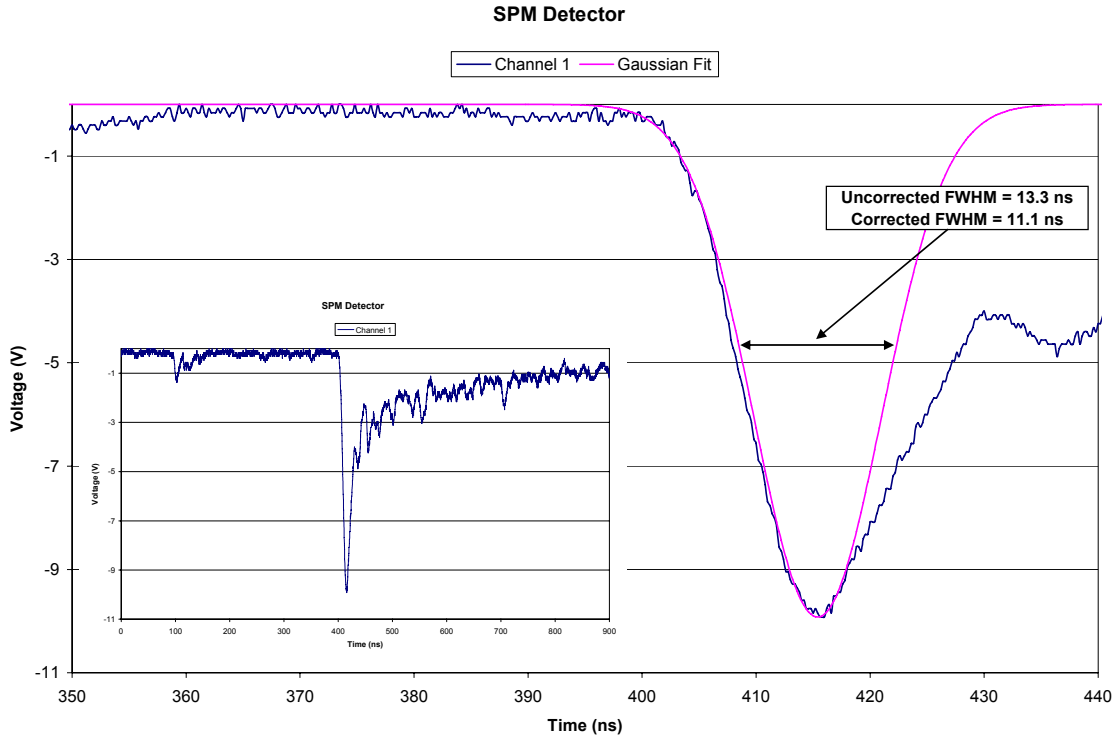


Figure 22. SPM Detector Signal for OMEGA Shot 34964

There is a signal tail that deviates from the Gaussian shape very soon after the peak of the signal. The major deviation occurs at a voltage of about 9 V. The neutron signal diverges from the Gaussian shape, starting only 2.0 ns after the peak. The single paddle detector is ~1 meter off the floor. The tail we are seeing could be an effect from neutrons scattering off the concrete floor, or effects from the lead directly in front of the detector. The Gaussian curve was fit by manually adjusting the mean time and FWHM to produce the “best” fit to the leading edge. The resulting FWHM of this fitted Gaussian was considered to be the “best guess” for the signal width if there were no scattering to increase the tail of the pulse. We note that this does not treat the true fall time of the detector correctly and, therefore, could be expected to underestimate the FWHM somewhat. The average detector response is unfolded from this fitted response width to determine the width of the signal solely due to neutron broadening. For the SPM detector, a

FWHM of 11.1 ns yielded the best fit to the curve. Using this FWHM, the ion temperature can be calculated. The temperature was determined to be 2.4 +/- 0.4 keV. This value agrees well with the reported value of 2.5 +/- 0.5 keV from the OMEGA diagnostics. The DPM detector was located farther from the lead and significantly closer to the concrete floor (~6 inches versus ~36 inches). Data from this signal could be used to see if the tail seen is caused from scattering from the floor or low angle scattering from the lead. A similar tail is seen (Figure 23) for the DPM detector.

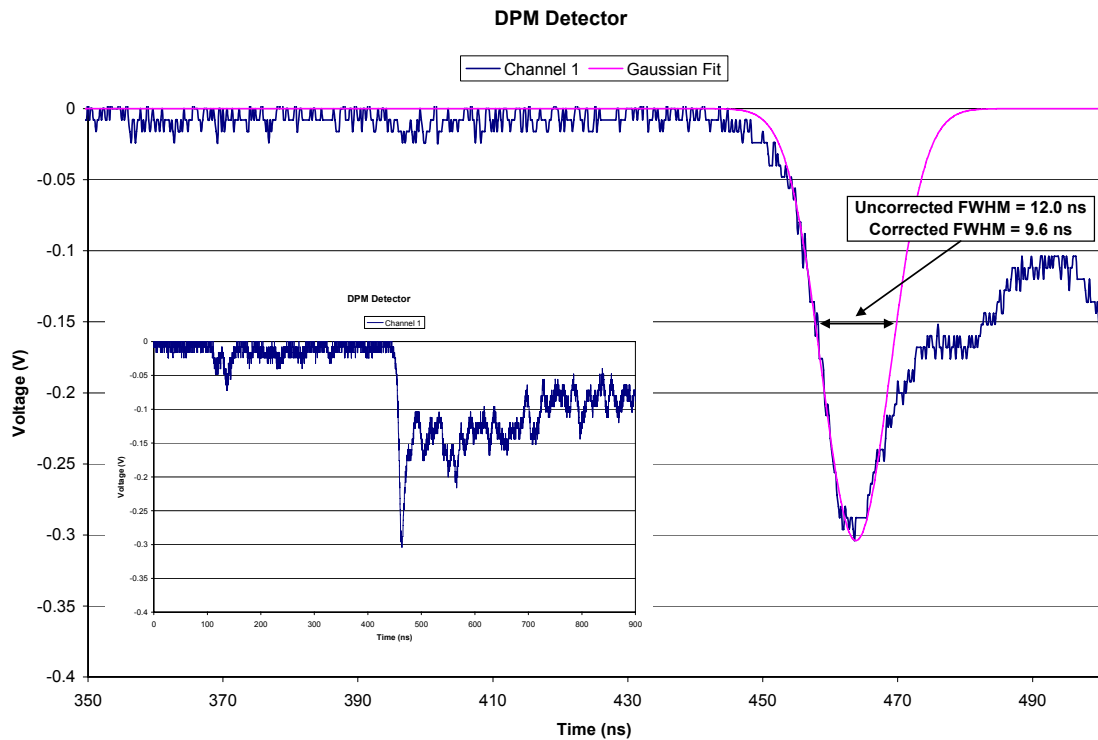


Figure 23. DPM Detector Signal for OMEGA Shot 34964

The tail again diverges from the Gaussian curve shortly after the peak and becomes quite noticeable at a voltage of ~0.20 V. The tail on both signals show similar characteristics. The detectors are in different locations with respect to the lead and the concrete floor. From this, one could ascertain that the distance from the lead to the scintillator makes no difference in the tail

seen in both signals. The concrete floor could contribute to the tail in the signal. The corrected FWHM for the DPM detector is 9.6 ns. This corresponds to an ion temperature of 1.5 ± 0.3 keV, slightly lower than the SPM detector ion temperature of 2.4 ± 0.4 keV.

Shot 35003

To determine if the floor is causing a large effect of scattering into the detectors, the DP detector was suspended off the floor. The SPM detector was still fielded in the cannon at a distance of 10 meters from the source (Figure 8). The DP detector was located in the 5.4 meter diagnostic location that is similarly used by an OMEGA neutron detector. This experiment gives the ability to explicitly determine any effects from the concrete floor. It will also give two ion temperature measurements from two different locations. Both the SPM and DP detectors had one-half inch lead shielding fielded in this shot. The SPM and DP detectors were powered with 2600 volts. A one-half inch thick Bicron 418 scintillator was fielded in during this shot. The OMEGA diagnostics reported a neutron yield of $5.63E8 \pm 4.18E7$ neutrons. Figure 24 shows the SPM signal and Gaussian fit for the shot. The corrected FWHM for this shot is 10.8 ns, which corresponds to an ion temperature of 1.9 ± 0.3 keV. This closely matches the OMEGA reported value of 2.0 ± 0.5 keV.

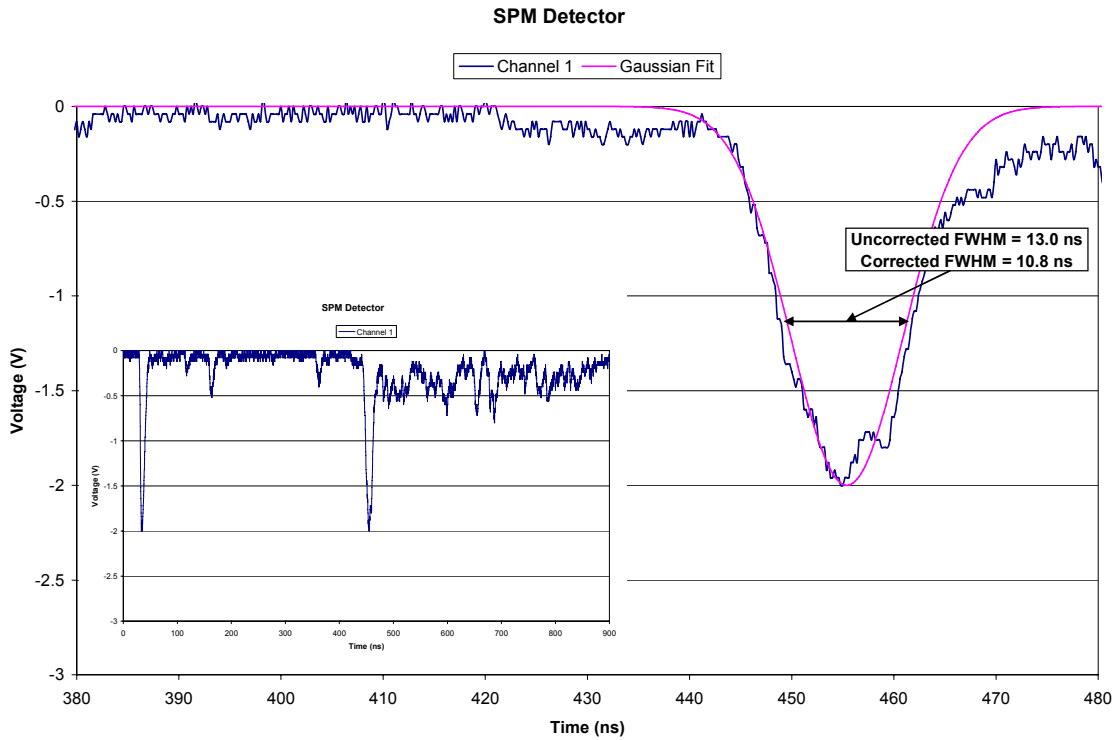


Figure 24. SPM Detector Signal for OMEGA Shot 35003

Data from the second channel of the SPM detector had slightly worse statistics but still yielded a signal that could be fit. The ion temperature calculated from channel 2 is 1.7 ± 0.3 keV. Note that, as seen in Figure 24, occasionally significant peaks are observed prior to the neutron signal. Some of the peaks are timed relative to the DD peak such that they could be due to 14.1 MeV neutrons generated in secondary reactions. Most of these peaks, however, appear to be due to prompt gamma rays generated by the neutrons interacting with the chamber wall.

The DP detector was located 5.4 meters from the neutron source. The signal from this detector can be compared to the SPM detector to see if the location has any effect on the tail end of the neutron signal. Figure 25 shows the neutron signal for shot 35003.

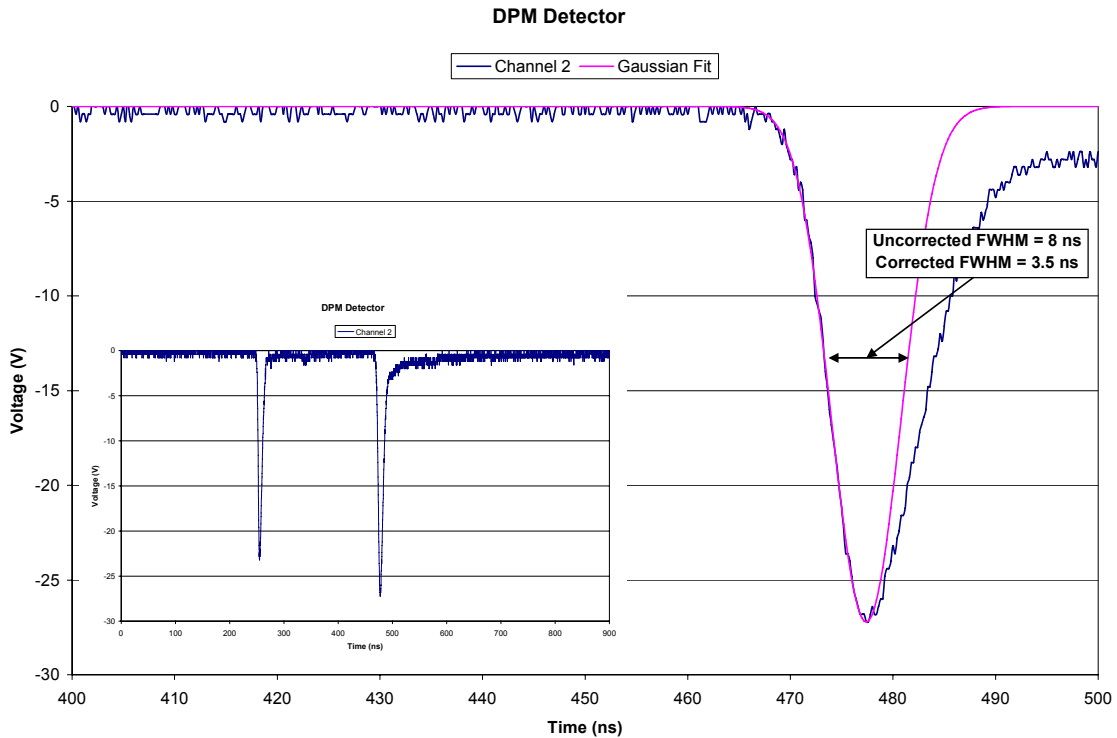


Figure 25. DPM Detector Signal for OMEGA Shot 35003

The curve shown in Figure 25 has a very clean signal, but the data may be misleading. With a corrected FWHM of 3.5 ns, the ion temperature would be 0.7 ± 0.4 keV. The temperature is within a factor of about 2 when compared to the SPM detector. The distance from the concrete floor is unknown and the aiming may be slightly off. Another reason for the inconsistency in temperatures may be the bias voltage applied to the detector. A negative bias of 2600 volts, which was applied on many shots, may be out of the optimal operating range for the photomultiplier; a fact not determined until after these experiments were completed. One would expect the tail seen on the signal to be less since the detector was located farther from the concrete floor and scattering should be lower. The tail on the DPM signal, however, seems to begin sooner after the peak than the SPM detector. The reason for difference observed in ion

temperature between the SPM and DPM detectors (1.7 ± 0.3 keV and 0.7 ± 0.4 keV) is unknown.

Shots 35004, 35005 and 35006

Shots 35004, 35005 and 35006 all have the same geometric setup as shot 35003. The only difference is that shots 35004, 35005 and 35006 have a different bias voltage of -1800 volts.

Figure 26 shows the DPM detector for shot 35004.

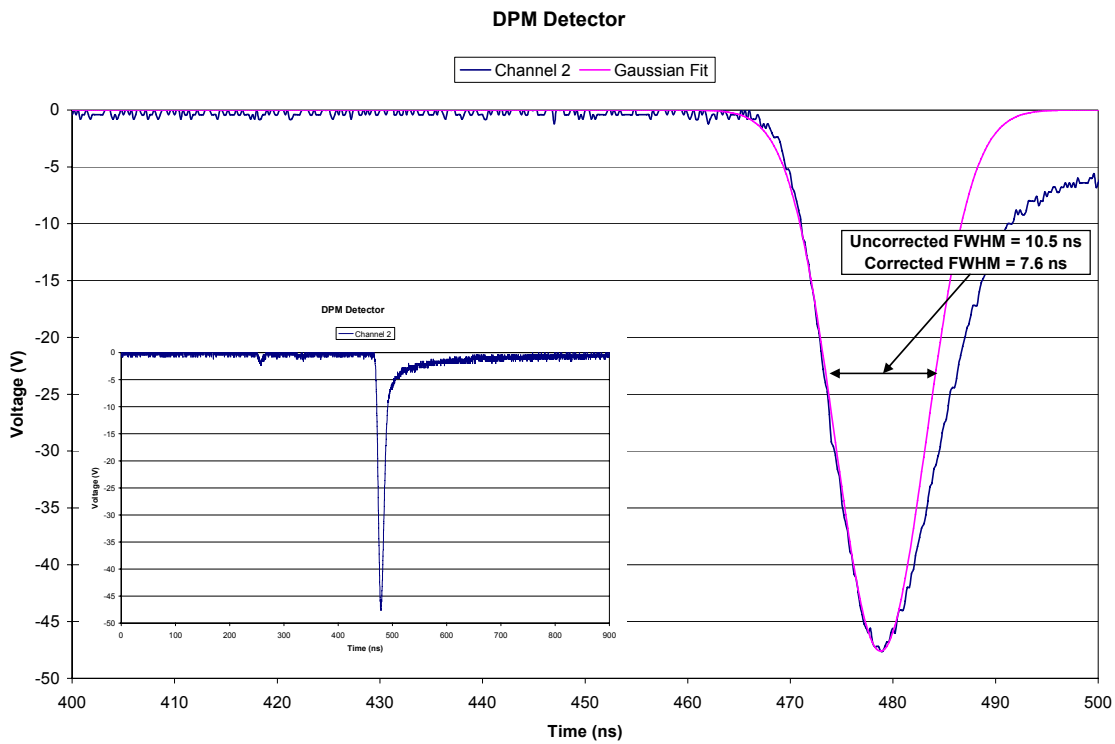


Figure 26. DPM Detector Signal for OMEGA Shot 35004

As shown in Figure 26, the rise time used in the Gaussian fit matches the rise time for the neutron signal well. The neutron yield reported for this shot was $1.55E10 \pm 2.20E8$ neutrons. The corrected FWHM is 7.6 ns, which corresponds to an ion temperature of 3.3 ± 0.7 keV. The OMEGA reported ion temperature was 4.3 ± 0.5 keV. The signal for the DPM detector for this

shot shows the same tail seen on shot 35003. The yield for shot 35004 is approximately 27.5 times higher than shot 35003. The signal from channel one yielded a saturated detector signal.

Shot 35005 had a yield of $8.56E9 \pm 1.63E8$ neutrons. OMEGA reported an ion temperature of 4.8 ± 0.9 keV. The DPM detector (Figure 27) consistently shows a similar signal to shots 35003 and 35004.

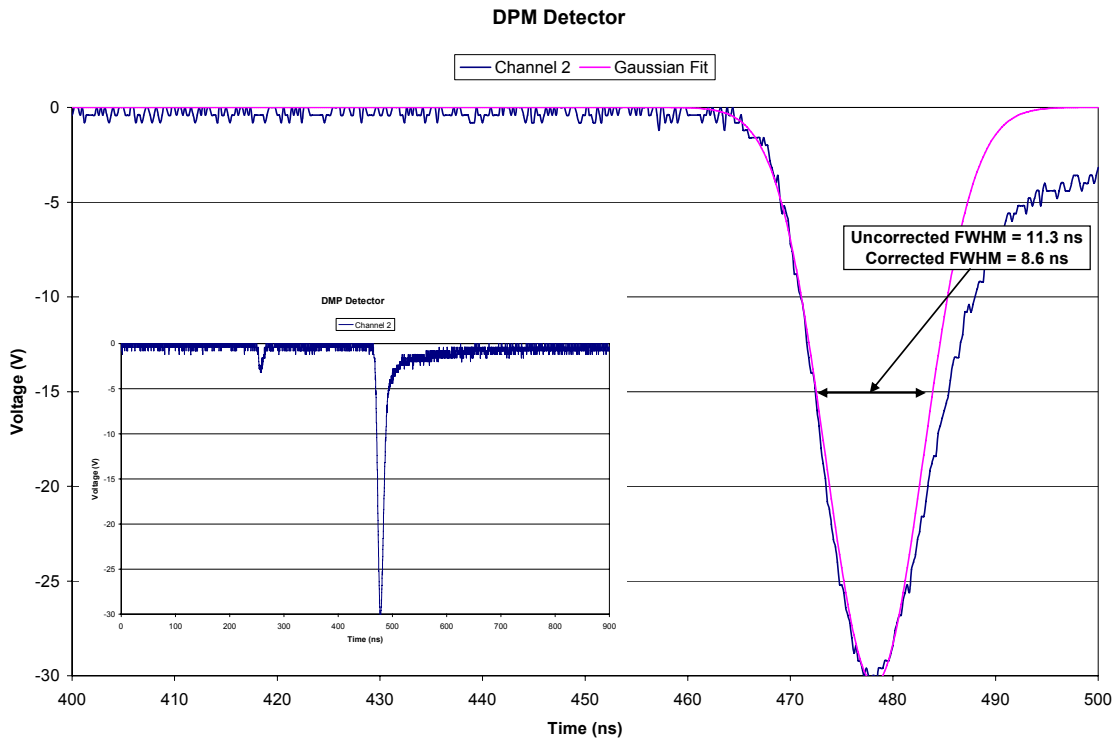


Figure 27. DPM Detector Signal for OMEGA Shot 35005

The corrected FWHM for the DPM detector is 8.6 ns. This corresponds to an ion temperature of 4.2 ± 0.9 keV. The neutron yield for shot 35005 is ~ 15 times greater than shot 35003. The OMEGA reported ion temperature is ~ 2.4 times greater for shot 35005. Channel one for shot 35005 had a saturated signal. The fit for the rise time to the saturation level (Figure 28) yields a corrected FWHM of 8.0 ns. This gives a temperature of 3.7 ± 0.8 ns. Although the signal is saturated, the temperatures for channels one and two are within the error bars of one another.

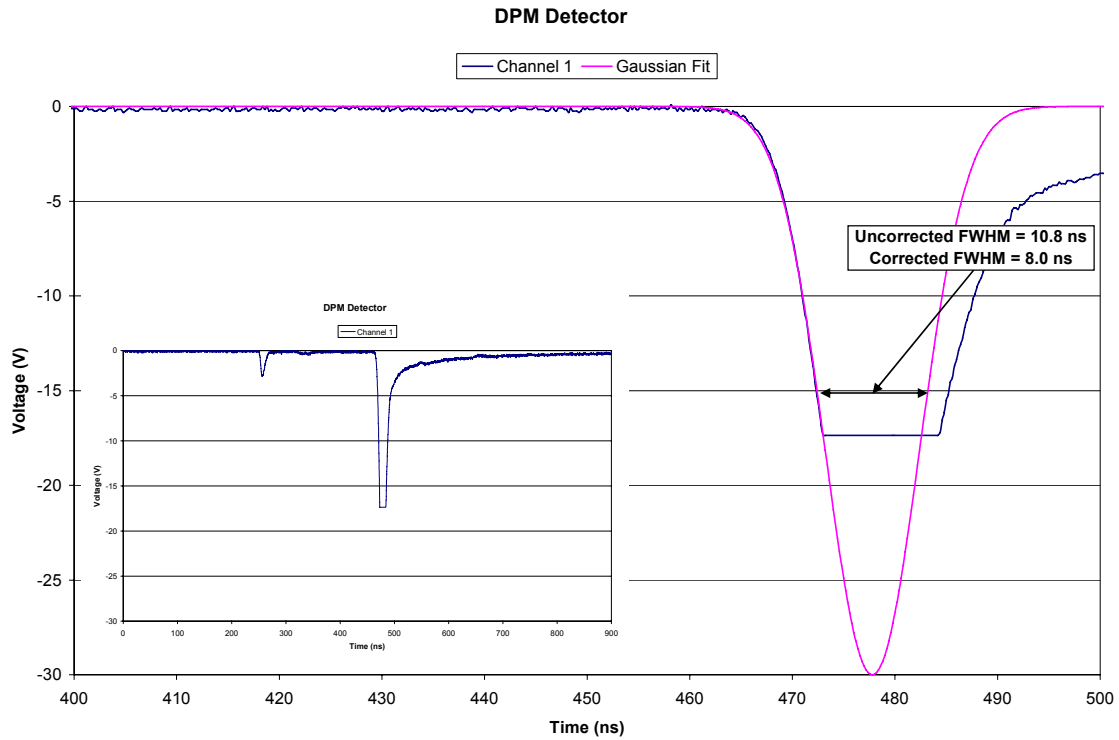


Figure 28. DPM (Channel 1) Detector Signal for OMEGA Shot 35005

Shot 35006 was similar to the previous three shots. The yield was reported as $1.62\text{E}9 \pm 7.09\text{E}7$ neutrons. OMEGA diagnostics recorded the ion temperature as 5.7 ± 0.9 keV. The DPM detector (Figure 29) shows characteristics similar to shots 35003, 35004 and 35005. There is a tail that deviates from the Gaussian shape soon after the peak. The DPM detector's corrected FWHM is 8.3 ns, which corresponds to a temperature of 3.9 ± 0.8 keV.

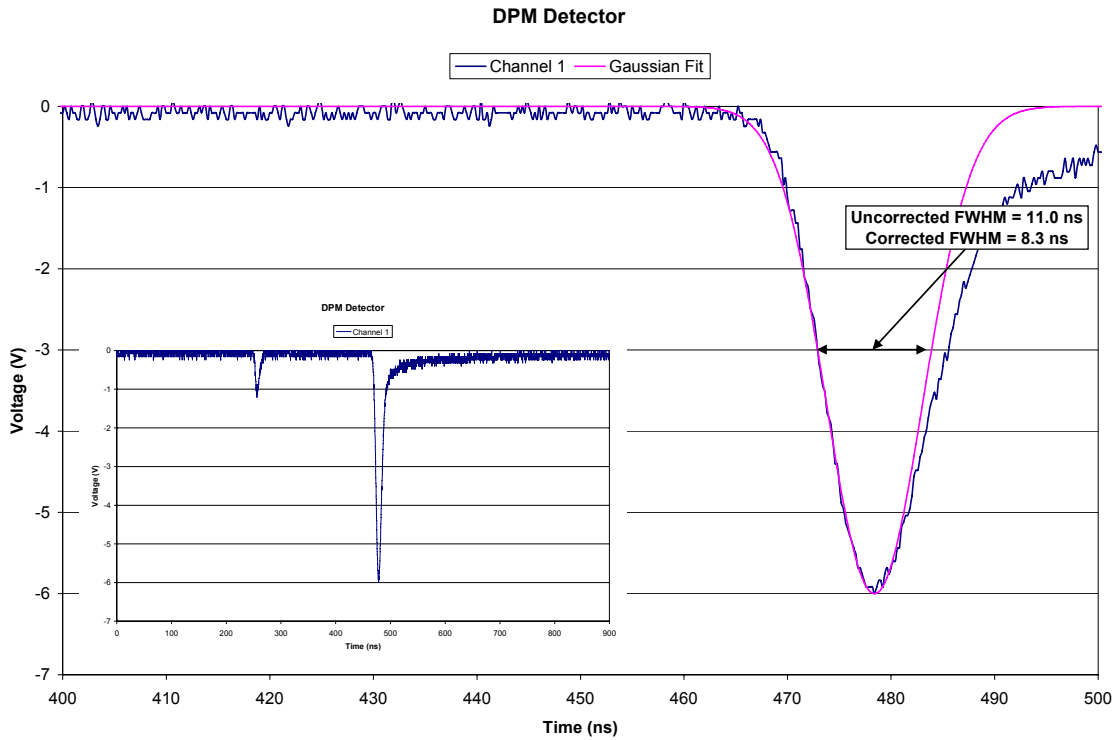


Figure 29. DPM Detector Signal for OMEGA Shot 35006

During the July 2004 shot series, the cannon was suspended (Figure 30) from a catwalk in the target bay. The DP detector was not available for this shot series. The cannon was suspended several meters above the concrete floor to decrease the chance of neutrons scattering into the scintillator. The SPM detector was aligned at a distance of 5.4 meters from the source. By hanging the cannon, various amounts of lead could be placed in the neutron line of sight. This allows for the determination of the effects of lead on ion temperature not tested in shots 35003 through 35006. Detector bias was not recorded during this series of shots.

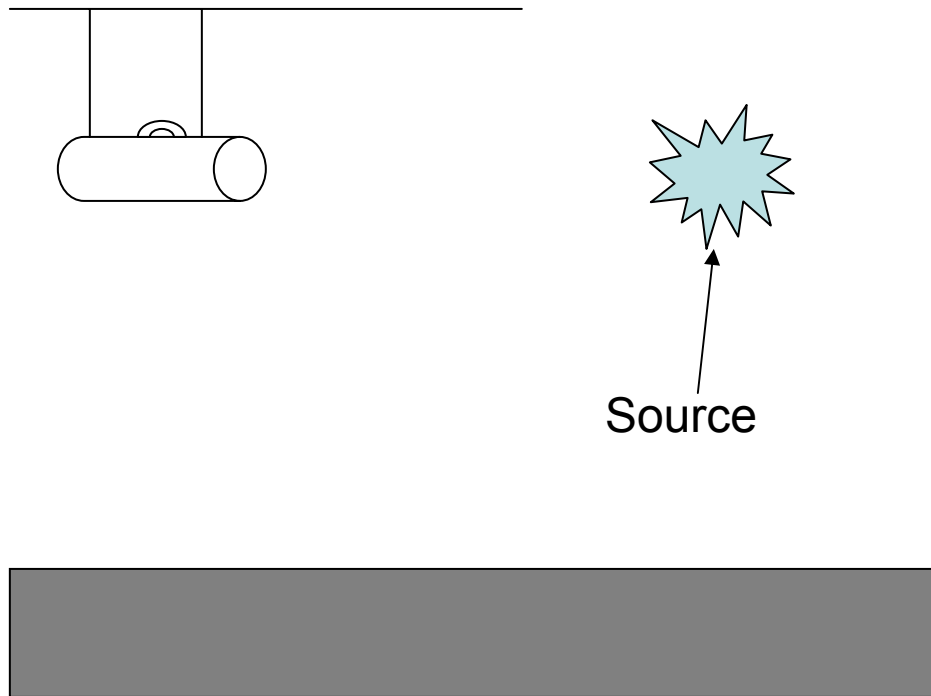


Figure 30. July Shot Series Geometry

Shot 36721

Shot 36721 was configured as seen in Figure 30. There was 4 inches of lead shielding placed 8 inches in front of the detector (Figure 31).

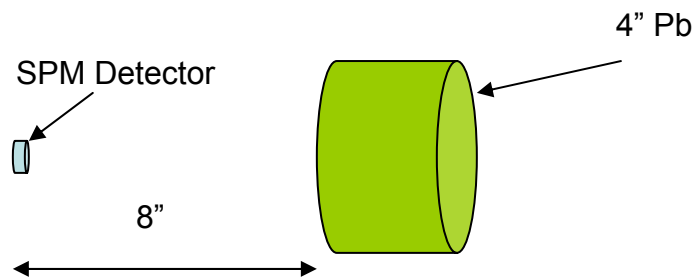


Figure 31. SPM Detector Configuration with 4" Pb Shielding

The scintillator used was one-half inch Bicron 418 plastic scintillator. The yield was reported at $6.76E9 \pm 1.45E8$ neutrons. The OMEGA determined ion temperature was 2.7 ± 0.5 keV.

Figure 32 shows the neutron signal for the SPM detector.

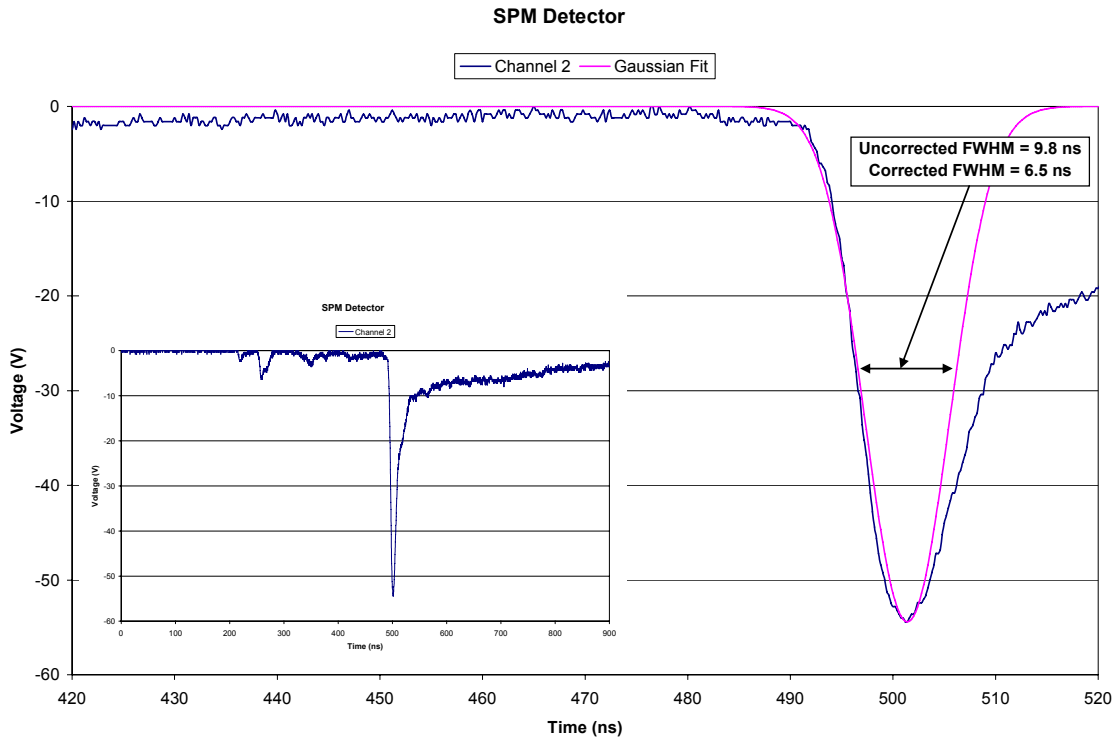


Figure 32. SPM Detector Signal for OMEGA Shot 36721

The corrected FWHM was 6.5 ns. This corresponds to an ion temperature of 2.4 ± 0.6 keV.

There is a significantly longer tail seen in Figure 32 than for shots 35003 through 35006. This can be explained by the amount of lead shielding present for shot 36721. The incoming neutrons have to interact with the lead shielding, contributing to scattered neutrons arriving at the detector later in time. With 4 inches of lead shielding, the SPM detector agrees well with the OMEGA reported temperature.

Shot 36723

Shot 36723 was similar to shot 36721, except only two inches of lead was used as shielding. The lead was 8 inches in front of the SPM detector. One-half inch of Bicorn 418 scintillator was used. Figure 33 depicts the geometry.

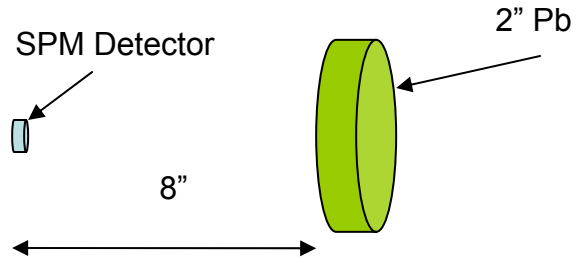


Figure 33. SPM Detector Configuration with 2" Pb Shielding

Both channels for the SPM detector had a saturated signal. Channel one saturated very early in the neutron signal, as seen in Figure 34.

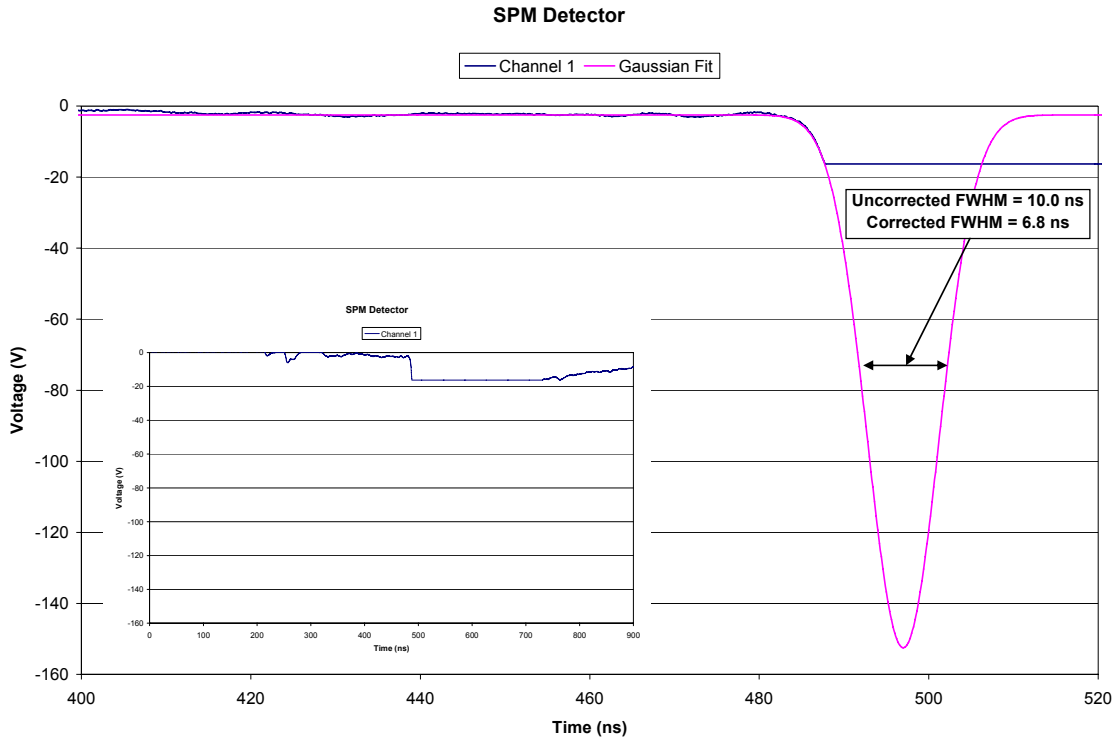


Figure 34. SPM Detector Signal for OMEGA Shot 36723

The channel two signal was also saturated, but at a time much later in the neutron signal. This difference in saturation time made fitting channel two's signal slightly more reliable. Figure 35 shows the fit for channel two.

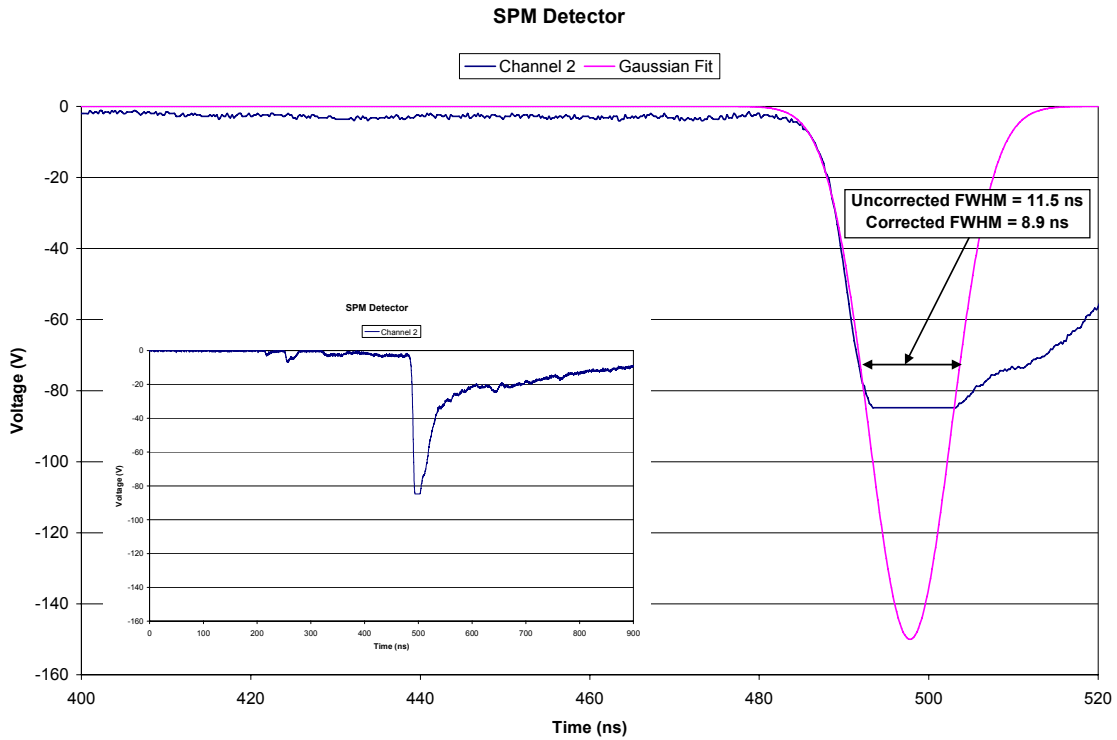


Figure 35. SPM (Channel 2) Detector for OMEGA Shot 36723

A Gaussian curve was used to estimate the data by fitting the rise time portion of the neutron signal and estimating the peak value. The corrected FWHM, 8.9 ns, was calculated by unfolding the detector response time in quadrature. The corrected FWHM yields an ion temperature of 4.5 +/- 0.9 keV. The value matches the OMEGA reported temperature of 4.8 +/- 1.5 keV. The yield for shot 36723 was 2.12E10 +/- 3.16E8 neutrons.

Shot 36730

For shot 36730, one-half inch of lead was located 8 inches in front of the scintillator. The scintillator was changed to one-eighth inch Bicron 422Q. One-half inch of lead was also placed directly behind the SPM detector (Figure 36) to shield against any neutrons or photons backscattering into the detector.

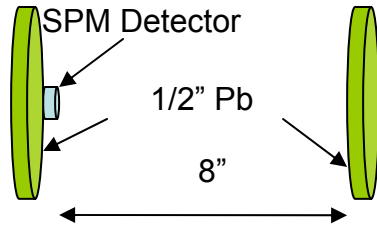


Figure 36. SPM Detector Configuration with 1/2" Pb Shielding (Front and Back)

The yield for shot 36730 was $2.02E10 \pm 3.08E8$ neutrons and OMEGA reported an ion temperature of 4.4 ± 0.5 keV. As seen in Figure 37, the Gaussian curve fits the neutron signal well. The corrected FWHM is 8.9 ns. This corresponds to an ion temperature of 4.5 ± 0.9 keV. This is very close to the ion temperature reported by OMEGA (4.4 ± 0.5 keV). One thing to note is the triple peak seen in the inset plot in Figure 37.

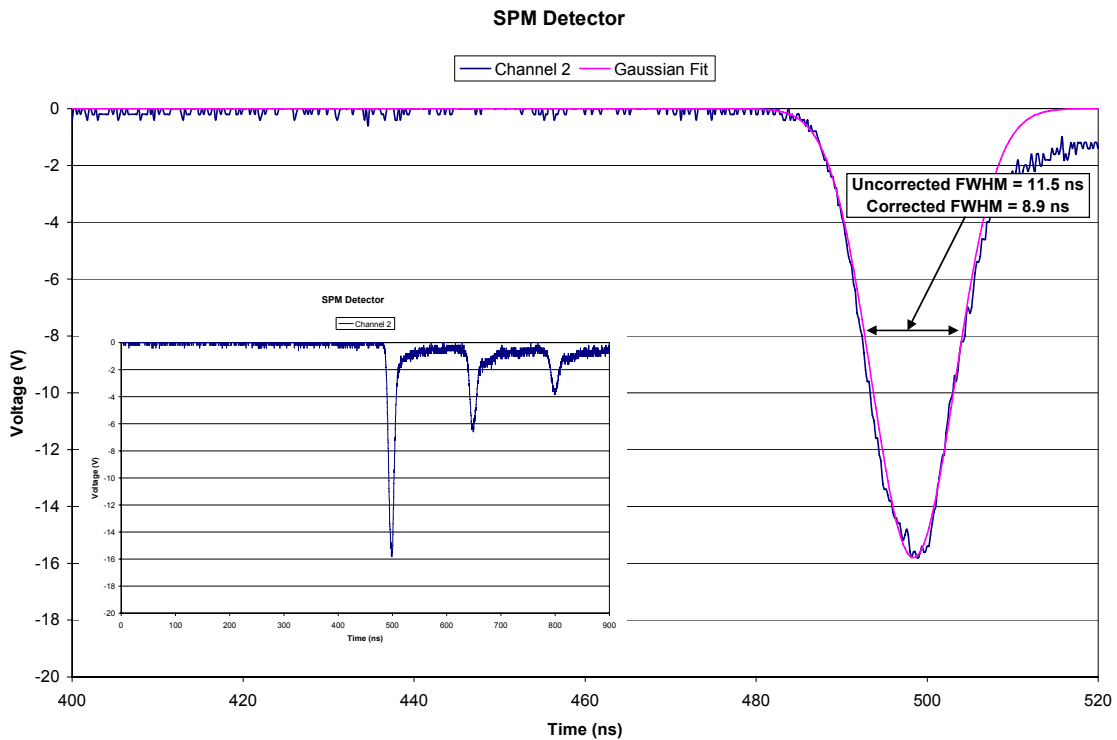


Figure 37. SPM Detector Signal for OMEGA Shot 36730

The most likely explanation for this multiple signal is a problem with the signal cable. The triple peak may be a signal reflection due to the digitizing scope not being terminated at 50 Ω properly on this shot. There is a very slight tail at the end of the neutron signal. This is caused by the small amount of lead shielding placed in front of the detector.

Shot 36731

For shot 36731, 7.5 inches of lead was located 8 inches in front of the SPM detector. Again, one-half inch of lead was placed directly behind the SPM detector to shield any possible backscattered neutrons and photons. One-eighth inch Bicron 422Q was used for scintillation. Figure 38 shows the geometric configuration for shot 36731.

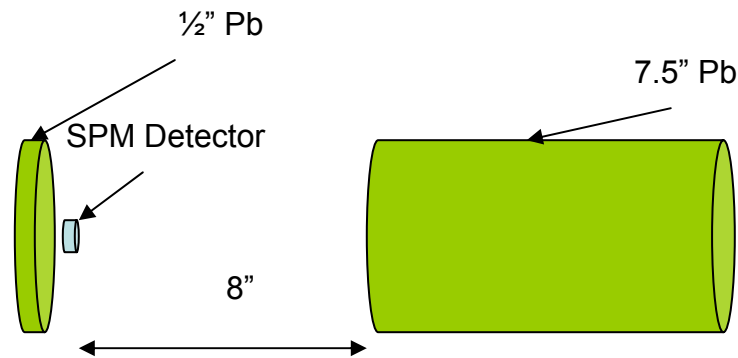


Figure 38. SPM Detector Configuration with 7.5" Pb Shielding

OMEGA diagnostics reported a yield of $1.35E11 \pm 7.98E8$ neutrons and an ion temperature of 4.9 ± 0.7 keV. The corrected FWHM is 9.5 ns. This yields an ion temperature of 5.1 ± 1.0 keV. The SPM detector's neutron signal (Figure 39) has a significant tail and structure. The large tail seen in Figure 39 is caused by the massive amount of lead shielding (7.5 inches) present.

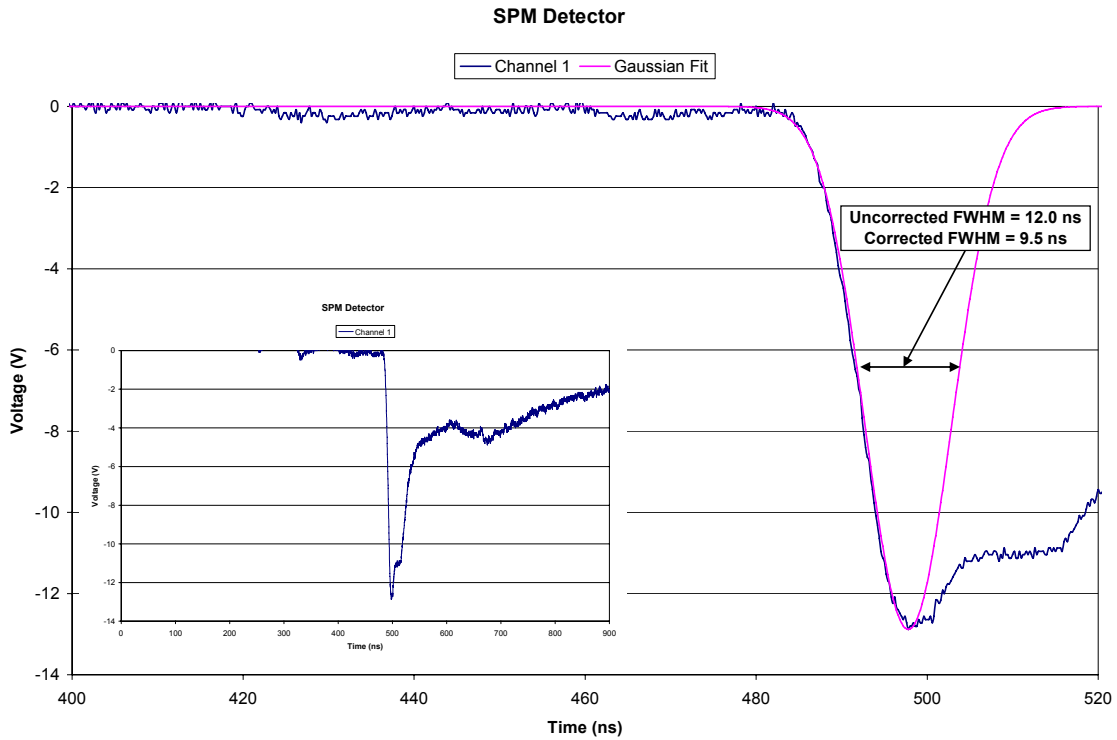


Figure 39. SPM Detector Signal for OMEGA Shot 36731

Shot 36732

Shot 36732 was configured the same as previous shots for the July series. Four inches of lead was placed 8 inches in front of the SPM detector, as shown in Figure 40. One-half inch of lead was located behind the detector to reduce any backscatter into the detector.

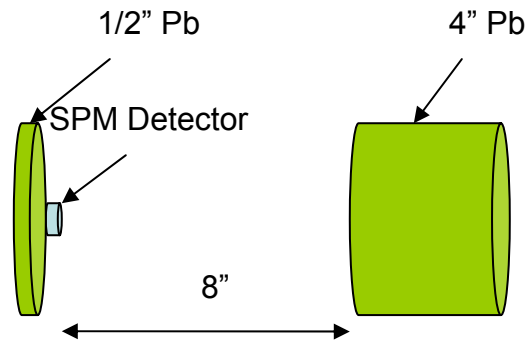


Figure 40. SPM Detector Configuration with 4" Pb Shielding

One-eighth inch Bicron 422Q scintillator was fielded in the SPM detector. The neutron yield was reported as $1.68E11 \pm 8.87E8$. OMEGA diagnostics reported a temperature of 3.6 ± 0.5 keV. The SPM detector signal was saturated on both channels. The signal on channel 2 had the most signal available to analyze. Figure 41 shows the neutron signal for channel 2 on the SPM detector.

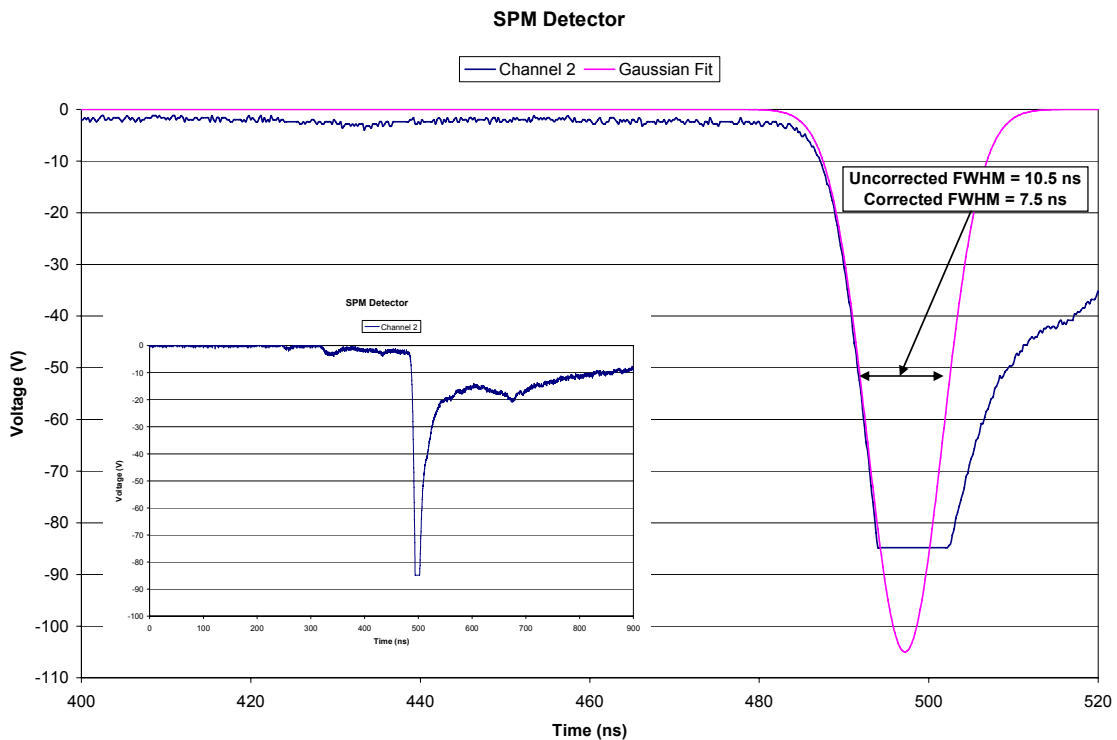


Figure 41. SPM (Channel 2) Detector Signal for OMEGA Shot 36732

The corrected FWHM is 7.5 ns, corresponding to an ion temperature of 3.2 ± 0.7 keV. There is still a tail that occurs during the fall time on the signal. As seen in shot 36731 (Figure 39), there is a small increase in signal around 660 ns. Slight backscattering from the lead behind the detector may cause these peaks. It is more likely the peaks are due to a reflection of the signal due to improper cable termination as seen on shot 36370, which are now partially hidden in a larger scattering tail. The slight “first peak” is present in shot 36732. This peak is present during

both shot series and occurs at similar times, relative to the neutron signal. This peak was present when the DP detector was located at 5.4 meters and when the SPM detector was located at 9.2 meters in the cannon. This “first peak” is approximately 145 ns before the main peak. This timing difference is approximately correct for 14.1 MeV neutrons, characteristic of a secondary DT reaction. Shots that had peaks with approximate timing for DT neutrons were 35003, 35004, 36721 and 36732.

CHAPTER 5

Results

The bremsstrahlung radiation environment at Z is very intense. In an attempt to shield the neutron time-of-flight detectors from this intense radiation source, as much as eight inches of lead is necessary. Experiments were performed at the University of Rochester's Laboratory for Laser Energetics to determine if the SPM and DP detectors can record a feasible neutron signal behind as much as eight inches of lead. Figure 42 shows a significant broadening to the SNL detectors when compared with the OMEGA diagnostics.

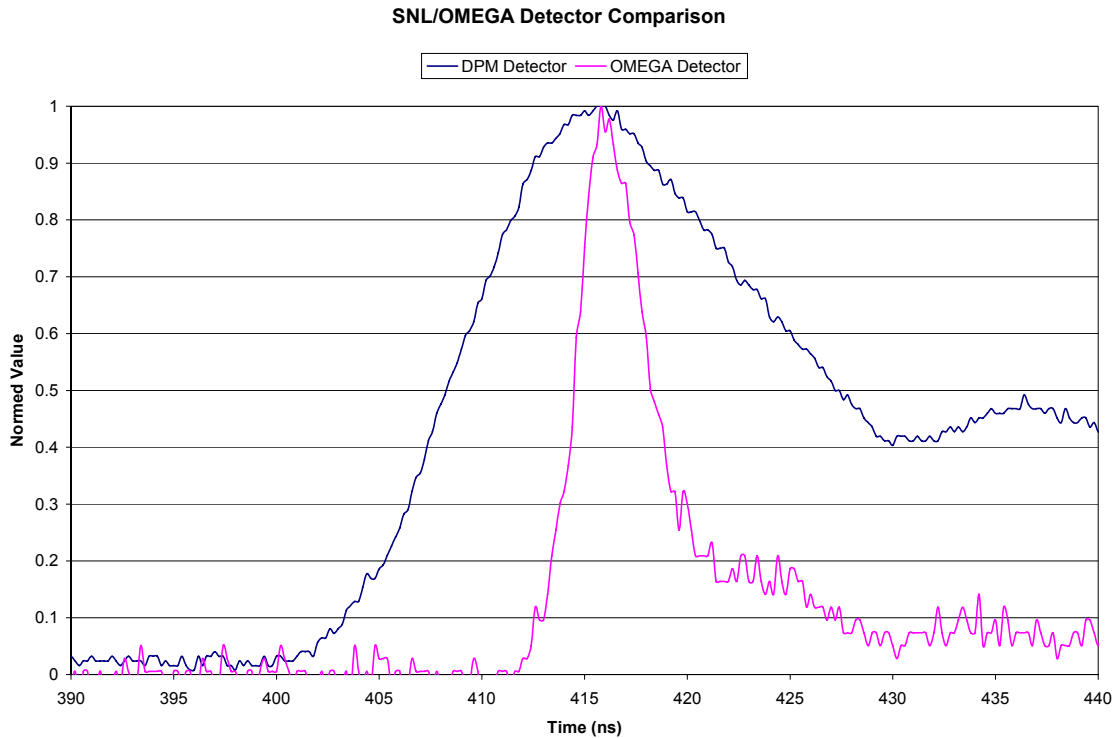


Figure 42. SNL/OMEGA Detector Comparison

As shown in Chapter 4, MCNPX calculations indicate that there are no effects on the neutron time signal when various materials are placed in the line of sight. These results suggest that the broadening seen during the experiments is largely caused by a response time inherent for the

detectors. Experiments were performed at ISU to determine the detector time response for both the SPM and DP detectors. These experiments yield a detector response time of 7.2 ns and 7.0 ns for the SPM detector and DPM detector, respectively. MCNPX and BROAD were used to computationally determine the detector time response as well. Table II shows the computational results.

Table II. MCNPX-Determined Detector Response Times

Shot	Rear Lead Thickness (in)	Front Lead Thickness (in)	SPM Detector (ns)	DPM Detector (ns)
34964	0.0	0.5	7.2 +/- 0.5	7.5 +/- 0.4
35003	0.0	0.0	6.1 +/- 0.5	7.0 +/- 0.3
35004	0.0	0.0	-	6.8 +/- 0.4
35005	0.0	0.0	-	7.4 +/- 0.4
35006	0.0	0.0	-	7.3 +/- 0.4
36719	0.0	8.0	7.6 +/- 0.4	-
36721	0.0	4.0	7.0 +/- 0.3	-
36723	0.0	2.0	7.5 +/- 0.4	-
36730	0.5	0.5	6.9 +/- 0.4	-
36731	0.5	7.5	8.2 +/- 0.4	-
36732	0.5	4.0	7.6 +/- 0.3	-
Shot Average	-	-	7.3 +/- 0.1	7.2 +/- 0.2

As shown, the computational response times compare well (7.3 ± 0.1 ns compared with 7.2 ns and 7.2 ± 0.2 ns compared with 7.0 ns) with the experimental response times. By using these averaged detector response times, a calculation for the ion temperature can be made.

After a simple Gaussian curve was fit to the rising edge of the raw data, an ion temperature was calculated using the average response times. Table III shows the results from the experimental analysis compared to OMEGA's results.

Table III. SNL/OMEGA Ion Temperature Comparison

Shot Number	Rear Lead Thickness (in)	Front Lead Thickness (in)	OMEGA (keV)	SPM Detector (keV)	DPM Detector (keV)
34964	0.0	0.5	2.5 ± 0.5	2.4 ± 0.4	1.5 ± 0.3
35003	0.0	0.5	2.0 ± 0.5	1.9 ± 0.3	0.7 ± 0.4
35004	0.0	0.5	4.3 ± 0.5	-	3.3 ± 0.7
35005	0.0	0.5	4.8 ± 0.7	3.7 ± 0.8	4.2 ± 0.9
35006	0.0	0.5	5.7 ± 0.9	-	3.9 ± 0.8
36721	0.0	4.0	2.7 ± 0.5	2.4 ± 0.6	-
36723	0.0	2.0	4.8 ± 1.5	4.5 ± 0.9	-
36730	0.5	0.5	4.4 ± 0.5	4.5 ± 0.9	-
36731	0.5	7.5	4.9 ± 0.7	5.1 ± 1.0	-
36732	0.5	4.0	3.6 ± 0.5	3.2 ± 0.7	-

As shown in Table III, by using the computationally determined response time, the ion temperature measurements from the SPM and DPM detectors compare well with the OMEGA detector diagnostics. Figure 43 plots the SNL and OMEGA ion temperatures with their

associated errors. Figure 44 shows that there is not a definitive trend in ion temperature ratios with respect to the amount of lead shielding present.

The origin of the tails seen on most shots is difficult to determine. The tail dramatically decreases when the detectors were placed away from the concrete floor. This may indicate that the concrete is a major source for scattering. This conclusion can be further supported by the fact that similar behavior is observed on the Z machine. In addition, however, the data suggests that the tail also increases as the thickness of the lead shield increases.

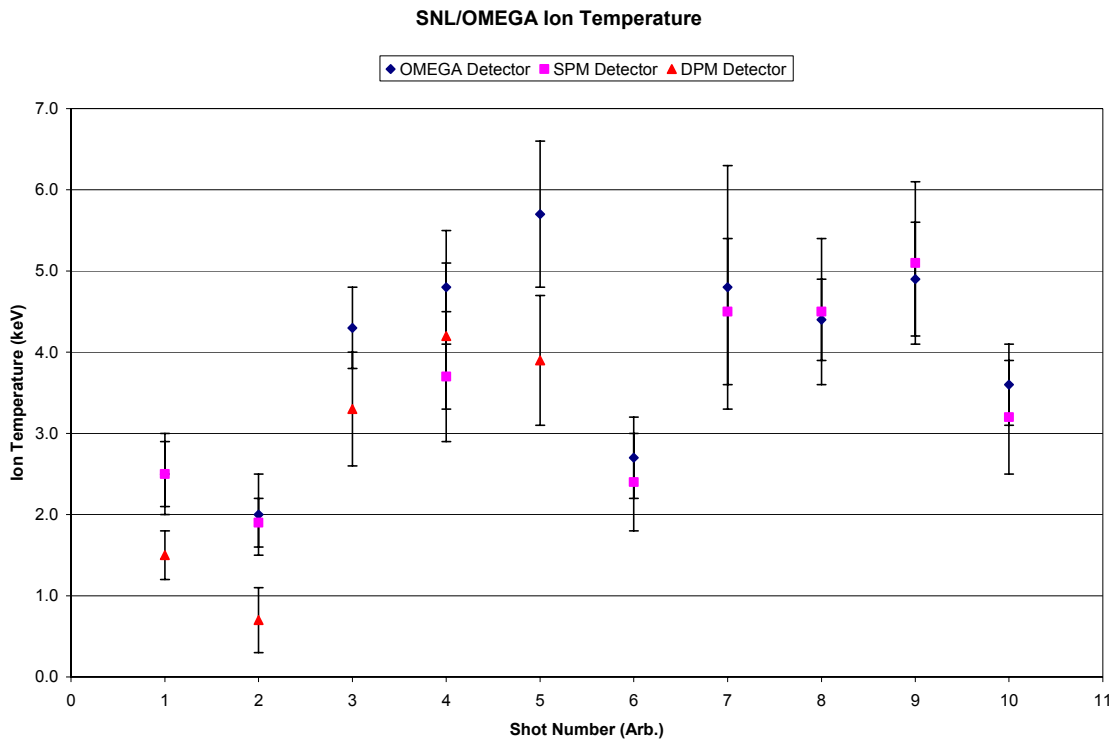


Figure 43. SNL/OMEGA Ion Temperature Comparison

MCNPX seems to show that any material in front of the detector has no broadening effect on the time signal. Modeling the full geometry to include large distances of void and concrete, with a point source, is currently not within the limits of MCNPX.

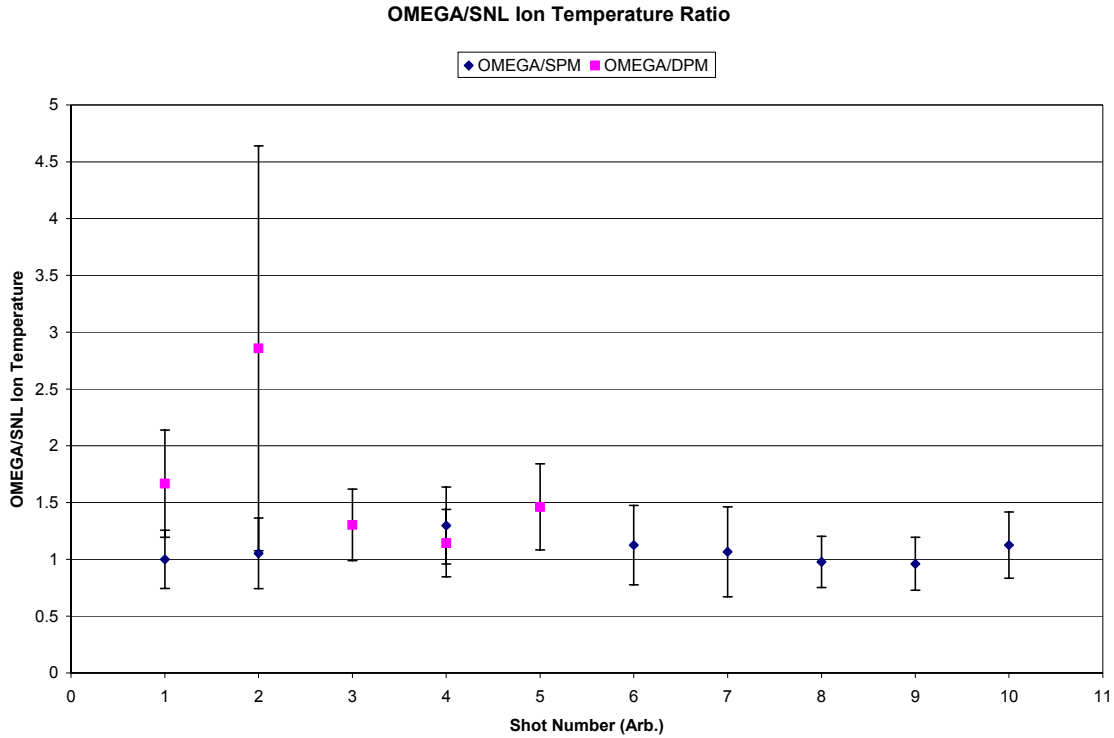


Figure 44. SNL/OMEGA Ion Temperature Ratio Comparison

At the time of this thesis, there is a beta version of MCNPX that allows for practically unlimited numbers of source particles, but it was unavailable for this work. More importantly, MCNPX cannot recreate the tails seen from experiments. Tails can be computationally seen with infinite spheres of lead, but for even simple geometries of right circular cylinders, there is no significant increase in the tail. MCNPX does indicate that the tail increases with increasing lead or the addition of a concrete floor near the detector but the size of the calculated tail is much smaller (by as much as an order-of-magnitude) than is observed experimentally. This difference has not been resolved. Even the inclusion of photons released via (n,γ) interactions did not resolve this discrepancy. Although it would be desirable to understand the physical nature of these tails, the fact remains that using the method described in this thesis, ion temperature measurements can be made with reasonable accuracy for the case of a detector that is shielded by 8 inches of lead as is necessary on Z.

CHAPTER 6

Conclusion

Accurate fusion ion temperature measurements are necessary to understand the basic physics of the fusion process. Thick x-ray shielding makes this measurement difficult. One asset to the fusion program would be the ability to computationally model and predict ion temperatures with radiation transport codes including MCNPX. The SPM and DPM detectors were found to have significantly larger response times than originally determined (~ 7.3 ns and ~ 7.2 ns versus ~ 4.3 ns). This large difference was determined by both experiments and computational simulations. The issues of large open spaces and small solid angles are still an issue when attempting to computationally model these geometries. It has been shown that by simplifying the geometry and source definition, one can closely predict neutron time signals using a basic model. For the experiments performed, these basic models are quite accurate when compared to data from OMEGA diagnostics.

For situations like those encountered on Z, large amounts of lead shielding are necessary to block out the intense bremsstrahlung radiation that would otherwise saturate the detector and prevent it from responding quickly enough to capture the neutron signal necessary to make the ion temperature measurement. It has been shown that MCNPX is able to accurately predict the ion temperature determined from the SPM and DPM detectors. The only variable that one must determine is the detector response time.

Future Work

More data is needed. I would suggest that we setup future experiments to focus on the SPM and DPM detectors with larger thicknesses of lead. I think either placing the detectors in the basement of the OMEGA facility or using the suspended geometry would be best to eliminate the scattering from the concrete floor. It would be beneficial to use the newly determined detector response time to re-evaluate some shots on Z. If possible, a standalone pulsed neutron source with a “short” pulse would also be an asset to the neutron diagnostic effort.

Further investigation into computationally modeling the Z environment would be useful to the program.

REFERENCES

Briesmeister, J. F., ed. MCNPTM - A General Monte Carlo N-Particle Transport Code, Version 4C. Technical Report LA-13709-M, LANL, 2000.

Brysk, H., "Fusion Neutron Energies and Spectra." Plasma Physics. 15 (1973): 611-617.

Carter, L.L. and E.D. Cashwell. Particle Transport Simulation with the Monte Carlo Method. Oak Ridge: U. S. Energy Research and Development Administration, 1975.

GE Co. and KAPL, Inc. "Nuclides and Isotopes." Chart of the Nuclides. 15th ed. San Jose: GE Nuclear Energy, 1996.

Lerche, R. A., L.W. Coleman, J. W. Houghton, D. R. Speck, and E.K. Storm. "Laser Fusion Ion Temperatures Determined by Neutron Time-of-Flight Techniques." Applied Physics Letters. 31.10 (1977): 645-647.

Murphy, T. J., J.L. Jimerson, R.R. Berggren, J.R. Faulkner, J.A. Oertel, and P.J. Walsh. "Neutron Time-of-Flight and Emission Time Diagnostics for the National Ignition Facility." Review of Scientific Instruments. 72.1 (2001): 850-853.

Murphy, T.J., R.A. Lerche, C. Bennett, and G. Howe. "Ion-temperature measurement of indirectly driven implosions using a geometry-compensated neutron time-of-flight detector." Review of Scientific Instruments. 66.1 (1995): 930-932.

Nuclear Wallet Cards. NNDC. 2005. Brookhaven National Laboratory.

<<http://www.nndc.bnl.gov/wallet/>>.

Taylor, J. R., An Introduction to Error Analysis. Sausalito: University Science Books, 1997.

APPENDICIES

APPENDIX A

MCNPX Description

Los Alamos National Laboratory developed a FORTRAN computer code (Briesmeister 2000) that performs particle transport using the Monte Carlo method (Carter and Cashwell 1975). Monte Carlo N-Particle (MCNP™) is that code. MCNP can be used for neutron, photon and electron transport. MCNP cannot only perform neutron, photon and electron transport, but can also be used for nuclear criticality calculations. MCNP uses explicit multi-dimensional volumes and/or surfaces to define arbitrary geometric configurations of materials with descriptive material compositions. MCNP can also utilize many different cross section data libraries. These libraries include point-wise neutron and photon cross-sections known as ENDF libraries. Photon libraries include coherent and incoherent scattering, possible fluorescence emission, pair production and bremsstrahlung. Electrons are modeled using a continuous slowing-down model. MCNP allows the user to geometrically plot the materials and specify tallies of calculated quantities. Every tally has an associated random error from the calculation. A new version of the code, MCNPX, includes a plethora of additional particles and can evaluate energies upwards of 100 GeV.

A brief note regarding the MCNPX modeling presented in this report is necessary. To simulate the basic geometry modeled for each shot, a compromise must be made with regard to the source information. The source was modeled using a beam source instead of an isotropic source. This change will neglect the angular distribution of the isotropic source. This was done to make sure the scintillator had enough neutron interactions to produce relatively good statistics. For shot models, this will not change the fact that regardless of the source's angular distribution, any small angle scatter of neutrons in the lead will not interact with the scintillator, due to the

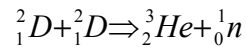
distance from the source to the scintillator and the small solid angle. The broadening of the source was considered more important for this work, thus, the angular dependence for the isotropic source was omitted.

APPENDIX B

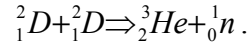
Nuclear Physics

To understand ion temperature calculations, we must first understand the physics behind the neutron source. In the fusion process, there are three main nuclear reactions that occur with isotopes of hydrogen. The first is the deuterium-deuterium reaction.

If there is enough energy in the system, two deuterium atoms can combine in nuclear fusion. Consider the following reaction:



For this to make sense, energy, charge, momentum and nucleons must be conserved. If this reaction is investigated further, one will notice that nucleons are conserved. On the left hand side of the equation we have a total atomic mass of 4. On the right, the total mass is also 4, showing that indeed nucleons are being conserved in this reaction. Conservation of energy must also be taken into consideration. This property can be checked by calculating the reaction's Q value. Q values are typically expressed in MeV. If the Q value is positive, the kinetic energy of the system is increasing, therefore we have an exothermic reaction. If the Q value is negative, this would indicate that we would need to inject energy into the system to sustain the reaction. For fusion applications an exothermic reaction is wanted. Since we must conserve energy, this increase in kinetic energy has to be dealt with. The excess energy is given off via heat. The Q value of the reaction can be calculated with a value known as the mass excess. The mass excess of deuterium, according to Brookhaven National Laboratories (NNDC 2005), is 13.1357 MeV. A neutron's mass excess is 8.0713 MeV. Finally, the mass excess of 3-He is 14.9312 MeV. If we find the difference between the sums of the products and reactants, we can balance the nuclear reaction with



$$13.1357MeV + 13.1357MeV \Rightarrow 14.9312MeV + 8.0713MeV + Q$$

The Q value for the DD reaction is 3.27 MeV, which makes this reaction useful in producing energy. Again, conservation of energy and momentum must be considered. The Q value energy must be separated between the two new particles created, namely the 3-He atom and the neutron.

Let's first consider the conservation of momentum

$$mv = MV,$$

where m is the mass of the neutron, v is the velocity of the neutron, M is the mass of the 3-He atom and V is its velocity. If we solve the above equation for V, we can use it to solve the conservation of energy equation.

$$\frac{1}{2}mv^2 + \frac{1}{2}MV^2 = Q,$$

where

$$V = \frac{mv}{M}.$$

Plugging this result into the conservation of energy equation gives

$$\frac{1}{2}mv^2 + \frac{1}{2}M\left(\frac{mv}{M}\right)^2 = Q.$$

By dividing out the 1/2's, combining like terms, and reducing we get

$$v^2\left(\frac{mM + m^2}{M}\right) = 2Q.$$

Finally, solving for v²

$$v^2 = \frac{2Q}{\frac{mM + m^2}{M}}.$$

To determine how much of the Q value goes to the neutron, we simply solve the following equation using our value for v^2 .

$$E_n = \frac{1}{2} m \frac{2Q}{\frac{mM + m^2}{M}}$$

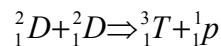
By reducing we can make the equation a little simpler to read.

$$E_n = \frac{Q}{1 + \frac{m}{M}}$$

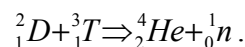
The emitted neutron energy is therefore

$$E_n = \frac{3.27 \text{ MeV}}{1 + \frac{1}{3}} = 2.4525 \text{ MeV} .$$

With this knowledge, we can set up our detection system to look for neutrons with energies of 2.45 MeV. We have two other reactions that occur when using deuterium. There is also a DD reaction that produces tritium and a proton.



Although this reaction may not look harmful, it needs to be accounted for. Neutrons are neutral particles, so we need not worry about the proton given off in the above reaction. This is because protons are charged particles and the methods of detection of neutrals versus charged particles are different. The tritium produced from the DD reaction can react with the deuterium we have in the system. This product would be



By using the same methods described above, we can calculate this reaction's Q value to be 17.5893 MeV. The neutron from this reaction will have 14.071 MeV. Since the DT neutron's energy is much greater than the DD neutron's (14.1 MeV vs. 2.45 MeV) we will not see

interference with our DD specific system. DT neutrons have a higher energy; therefore, they will reach our detector sooner. One must remember that the production rate of the DT neutrons is significantly less than the production rate of the DD neutrons. Our detectors will detect the DT neutrons, but the signal will be very small and will not interfere with the DD neutron signal.

APPENDIX C

Bicron 418/422Q Specification Sheets

Bicron 418 Specification Sheet

BC-418, BC-420, BC-422 Premium Plastic Scintillators

The premium plastic scintillators described in this data sheet are intended for use in ultra-fast timing and ultra-fast counting applications. BC-418 and BC-422 are recommended for use in small sizes, i.e. when any dimension is less than 4" (100mm). BC-420 is substantially less expensive than BC-418.

Scintillation Properties –

	BC-418	BC-420	BC-422
Light Output, % Anthracene	67	64	55
Rise Time, ns	0.5	0.5	0.35
Decay Time, ns	1.4	1.5	1.6
Pulse Width, FWHM, ns	1.2	1.3	1.3
Wavelength of Max. Emission, nm	391	391	370
Light Attenuation Length, cm*	NA**	140	NA**
Bulk Light Attenuation Length, cm	100	110	8

Atomic Composition –

No. H Atoms per cm ³ (x10 ²³)	5.21	5.21	5.19
No. C Atoms per cm ³ (x10 ²³)	4.74	4.74	4.71
Ratio (H:C) Atoms	1.100	1.100	1.102
No. of Electrons per cm ³ (x10 ²³)	3.37	3.37	3.34

* The typical 1/e attenuation length of a 1x20x200cm cast sheet with edges polished as measured with a bialkali photomultiplier tube coupled to one end.

** Scintillator recommended for use in small sizes; therefore, the 1/e attenuation length values are not applicable.

General Technical Data –

Base Polyvinyltoluene

Density 1.032 g/cc

Refractive Index 1.58

Coefficient of Linear Expansion
..... 7.8x10⁻⁵ below 67°C

Light Output Temperature Dependence:
at +60°C = 95% of that at +20°C; independent
of temperature from -60°C to +20°C

Vapor Pressure . May be used in a vacuum

Solubility Soluble in aromatic
solvents, chlorine, acetone, etc. Insoluble
in water, dilute acids, lower alcohols,
silicone fluid, grease and alkalis.



SAINT-GOBAIN
CRYSTALS

Scintillation Products
Organic Scintillators



USA

Saint-Gobain Crystals
12345 Kinsman Road
Newbury, OH 44065
Tel: (440) 564-2251
Fax: (440) 564-8047

Europe

Saint-Gobain Crystals
104 Route de Larchant
BP 521
77794 Nemours Cedex, France
Tel: 33 (1) 64 45 10 10
Fax: 33 (1) 64 45 10 01

P.O. Box 3093
3760 DB Soest
The Netherlands
Tel: 31 35 60 29 700
Fax: 31 35 60 29 214

Japan

Saint-Gobain KK, Crystals Division
3-7, Kojimachi, Chiyoda-ku,
Tokyo 102-0083 Japan
Tel: 81 (0) 3 3263 0559
Fax: 81 (0) 3 5212 2196

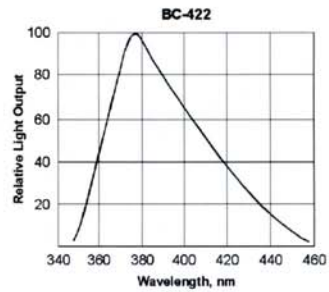
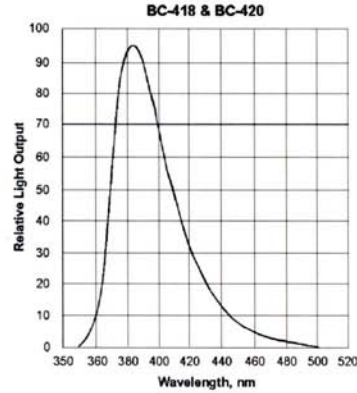
China

Saint-Gobain (China) Investment Co.,
Ltd.
15-01 CITIC Building
19 Jianguomenwai Ave.
Beijing 100004 China
Tel: 86 (0) 10 6513 0311
Fax: 86 (0) 10 6512 9843

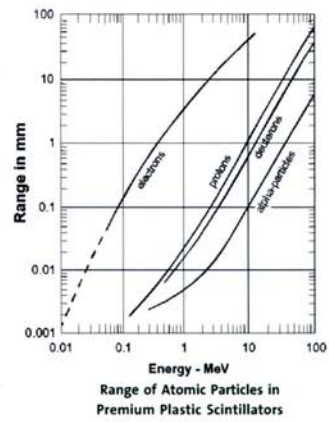
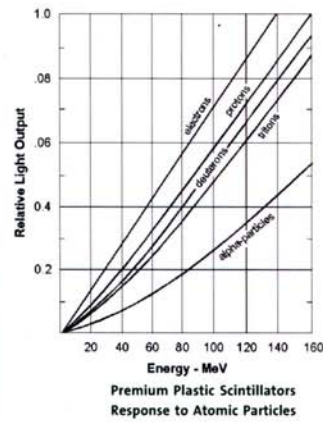
www.detectors.saint-gobain.com

**BC-418, BC-420, BC-422
Premium
Plastic Scintillators**

Emission Spectra –



Atomic Particles Response –



Manufacturer reserves the right to alter specifications.
©2005 Saint-Gobain Ceramics & Plastics, Inc. All rights reserved.

(10-05)

Bicron 422Q Specification Sheet

BC-422Q Ultra-fast Timing Plastic Scintillator

BC-422Q premium plastic scintillator is intended for use in ultra-fast timing and ultra-fast counting applications. It is quenched with various weight percentages of benzophenone (specified at time of order) to improve timing properties. The faster timing comes at the expense of total light output, however.

Scintillation Properties –

	Weight % Benzophenone					
	None*	0.5	1.0	2.0	3.0	5.0
Light Output, %Anthracene	55	19	11	5	4	3
Rise Time, ps	350	110	105	100	100	100
Decay Time, ns	1.6	0.7	0.7	0.7	0.7	0.7
Pulse Width, FWHM, ps	1300	360	290	260	240	220

*BC-422

General Technical Data –

Base Polyvinyltoluene
 Density 1.032 g/cc
 Refractive Index 1.58
 Ratio H:C Atoms ~1.1
 Coefficient of Linear Expansion
 7.8×10^{-5} below 67°C
 Light Output Temperature Dependence
 at +60°C = 95% of that at +20°C; independent of temperature from -60°C to +20°C
 Vapor Pressure May be used in a vacuum
 Solubility Soluble in aromatic solvents, chlorine, acetone, etc. Insoluble in water, dilute acids, lower alcohols, silicone fluid, grease and alkalis.
 Softening Point 70°C



SAINT-GOBAIN
CRYSTALS

Scintillation Products
Organic Scintillators



USA

Saint-Gobain Crystals
12345 Kinsman Road
Newbury, OH 44065
Tel: (440) 564-2251
Fax: (440) 564-8047

Europe

Saint-Gobain Crystals
104 Route de Larchant
BP 521
77794 Nemours Cedex, France
Tel: 33 (1) 64 45 10 10
Fax: 33 (1) 64 45 10 01

P.O. Box 3093
3760 DB Soest
The Netherlands
Tel: 31 35 60 29 700
Fax: 31 35 60 29 214

Japan

Saint-Gobain KK, Crystals Division
3-7, Kojimachi, Chiyoda-ku,
Tokyo 102-0083 Japan
Tel: 81 (0) 3 3263 0559
Fax: 81 (0) 3 5212 2196

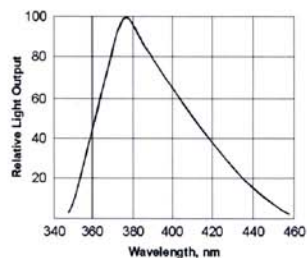
China

Saint-Gobain (China) Investment Co., Ltd.
15-01 CITIC Building
19 Jianguomenwai Ave.
Beijing 100004 China
Tel: 86 (0) 10 6513 0311
Fax: 86 (0) 10 6512 9843

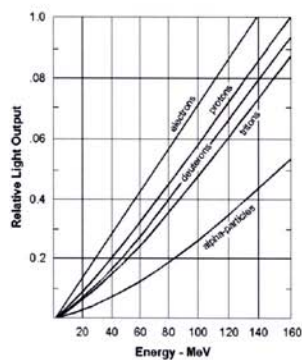
www.detectors.saint-gobain.com

BC-422Q Ultra-fast Timing Plastic Scintillator

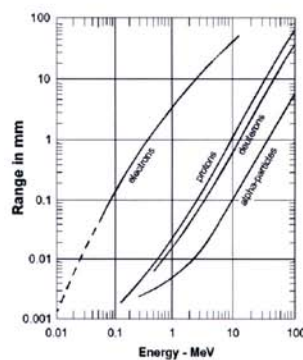
Emission Spectra –



Atomic Particles Response –



Premium Plastic Scintillators
Response to Atomic Particles



Range of Atomic Particles in
Premium Plastic Scintillators

Manufacturer reserves the right to alter specifications.
©2005 Saint-Gobain Ceramics & Plastics, Inc. All rights reserved.

(01-05)

APPENDIX D

Basic Error Analysis

To compare computational results with experimental results, basic error analysis methods need to be understood. MCNPX calculates relative error for the one sigma (68%) standard deviation of the mean. When the uncertainties in a calculation are random and independent, there are four main ways for the uncertainties in the measurement or calculation to progress. Sums and differences will be discussed first. For example, consider the following sum:

$$q = (x + \dots + z) - (u + \dots + w)$$

We will also assume that x, \dots, z, u, \dots, w have corresponding uncertainties of $dx, \dots, dz, du, \dots, dw$. Provided that all uncertainties are random and independent, the associated uncertainty of the value of q is dq . The definition of dq is as follows:

$$dq = \sqrt{dx^2 + \dots + dz^2 + du^2 + \dots + dw^2}$$

This method is commonly known as propagation of error in quadrature. One must take care that

$$dz \leq dx + \dots + dz + du + \dots + dw.$$

In the case of products and quotients, we see the uncertainties propagate slightly differently. Let's assume that x, \dots, z, u, \dots, w all have the same uncertainties as above. If this time we would like to find

$$q = \frac{x * \dots * z}{u * \dots * w},$$

the uncertainty in q , dq , will be

$$dq = |q| \sqrt{\left(\frac{dx}{x}\right)^2 + \dots + \left(\frac{dz}{z}\right)^2 + \left(\frac{du}{u}\right)^2 + \dots + \left(\frac{dw}{w}\right)^2}.$$

Again, the rule for dq is

$$dq \leq |q| * \left(\frac{dx}{x} + \dots + \frac{dz}{z} + \frac{du}{u} + \dots + \frac{dw}{w} \right).$$

If the case arises where we are trying to find quantity q if B is absolute known, then

$$q = Bx .$$

The uncertainty in this calculation would be

$$dq = |B|dx .$$

If we are using exact numbers for powers, and n is the exact number, then

$$q = x^n ,$$

with the uncertainty in q being

$$dq = |q| * \left(|n| * \frac{dx}{|x|} \right).$$

With these simple methods to propagate random and independent errors, comparison between computational results and experimental results from OMEGA can be made.

APPENDIX E

Truncated MCNPX Output Files


```

67-      C +-----+
68-      C |
69-      C |                               Data Card
70-      C |
71-      C +-----+
72-      C *****
73-      C * Source Definition
74-      C * +-----+
75-      C * | 4.4 keV Gaussian Neutron Source | *
76-      C * | Perpendicular Beam              | *
77-      C * | Radius = 7.62 cm                | *
78-      C * | Center = 0.0, 0.0, 0.0         | *
79-      C * | Direction = +Y                  | *
80-      C * +-----+
81-      C *****
82-      sdef par=1 erg=d1 sur=4 rad=d2 vec=0 1 0 dir=1 pos=0.0 0.0 0.0
83-      sp1 -4 -0.0044 -2
84-      si2 0 7.6199
85-      sp2 0 1
86-      C +-----+
87-      C |
88-      C |                               Material Card
89-      C |
90-      C +-----+
91-      C *****
92-      C * Plastic Scintillator (Mass Density = 1.032 gm/cc) *
93-      C *****
94-      m1 1001 1.0 6012 1.0
95-      C *****
96-      C * Natural Aluminum (Mass Density = 2.699 g/cc) *
97-      C *****
98-      m2 13027 -1.0
99-      C +-----+
100-     C |
101-     C |                               Tally Card
102-     C |
103-     C +-----+
104-     C *****
105-     C * Energy Deposition Tally (Type 6) *
106-     C *****
107-     f6:n 2
108-     C 0.2 ns time binning
109-     t6 20.0 499i 30.0
110-     fq6 t s
111-     C +-----+
112-     C |
113-     C |                               Control Card
114-     C |
115-     C +-----+
116-     C *****
117-     C * Number of Source Particles *
118-     C *****
119-     nps 20000000
120-     C *****
121-     C * Output Options *
122-     C *****
123-     print -30

```

probability distribution 1 for source variable erg
energy function 4: gaussian (fusion) spectrum

$$f(e) = c * \exp(-((e-b)/a)**2)$$

fusion temperature	fusion width(a)	fusion energy(b)	fusion constant(c)	fusion fwhm
4.4000E-03	1.0421E-01	2.4637E+00	5.4138E+00	1.7353E-01

the mean of source distribution 1 is 2.4637E+00

warning. source variable rad is sampled uniformly.

probability distribution 2 for source variable rad
 unbiased histogram distribution

source entry	source value	cumulative probability	probability of bin
1	0.00000E+00	0.000000E+00	0.000000E+00
2	7.61990E+00	1.000000E+00	1.000000E+00

the mean of source distribution 2 is 3.8100E+00

print table 126

average weight (relative)	tracks average cell track mfp (cm)	population	collisions entering	collisions * weight (per history)	number weighted energy	flux weighted energy	track
1.0000E+00	1 20351131	20000000	0	0.0000E+00	2.4614E+00	2.4634E+00	
9.9999E-01	2 10030697	9906946	748408	3.7420E-02	2.0548E+00	2.3532E+00	
9.9999E-01	3 4.8577E+00	10833857	675837	3.3792E-02	2.2505E+00	2.4046E+00	
9.9999E-01	4 11075411	877610	50696	2.5348E-03	2.2598E+00	2.3998E+00	
9.9999E-01	5 882945	10532452	669890	3.3494E-02	2.0877E+00	2.3383E+00	
9.9999E-01	6 5.8291E+00	9329975	0	0.0000E+00	2.3940E+00	2.4453E+00	
1.0000E+00	0.0000E+00						
	total	62213895	61480840	2144831	1.0724E-01		

ltally 6 nps = 20000000
 tally type 6 track length estimate of heating. units mev/gram
 particle(s): neutron

masses
 cell: 2
 1.49425E+01

cell 2

time		
2.4000E+01	0.00000E+00	0.0000
2.4020E+01	0.00000E+00	0.0000
2.4040E+01	0.00000E+00	0.0000
2.4060E+01	1.05381E-10	1.0000
2.4080E+01	1.14082E-10	1.0000
2.4100E+01	0.00000E+00	0.0000
2.4120E+01	0.00000E+00	0.0000
2.4140E+01	1.49035E-10	1.0000
2.4160E+01	1.35725E-10	0.6983
2.4180E+01	4.47489E-10	0.6163
2.4200E+01	3.01433E-10	0.7093
2.4220E+01	1.59561E-10	0.5234
2.4240E+01	1.21691E-09	0.3772
2.4260E+01	8.98404E-10	0.3727
2.4280E+01	2.61083E-09	0.2686
2.4300E+01	3.55494E-09	0.2179
2.4320E+01	3.79792E-09	0.2118
2.4340E+01	4.64392E-09	0.1918
2.4360E+01	7.57626E-09	0.1538
2.4380E+01	7.07151E-09	0.1523
2.4400E+01	8.79259E-09	0.1423
2.4420E+01	1.03777E-08	0.1296
2.4440E+01	1.30030E-08	0.1119

2.4460E+01	1.90400E-08	0.0929
2.4480E+01	1.89405E-08	0.0908
2.4500E+01	2.64187E-08	0.0781
2.4520E+01	3.38648E-08	0.0675
2.4540E+01	4.52564E-08	0.0585
2.4560E+01	5.54066E-08	0.0539
2.4580E+01	6.03693E-08	0.0516
2.4600E+01	7.74864E-08	0.0454
2.4620E+01	1.05363E-07	0.0392
2.4640E+01	1.26819E-07	0.0353
2.4660E+01	1.65893E-07	0.0311
2.4680E+01	1.92751E-07	0.0287
2.4700E+01	2.25687E-07	0.0264
2.4720E+01	2.82621E-07	0.0237
2.4740E+01	3.28796E-07	0.0218
2.4760E+01	4.10197E-07	0.0196
2.4780E+01	4.73217E-07	0.0182
2.4800E+01	5.66395E-07	0.0167
2.4820E+01	6.66965E-07	0.0153
2.4840E+01	8.03834E-07	0.0139
2.4860E+01	9.64814E-07	0.0127
2.4880E+01	1.10017E-06	0.0119
2.4900E+01	1.26211E-06	0.0111
2.4920E+01	1.51631E-06	0.0102
2.4940E+01	1.75300E-06	0.0094
2.4960E+01	2.02130E-06	0.0088
2.4980E+01	2.32414E-06	0.0082
2.5000E+01	2.64417E-06	0.0077
2.5020E+01	3.04815E-06	0.0071
2.5040E+01	3.50567E-06	0.0066
2.5060E+01	3.95424E-06	0.0062
2.5080E+01	4.45134E-06	0.0059
2.5100E+01	5.00096E-06	0.0055
2.5120E+01	5.61260E-06	0.0052
2.5140E+01	6.25787E-06	0.0049
2.5160E+01	7.04189E-06	0.0047
2.5180E+01	7.73275E-06	0.0044
2.5200E+01	8.54691E-06	0.0042
2.5220E+01	9.47947E-06	0.0040
2.5240E+01	1.05365E-05	0.0038
2.5260E+01	1.15166E-05	0.0036
2.5280E+01	1.25860E-05	0.0035
2.5300E+01	1.36650E-05	0.0033
2.5320E+01	1.47898E-05	0.0032
2.5340E+01	1.60956E-05	0.0031
2.5360E+01	1.73631E-05	0.0030
2.5380E+01	1.87077E-05	0.0028
2.5400E+01	2.00598E-05	0.0027
2.5420E+01	2.13059E-05	0.0027
2.5440E+01	2.26020E-05	0.0026
2.5460E+01	2.39235E-05	0.0025
2.5480E+01	2.53643E-05	0.0024
2.5500E+01	2.67378E-05	0.0024
2.5520E+01	2.81655E-05	0.0023
2.5540E+01	2.93550E-05	0.0023
2.5560E+01	3.08052E-05	0.0022
2.5580E+01	3.20622E-05	0.0022
2.5600E+01	3.34634E-05	0.0021
2.5620E+01	3.44842E-05	0.0021
2.5640E+01	3.58189E-05	0.0020
2.5660E+01	3.69387E-05	0.0020
2.5680E+01	3.79308E-05	0.0020
2.5700E+01	3.88619E-05	0.0020
2.5720E+01	3.97713E-05	0.0019
2.5740E+01	4.04604E-05	0.0019
2.5760E+01	4.12016E-05	0.0019
2.5780E+01	4.15801E-05	0.0019
2.5800E+01	4.16984E-05	0.0019
2.5820E+01	4.19866E-05	0.0019
2.5840E+01	4.21219E-05	0.0019
2.5860E+01	4.21325E-05	0.0019

2.5880E+01	4.19867E-05	0.0019
2.5900E+01	4.14599E-05	0.0019
2.5920E+01	4.11915E-05	0.0019
2.5940E+01	4.07425E-05	0.0019
2.5960E+01	4.02159E-05	0.0019
2.5980E+01	3.95812E-05	0.0019
2.6000E+01	3.89143E-05	0.0019
2.6020E+01	3.81792E-05	0.0019
2.6040E+01	3.72548E-05	0.0020
2.6060E+01	3.62489E-05	0.0020
2.6080E+01	3.53903E-05	0.0020
2.6100E+01	3.43363E-05	0.0020
2.6120E+01	3.32878E-05	0.0021
2.6140E+01	3.21984E-05	0.0021
2.6160E+01	3.10601E-05	0.0021
2.6180E+01	2.98428E-05	0.0022
2.6200E+01	2.86404E-05	0.0022
2.6220E+01	2.73627E-05	0.0023
2.6240E+01	2.61517E-05	0.0023
2.6260E+01	2.49716E-05	0.0024
2.6280E+01	2.36371E-05	0.0025
2.6300E+01	2.24045E-05	0.0025
2.6320E+01	2.10968E-05	0.0026
2.6340E+01	1.98689E-05	0.0027
2.6360E+01	1.87564E-05	0.0028
2.6380E+01	1.76570E-05	0.0028
2.6400E+01	1.64286E-05	0.0029
2.6420E+01	1.53074E-05	0.0030
2.6440E+01	1.43032E-05	0.0032
2.6460E+01	1.34045E-05	0.0033
2.6480E+01	1.24463E-05	0.0034
2.6500E+01	1.15965E-05	0.0035
2.6520E+01	1.07073E-05	0.0036
2.6540E+01	9.83253E-06	0.0038
2.6560E+01	9.03013E-06	0.0040
2.6580E+01	8.38604E-06	0.0041
2.6600E+01	7.65764E-06	0.0043
2.6620E+01	7.07994E-06	0.0045
2.6640E+01	6.41899E-06	0.0047
2.6660E+01	5.85642E-06	0.0049
2.6680E+01	5.26941E-06	0.0052
2.6700E+01	4.83448E-06	0.0054
2.6720E+01	4.40816E-06	0.0057
2.6740E+01	4.02739E-06	0.0059
2.6760E+01	3.60943E-06	0.0062
2.6780E+01	3.21892E-06	0.0066
2.6800E+01	2.89920E-06	0.0070
2.6820E+01	2.61764E-06	0.0073
2.6840E+01	2.34614E-06	0.0078
2.6860E+01	2.08687E-06	0.0082
2.6880E+01	1.86236E-06	0.0087
2.6900E+01	1.66304E-06	0.0092
2.6920E+01	1.49016E-06	0.0097
2.6940E+01	1.30934E-06	0.0103
2.6960E+01	1.17096E-06	0.0110
2.6980E+01	1.03908E-06	0.0116
2.7000E+01	9.10174E-07	0.0124
2.7020E+01	7.83345E-07	0.0133
2.7040E+01	7.04812E-07	0.0140
2.7060E+01	6.32474E-07	0.0149
2.7080E+01	5.54946E-07	0.0159
2.7100E+01	4.64363E-07	0.0173
2.7120E+01	4.21267E-07	0.0182
2.7140E+01	3.51505E-07	0.0196
2.7160E+01	3.19616E-07	0.0209
2.7180E+01	2.69674E-07	0.0227
2.7200E+01	2.37618E-07	0.0242
2.7220E+01	1.95984E-07	0.0263
2.7240E+01	1.71858E-07	0.0283
2.7260E+01	1.54948E-07	0.0298
2.7280E+01	1.31196E-07	0.0321

2.7300E+01	1.23575E-07	0.0336
2.7320E+01	9.56940E-08	0.0375
2.7340E+01	8.94358E-08	0.0389
2.7360E+01	7.78128E-08	0.0416
2.7380E+01	6.61561E-08	0.0451
2.7400E+01	5.37889E-08	0.0499
2.7420E+01	4.62674E-08	0.0531
2.7440E+01	4.33327E-08	0.0557
2.7460E+01	3.47886E-08	0.0615
2.7480E+01	2.88830E-08	0.0684
2.7500E+01	2.12376E-08	0.0788
2.7520E+01	2.06199E-08	0.0792
2.7540E+01	1.98901E-08	0.0809
2.7560E+01	1.56155E-08	0.0912
2.7580E+01	1.21427E-08	0.1026
2.7600E+01	1.16526E-08	0.1058
2.7620E+01	7.13840E-09	0.1288
2.7640E+01	6.82195E-09	0.1366
2.7660E+01	5.96421E-09	0.1456
2.7680E+01	5.49755E-09	0.1513
2.7700E+01	3.58835E-09	0.1858
2.7720E+01	4.77556E-09	0.1719
2.7740E+01	4.61014E-09	0.1699
2.7760E+01	3.07307E-09	0.1906
2.7780E+01	3.39605E-09	0.1940
2.7800E+01	2.14571E-09	0.2272
2.7820E+01	2.02327E-09	0.2417
2.7840E+01	1.68946E-09	0.2426
2.7860E+01	2.11262E-09	0.2329
2.7880E+01	1.50556E-09	0.2672
2.7900E+01	1.16818E-09	0.2964
2.7920E+01	1.24303E-09	0.2993
2.7940E+01	8.51706E-10	0.3035
2.7960E+01	5.81037E-10	0.2800
2.7980E+01	2.91897E-10	0.1345
2.8000E+01	5.52585E-10	0.4018
2.8020E+01	4.64769E-10	0.3866
2.8040E+01	5.05477E-10	0.4257
2.8060E+01	2.36125E-10	0.1884
2.8080E+01	2.19077E-10	0.1510
2.8100E+01	2.13431E-10	0.1580
2.8120E+01	2.01850E-10	0.1643
2.8140E+01	1.97296E-10	0.1677
2.8160E+01	1.92864E-10	0.1620
2.8180E+01	1.68523E-10	0.1617
2.8200E+01	1.35816E-10	0.1166
2.8220E+01	1.20111E-10	0.1108
2.8240E+01	1.13530E-10	0.1132
2.8260E+01	1.05291E-10	0.1125
2.8280E+01	2.44749E-10	0.5647
2.8300E+01	1.43614E-10	0.2970
2.8320E+01	9.62170E-11	0.1303
2.8340E+01	9.34873E-11	0.1306
2.8360E+01	8.36481E-11	0.1308
2.8380E+01	7.70023E-11	0.1324
2.8400E+01	7.60887E-11	0.1330
2.8420E+01	7.30506E-11	0.1328
2.8440E+01	7.01372E-11	0.1322
2.8460E+01	6.82505E-11	0.1358
2.8480E+01	5.87982E-11	0.1104
2.8500E+01	5.41862E-11	0.1107
2.8520E+01	5.40487E-11	0.1126
2.8540E+01	5.32019E-11	0.1151
2.8560E+01	5.21775E-11	0.1183
2.8580E+01	4.93077E-11	0.1174
2.8600E+01	4.72305E-11	0.1182
2.8620E+01	4.62926E-11	0.1186
2.8640E+01	4.39263E-11	0.1199
2.8660E+01	4.24317E-11	0.1224
2.8680E+01	4.13044E-11	0.1247
2.8700E+01	4.02844E-11	0.1265

2.8720E+01	3.97823E-11	0.1283
2.8740E+01	3.68467E-11	0.1280
2.8760E+01	3.44035E-11	0.1238
2.8780E+01	3.18776E-11	0.1232
2.8800E+01	3.08131E-11	0.1265
2.8820E+01	3.06115E-11	0.1273
2.8840E+01	2.87453E-11	0.1227
2.8860E+01	2.67621E-11	0.1266
2.8880E+01	2.54786E-11	0.1288
2.8900E+01	2.37049E-11	0.1344
2.8920E+01	2.33024E-11	0.1356
2.8940E+01	2.32999E-11	0.1372
2.8960E+01	2.44670E-11	0.1551
2.8980E+01	2.30929E-11	0.1545
2.9000E+01	2.25199E-11	0.1558
2.9020E+01	2.21865E-11	0.1581
2.9040E+01	2.18556E-11	0.1604
2.9060E+01	2.14651E-11	0.1615
2.9080E+01	2.04020E-11	0.1652
2.9100E+01	2.05922E-11	0.1643
2.9120E+01	2.03881E-11	0.1659
2.9140E+01	2.02747E-11	0.1668
2.9160E+01	2.03351E-11	0.1665
2.9180E+01	1.95653E-11	0.1484
2.9200E+01	1.88737E-11	0.1444
2.9220E+01	1.86349E-11	0.1463
2.9240E+01	1.86982E-11	0.1459
2.9260E+01	1.78065E-11	0.1486
2.9280E+01	1.71386E-11	0.1521
2.9300E+01	1.68217E-11	0.1543
2.9320E+01	1.65596E-11	0.1564
2.9340E+01	1.60617E-11	0.1522
2.9360E+01	1.36898E-11	0.1399
2.9380E+01	1.30659E-11	0.1443
2.9400E+01	1.24715E-11	0.1392
2.9420E+01	1.20009E-11	0.1420
2.9440E+01	1.18799E-11	0.1433
2.9460E+01	1.18077E-11	0.1440
2.9480E+01	1.16754E-11	0.1454
2.9500E+01	1.14911E-11	0.1474
2.9520E+01	1.13551E-11	0.1490
2.9540E+01	1.11460E-11	0.1508
2.9560E+01	1.06322E-11	0.1539
2.9580E+01	1.09730E-11	0.1564
2.9600E+01	1.08148E-11	0.1577
2.9620E+01	1.05003E-11	0.1594
2.9640E+01	1.04472E-11	0.1602
2.9660E+01	1.06774E-11	0.1594
2.9680E+01	1.07656E-11	0.1603
2.9700E+01	1.02278E-11	0.1618
2.9720E+01	9.84942E-12	0.1655
2.9740E+01	9.53443E-12	0.1681
2.9760E+01	9.87983E-12	0.1684
2.9780E+01	9.83964E-12	0.1691
2.9800E+01	9.44587E-12	0.1715
2.9820E+01	9.20433E-12	0.1752
2.9840E+01	8.78051E-12	0.1793
2.9860E+01	8.16172E-12	0.1757
2.9880E+01	7.75339E-12	0.1812
2.9900E+01	7.67996E-12	0.1826
2.9920E+01	7.50366E-12	0.1852
2.9940E+01	7.32191E-12	0.1887
2.9960E+01	6.51192E-12	0.1915
2.9980E+01	6.28546E-12	0.1971
3.0000E+01	6.37419E-12	0.2012
total	2.02894E-03	0.0003

dump no. 2 on file runtpe nps = 2000000 coll = 2144831 ctm = 4.91
nrn = 142208338

6 warning messages so far.

run terminated when 20000000 particle histories were done.

computer time = 4.92 minutes

mcnp version 2.5e Mon Feb 23 09:00:00 MST 2004
= 04/20/05 14:14:04

04/20/05 14:17:10 probid

MCNPX Output File – Light Guide

```

1- Scintillator Broadening Deck
2- C
3- C PROBLEM DESCRIPTION
4- C One-eighth inch thick scintillator at a distance of 5.6 meters
5- C from the source. Including the light guides out to 4.5 inches
6- C from the scintillator. This represents the OMEGA geometry.
7- C See page 67 of MS thesis notebook.
8- C
9- C 345678901234567890123456789012345678901234567890123456789012
10- C 1 2 3 4 5 6 7
11- C
12- C +-----+
13- C | |
14- C | | Geometry Card |
15- C | |
16- C +-----+
17- C *****
18- C * Source Void *
19- C *****
20- C 1 0 -2 3 -4
21- C *****
22- C * Scintillator *
23- C *****
24- C 2 1 -1.032 -1 4 -5
25- C *****
26- C * Light Guide *
27- C *****
28- C 3 1 -1.032 -2 1 -5 4
29- C *****
30- C * Particle Death *
31- C *****
32- C 999 0 2:-3:5
33- C
34- C +-----+
35- C | |
36- C | | Surface Card |
37- C | |
38- C +-----+
39- C *****
40- C * Global Surfaces *
41- C *****
42- C 1 cy 3.8100
43- C 2 cy 15.2400
44- C 3 py 0.0000
45- C *****
46- C * Scintillator Planes *
47- C *****
48- C 4 py 560.0000
49- C 5 py 560.3175
50- C
51- C *****
52- C * Importance Function *
53- C *****
54- C imp:n 1 1 1 0
55- C +-----+
56- C | |
57- C | | Data Card |
58- C | |
59- C +-----+
60- C *****
61- C * Source Definition *
62- C * +-----+ *
63- C * | 4.4 keV Gaussian Neutron Source | *
64- C * | Perpendicular Beam | *
65- C * | Radius = 15.24 cm | *
66- C * | Center = 0.0, 0.0, 0.0 | *

```



```

67-      C * | Direction = +Y          | *
68-      C * +-----+ *
69-      C *****
70-      sdef par=1 erg=d1 sur=3 rad=d2 vec=0 1 0 dir=1 pos=0.0 0.0 0.0
71-      sp1 -4 -0.0044 -2
72-      si2 0 15.2399
73-      sp2 0 1
74-      C +-----+
75-      C |
76-      C |                               Material Card
77-      C |
78-      C +-----+
79-      C *****
80-      C * Plastic Scintillator (Mass Density = 1.032 gm/cc) *
81-      C *****
82-      m1 1001 1.0 6012 1.0
83-      C +-----+
84-      C |
85-      C |                               Tally Card
86-      C |
87-      C +-----+
88-      C *****
89-      C * Energy Deposition Tally (Type 6) *
90-      C *****
91-      f6:n 2
92-      C 0.2 ns time binning
93-      t6 20.0 499i 30.0
94-      fq6 t s
95-      C Flag neutrons entering from light guide
96-      cf6 3
97-      C +-----+
98-      C |
99-      C |                               Control Card
100-     C |
101-     C +-----+
102-     C *****
103-     C * Number of Source Particles *
104-     C *****
105-     nps 20000000
106-     C *****
107-     C * Output Options *
108-     C *****
109-     print -30

```

probability distribution 1 for source variable erg
energy function 4: gaussian (fusion) spectrum

$$f(e)=c*\exp(-((e-b)/a)**2)$$

fusion temperature	fusion width(a)	fusion energy(b)	fusion constant(c)	fusion fwhm
4.4000E-03	1.0421E-01	2.4637E+00	5.4138E+00	1.7353E-01

the mean of source distribution 1 is 2.4637E+00

warning. source variable rad is sampled uniformly.

probability distribution 2 for source variable rad
unbiased histogram distribution

source entry	source value	cumulative probability	probability of bin
1	0.00000E+00	0.000000E+00	0.000000E+00
2	1.52399E+01	1.000000E+00	1.000000E+00

the mean of source distribution 2 is 7.6200E+00

print table 126

average	tracks	population	collisions	collisions	number	flux	
weight	average			* weight	weighted	weighted	
(relative)	cell	entering		(per history)	energy	energy	
	track	mfp				track	
	(cm)						
1	1	20251699	20000000	0	0.0000E+00	2.4592E+00	2.4632E+00
1.0000E+00	0.0000E+00						
2	2	5010556	5010415	349990	1.7499E-02	2.1200E+00	2.3893E+00
1.0000E+00	4.9033E+00						
3	3	15006581	15006248	1053622	5.2681E-02	2.1152E+00	2.3879E+00
1.0000E+00	4.9012E+00						
total		40268836	40016663	1403612	7.0180E-02		

ltally 6 nps = 20000000
tally type 6 track length estimate of heating. units mev/gram
particle(s): neutron
flagging cells: 3

masses
cell: 2
1.49425E+01

cell 2
time

2.4000E+01	0.00000E+00	0.0000
2.4020E+01	0.00000E+00	0.0000
2.4040E+01	2.80772E-12	1.0000
2.4060E+01	2.16655E-10	1.0000
2.4080E+01	0.00000E+00	0.0000
2.4100E+01	0.00000E+00	0.0000
2.4120E+01	0.00000E+00	0.0000
2.4140E+01	0.00000E+00	0.0000
2.4160E+01	2.17675E-10	1.0000
2.4180E+01	2.18424E-10	1.0000
2.4200E+01	0.00000E+00	0.0000
2.4220E+01	6.18215E-10	0.5777
2.4240E+01	3.58584E-10	0.6517
2.4260E+01	9.49886E-10	0.4125
2.4280E+01	1.22955E-09	0.3276
2.4300E+01	2.51089E-09	0.2610
2.4320E+01	1.75593E-09	0.2960
2.4340E+01	1.95703E-09	0.2503
2.4360E+01	4.22932E-09	0.1944
2.4380E+01	3.73697E-09	0.2106
2.4400E+01	4.79439E-09	0.1858
2.4420E+01	5.44120E-09	0.1666
2.4440E+01	8.64487E-09	0.1346
2.4460E+01	8.32109E-09	0.1374
2.4480E+01	1.15055E-08	0.1220
2.4500E+01	1.42352E-08	0.1071
2.4520E+01	2.04643E-08	0.0885
2.4540E+01	2.91541E-08	0.0748
2.4560E+01	3.12471E-08	0.0718
2.4580E+01	3.49829E-08	0.0669
2.4600E+01	5.13016E-08	0.0559
2.4620E+01	5.63308E-08	0.0524
2.4640E+01	7.80180E-08	0.0455
2.4660E+01	8.63990E-08	0.0424
2.4680E+01	1.03661E-07	0.0387
2.4700E+01	1.29436E-07	0.0348
2.4720E+01	1.50935E-07	0.0321
2.4740E+01	1.93795E-07	0.0285
2.4760E+01	2.25429E-07	0.0263
2.4780E+01	2.71955E-07	0.0240
2.4800E+01	3.13822E-07	0.0222
2.4820E+01	3.79568E-07	0.0202
2.4840E+01	4.54491E-07	0.0184
2.4860E+01	5.25043E-07	0.0171

2.4880E+01	5.94084E-07	0.0161
2.4900E+01	7.04600E-07	0.0148
2.4920E+01	8.14643E-07	0.0137
2.4940E+01	9.39767E-07	0.0127
2.4960E+01	1.10436E-06	0.0118
2.4980E+01	1.25212E-06	0.0110
2.5000E+01	1.45294E-06	0.0102
2.5020E+01	1.67851E-06	0.0095
2.5040E+01	1.88248E-06	0.0090
2.5060E+01	2.12078E-06	0.0085
2.5080E+01	2.33954E-06	0.0080
2.5100E+01	2.66738E-06	0.0075
2.5120E+01	2.94831E-06	0.0071
2.5140E+01	3.32344E-06	0.0067
2.5160E+01	3.65440E-06	0.0064
2.5180E+01	4.05966E-06	0.0061
2.5200E+01	4.52246E-06	0.0058
2.5220E+01	5.00405E-06	0.0055
2.5240E+01	5.43154E-06	0.0053
2.5260E+01	5.93043E-06	0.0050
2.5280E+01	6.49421E-06	0.0048
2.5300E+01	7.03156E-06	0.0046
2.5320E+01	7.57104E-06	0.0044
2.5340E+01	8.27454E-06	0.0042
2.5360E+01	8.82988E-06	0.0041
2.5380E+01	9.46971E-06	0.0040
2.5400E+01	1.00934E-05	0.0038
2.5420E+01	1.07616E-05	0.0037
2.5440E+01	1.14084E-05	0.0036
2.5460E+01	1.20783E-05	0.0035
2.5480E+01	1.27601E-05	0.0034
2.5500E+01	1.34871E-05	0.0033
2.5520E+01	1.39899E-05	0.0032
2.5540E+01	1.47300E-05	0.0032
2.5560E+01	1.52890E-05	0.0031
2.5580E+01	1.59890E-05	0.0030
2.5600E+01	1.65651E-05	0.0030
2.5620E+01	1.71269E-05	0.0029
2.5640E+01	1.76494E-05	0.0029
2.5660E+01	1.80068E-05	0.0028
2.5680E+01	1.85022E-05	0.0028
2.5700E+01	1.88218E-05	0.0028
2.5720E+01	1.91438E-05	0.0027
2.5740E+01	1.95271E-05	0.0027
2.5760E+01	1.98272E-05	0.0027
2.5780E+01	1.98986E-05	0.0027
2.5800E+01	2.00774E-05	0.0027
2.5820E+01	2.01595E-05	0.0027
2.5840E+01	2.02143E-05	0.0027
2.5860E+01	2.01467E-05	0.0027
2.5880E+01	2.00161E-05	0.0027
2.5900E+01	2.00308E-05	0.0027
2.5920E+01	1.97969E-05	0.0027
2.5940E+01	1.95824E-05	0.0027
2.5960E+01	1.93292E-05	0.0027
2.5980E+01	1.89783E-05	0.0027
2.6000E+01	1.85836E-05	0.0028
2.6020E+01	1.82336E-05	0.0028
2.6040E+01	1.76986E-05	0.0028
2.6060E+01	1.71907E-05	0.0029
2.6080E+01	1.66677E-05	0.0029
2.6100E+01	1.61075E-05	0.0030
2.6120E+01	1.55831E-05	0.0030
2.6140E+01	1.50447E-05	0.0031
2.6160E+01	1.44391E-05	0.0031
2.6180E+01	1.38495E-05	0.0032
2.6200E+01	1.32228E-05	0.0033
2.6220E+01	1.26374E-05	0.0033
2.6240E+01	1.20903E-05	0.0034
2.6260E+01	1.14945E-05	0.0035
2.6280E+01	1.08891E-05	0.0036

2.6300E+01	1.03130E-05	0.0037
2.6320E+01	9.67314E-06	0.0038
2.6340E+01	9.13790E-06	0.0039
2.6360E+01	8.59761E-06	0.0040
2.6380E+01	8.01599E-06	0.0042
2.6400E+01	7.47920E-06	0.0043
2.6420E+01	6.93660E-06	0.0045
2.6440E+01	6.49524E-06	0.0046
2.6460E+01	6.02423E-06	0.0048
2.6480E+01	5.60543E-06	0.0050
2.6500E+01	5.19383E-06	0.0052
2.6520E+01	4.73310E-06	0.0054
2.6540E+01	4.36944E-06	0.0057
2.6560E+01	4.00434E-06	0.0059
2.6580E+01	3.65930E-06	0.0062
2.6600E+01	3.40071E-06	0.0064
2.6620E+01	3.11870E-06	0.0067
2.6640E+01	2.81031E-06	0.0070
2.6660E+01	2.52983E-06	0.0074
2.6680E+01	2.30096E-06	0.0077
2.6700E+01	2.11879E-06	0.0081
2.6720E+01	1.91639E-06	0.0085
2.6740E+01	1.73601E-06	0.0089
2.6760E+01	1.54955E-06	0.0094
2.6780E+01	1.39970E-06	0.0099
2.6800E+01	1.23700E-06	0.0105
2.6820E+01	1.10513E-06	0.0112
2.6840E+01	9.86381E-07	0.0118
2.6860E+01	8.95116E-07	0.0124
2.6880E+01	8.00765E-07	0.0131
2.6900E+01	6.94257E-07	0.0140
2.6920E+01	6.16910E-07	0.0148
2.6940E+01	5.52093E-07	0.0157
2.6960E+01	4.83212E-07	0.0168
2.6980E+01	4.28550E-07	0.0178
2.7000E+01	3.62537E-07	0.0193
2.7020E+01	3.25527E-07	0.0204
2.7040E+01	2.95143E-07	0.0214
2.7060E+01	2.58525E-07	0.0228
2.7080E+01	2.17476E-07	0.0250
2.7100E+01	1.88487E-07	0.0269
2.7120E+01	1.62050E-07	0.0289
2.7140E+01	1.46239E-07	0.0307
2.7160E+01	1.29566E-07	0.0324
2.7180E+01	1.07509E-07	0.0352
2.7200E+01	9.42290E-08	0.0377
2.7220E+01	8.02078E-08	0.0409
2.7240E+01	6.98777E-08	0.0434
2.7260E+01	6.25496E-08	0.0459
2.7280E+01	5.82489E-08	0.0485
2.7300E+01	4.20937E-08	0.0552
2.7320E+01	4.19253E-08	0.0565
2.7340E+01	3.55928E-08	0.0605
2.7360E+01	3.12512E-08	0.0648
2.7380E+01	2.55684E-08	0.0717
2.7400E+01	2.05686E-08	0.0799
2.7420E+01	1.92943E-08	0.0832
2.7440E+01	1.60362E-08	0.0888
2.7460E+01	1.40722E-08	0.0971
2.7480E+01	8.91607E-09	0.1170
2.7500E+01	8.69720E-09	0.1158
2.7520E+01	1.00857E-08	0.1121
2.7540E+01	7.02801E-09	0.1343
2.7560E+01	5.43700E-09	0.1550
2.7580E+01	5.06461E-09	0.1619
2.7600E+01	2.96855E-09	0.1991
2.7620E+01	2.39323E-09	0.2270
2.7640E+01	2.13045E-09	0.2407
2.7660E+01	2.67423E-09	0.2289
2.7680E+01	1.11348E-09	0.3167
2.7700E+01	1.43892E-09	0.3167

2.7720E+01	2.06686E-09	0.2631
2.7740E+01	8.03833E-10	0.3049
2.7760E+01	1.26837E-09	0.3256
2.7780E+01	4.97221E-10	0.5131
2.7800E+01	5.63960E-10	0.4538
2.7820E+01	4.11602E-10	0.4523
2.7840E+01	9.19739E-10	0.3817
2.7860E+01	4.12335E-10	0.5194
2.7880E+01	7.30076E-11	0.2630
2.7900E+01	6.68751E-11	0.2264
2.7920E+01	7.89930E-11	0.2624
2.7940E+01	2.25893E-10	0.7266
2.7960E+01	6.05348E-11	0.2466
2.7980E+01	2.30024E-10	0.7522
2.8000E+01	6.25319E-11	0.2507
2.8020E+01	2.31217E-10	0.7758
2.8040E+01	5.00234E-11	0.2417
2.8060E+01	4.79659E-11	0.2504
2.8080E+01	2.23878E-10	0.7923
2.8100E+01	5.02678E-11	0.2492
2.8120E+01	4.59236E-11	0.2610
2.8140E+01	3.87671E-11	0.2440
2.8160E+01	3.33535E-11	0.2187
2.8180E+01	2.58208E-11	0.1194
2.8200E+01	2.53251E-11	0.1203
2.8220E+01	2.46762E-11	0.1204
2.8240E+01	2.30087E-11	0.1251
2.8260E+01	1.15873E-10	0.8057
2.8280E+01	1.06809E-10	0.7956
2.8300E+01	2.10855E-11	0.1330
2.8320E+01	2.05067E-11	0.1344
2.8340E+01	2.00301E-11	0.1370
2.8360E+01	1.97040E-11	0.1389
2.8380E+01	1.91551E-11	0.1422
2.8400E+01	1.89510E-11	0.1435
2.8420E+01	1.86150E-11	0.1453
2.8440E+01	1.80866E-11	0.1485
2.8460E+01	1.77182E-11	0.1511
2.8480E+01	1.73525E-11	0.1537
2.8500E+01	1.69949E-11	0.1566
2.8520E+01	1.67363E-11	0.1577
2.8540E+01	1.59894E-11	0.1604
2.8560E+01	1.46932E-11	0.1426
2.8580E+01	1.36394E-11	0.1454
2.8600E+01	1.31198E-11	0.1490
2.8620E+01	1.27776E-11	0.1517
2.8640E+01	1.14685E-11	0.1543
2.8660E+01	1.11480E-11	0.1570
2.8680E+01	1.11228E-11	0.1574
2.8700E+01	1.08589E-11	0.1592
2.8720E+01	1.08591E-11	0.1593
2.8740E+01	1.06305E-11	0.1615
2.8760E+01	1.01415E-11	0.1654
2.8780E+01	9.35486E-12	0.1651
2.8800E+01	8.71374E-12	0.1691
2.8820E+01	8.63317E-12	0.1704
2.8840E+01	8.37808E-12	0.1742
2.8860E+01	7.86802E-12	0.1823
2.8880E+01	7.84061E-12	0.1829
2.8900E+01	7.53000E-12	0.1849
2.8920E+01	7.30983E-12	0.1891
2.8940E+01	6.42154E-12	0.1555
2.8960E+01	6.15284E-12	0.1602
2.8980E+01	6.00515E-12	0.1620
2.9000E+01	5.86428E-12	0.1646
2.9020E+01	5.83317E-12	0.1645
2.9040E+01	5.48950E-12	0.1693
2.9060E+01	5.35864E-12	0.1728
2.9080E+01	5.30924E-12	0.1740
2.9100E+01	5.20402E-12	0.1769
2.9120E+01	5.14322E-12	0.1788

2.9140E+01	5.08082E-12	0.1808
2.9160E+01	5.05974E-12	0.1812
2.9180E+01	4.85295E-12	0.1737
2.9200E+01	4.50934E-12	0.1748
2.9220E+01	4.51643E-12	0.1745
2.9240E+01	4.51718E-12	0.1747
2.9260E+01	4.49408E-12	0.1755
2.9280E+01	4.45791E-12	0.1766
2.9300E+01	4.45547E-12	0.1767
2.9320E+01	4.40183E-12	0.1787
2.9340E+01	4.35070E-12	0.1799
2.9360E+01	4.22926E-12	0.1830
2.9380E+01	4.25992E-12	0.1820
2.9400E+01	4.17599E-12	0.1849
2.9420E+01	4.10124E-12	0.1863
2.9440E+01	4.05503E-12	0.1879
2.9460E+01	4.04276E-12	0.1884
2.9480E+01	4.00141E-12	0.1899
2.9500E+01	3.67025E-12	0.1583
2.9520E+01	3.20315E-12	0.1443
2.9540E+01	3.01770E-12	0.1418
2.9560E+01	2.98970E-12	0.1429
2.9580E+01	2.97219E-12	0.1436
2.9600E+01	2.90976E-12	0.1453
2.9620E+01	2.81783E-12	0.1484
2.9640E+01	2.77975E-12	0.1500
2.9660E+01	2.73956E-12	0.1515
2.9680E+01	2.68752E-12	0.1536
2.9700E+01	2.58416E-12	0.1541
2.9720E+01	2.46673E-12	0.1588
2.9740E+01	2.38802E-12	0.1629
2.9760E+01	2.34652E-12	0.1622
2.9780E+01	2.23514E-12	0.1636
2.9800E+01	2.21882E-12	0.1644
2.9820E+01	2.17721E-12	0.1666
2.9840E+01	2.10862E-12	0.1707
2.9860E+01	2.00659E-12	0.1636
2.9880E+01	1.92048E-12	0.1664
2.9900E+01	1.90285E-12	0.1673
2.9920E+01	1.88720E-12	0.1683
2.9940E+01	1.86316E-12	0.1698
2.9960E+01	1.83226E-12	0.1719
2.9980E+01	1.82130E-12	0.1727
3.0000E+01	1.81881E-12	0.1729
total	9.74814E-04	0.0004

cell 2
 flagged tallies
 time

2.4400E+01	0.00000E+00	0.0000
2.4420E+01	0.00000E+00	0.0000
2.4440E+01	0.00000E+00	0.0000
2.4460E+01	2.16961E-10	1.0000
2.4480E+01	1.87671E-10	1.0000
2.4500E+01	0.00000E+00	0.0000
2.4520E+01	0.00000E+00	0.0000
2.4540E+01	2.20523E-10	0.7401
2.4560E+01	4.90728E-10	0.7074
2.4580E+01	4.90728E-10	0.7074
2.4600E+01	2.36770E-10	0.8089
2.4620E+01	0.00000E+00	0.0000
2.4640E+01	0.00000E+00	0.0000
2.4660E+01	0.00000E+00	0.0000
2.4680E+01	0.00000E+00	0.0000
2.4700E+01	0.00000E+00	0.0000
2.4720E+01	0.00000E+00	0.0000
2.4740E+01	0.00000E+00	0.0000
2.4760E+01	0.00000E+00	0.0000
2.4780E+01	1.13092E-10	0.9663
2.4800E+01	1.72633E-10	0.5210
2.4820E+01	2.42970E-10	0.4816

2.4840E+01	1.97712E-10	0.8586
2.4860E+01	8.67033E-11	0.6732
2.4880E+01	3.97437E-10	0.5051
2.4900E+01	2.60325E-10	0.8924
2.4920E+01	4.33379E-10	0.6841
2.4940E+01	5.05639E-10	0.5317
2.4960E+01	4.94077E-10	0.4193
2.4980E+01	4.53682E-10	0.3351
2.5000E+01	1.51364E-09	0.3170
2.5020E+01	9.05757E-10	0.4416
2.5040E+01	1.14515E-09	0.3533
2.5060E+01	1.52024E-09	0.2903
2.5080E+01	2.09187E-09	0.2647
2.5100E+01	2.37058E-09	0.2631
2.5120E+01	2.77440E-09	0.2487
2.5140E+01	2.76957E-09	0.2478
2.5160E+01	3.54363E-09	0.2019
2.5180E+01	4.81818E-09	0.1852
2.5200E+01	5.60608E-09	0.1744
2.5220E+01	6.37954E-09	0.1631
2.5240E+01	6.87452E-09	0.1603
2.5260E+01	7.58860E-09	0.1527
2.5280E+01	8.37051E-09	0.1382
2.5300E+01	9.19015E-09	0.1383
2.5320E+01	9.26852E-09	0.1348
2.5340E+01	8.58430E-09	0.1378
2.5360E+01	9.58631E-09	0.1282
2.5380E+01	1.12245E-08	0.1241
2.5400E+01	1.17087E-08	0.1165
2.5420E+01	1.18434E-08	0.1165
2.5440E+01	1.36915E-08	0.1079
2.5460E+01	1.40924E-08	0.1083
2.5480E+01	1.64484E-08	0.1000
2.5500E+01	1.78438E-08	0.0940
2.5520E+01	1.83557E-08	0.0941
2.5540E+01	1.81697E-08	0.0926
2.5560E+01	2.06818E-08	0.0875
2.5580E+01	2.20533E-08	0.0885
2.5600E+01	2.64232E-08	0.0781
2.5620E+01	2.84919E-08	0.0765
2.5640E+01	2.82809E-08	0.0769
2.5660E+01	2.86231E-08	0.0772
2.5680E+01	3.10018E-08	0.0734
2.5700E+01	3.19395E-08	0.0732
2.5720E+01	3.44357E-08	0.0712
2.5740E+01	3.50449E-08	0.0694
2.5760E+01	3.68888E-08	0.0676
2.5780E+01	3.93947E-08	0.0660
2.5800E+01	4.15533E-08	0.0648
2.5820E+01	4.16616E-08	0.0647
2.5840E+01	4.29175E-08	0.0635
2.5860E+01	4.19576E-08	0.0647
2.5880E+01	4.23668E-08	0.0645
2.5900E+01	4.40336E-08	0.0628
2.5920E+01	4.42065E-08	0.0617
2.5940E+01	4.42287E-08	0.0633
2.5960E+01	4.42270E-08	0.0626
2.5980E+01	4.50507E-08	0.0627
2.6000E+01	4.63019E-08	0.0626
2.6020E+01	4.52686E-08	0.0633
2.6040E+01	4.22030E-08	0.0651
2.6060E+01	3.84034E-08	0.0672
2.6080E+01	4.09330E-08	0.0659
2.6100E+01	4.00114E-08	0.0669
2.6120E+01	4.10295E-08	0.0662
2.6140E+01	3.91797E-08	0.0675
2.6160E+01	3.84089E-08	0.0678
2.6180E+01	3.73279E-08	0.0685
2.6200E+01	3.48509E-08	0.0714
2.6220E+01	3.52760E-08	0.0704
2.6240E+01	3.59288E-08	0.0698

2.6260E+01	3.40587E-08	0.0719
2.6280E+01	3.39841E-08	0.0712
2.6300E+01	3.21698E-08	0.0723
2.6320E+01	2.94104E-08	0.0750
2.6340E+01	3.03840E-08	0.0743
2.6360E+01	2.90896E-08	0.0746
2.6380E+01	2.81739E-08	0.0765
2.6400E+01	2.60161E-08	0.0802
2.6420E+01	2.51696E-08	0.0817
2.6440E+01	2.53371E-08	0.0823
2.6460E+01	2.40108E-08	0.0837
2.6480E+01	2.24706E-08	0.0879
2.6500E+01	2.14706E-08	0.0882
2.6520E+01	2.09258E-08	0.0905
2.6540E+01	1.86039E-08	0.0947
2.6560E+01	1.85636E-08	0.0958
2.6580E+01	1.97300E-08	0.0919
2.6600E+01	1.81753E-08	0.0960
2.6620E+01	1.72409E-08	0.0996
2.6640E+01	1.64553E-08	0.1027
2.6660E+01	1.59513E-08	0.1028
2.6680E+01	1.44504E-08	0.1090
2.6700E+01	1.32664E-08	0.1115
2.6720E+01	1.42404E-08	0.1101
2.6740E+01	1.36291E-08	0.1121
2.6760E+01	1.27075E-08	0.1136
2.6780E+01	1.04618E-08	0.1258
2.6800E+01	9.39237E-09	0.1351
2.6820E+01	8.66770E-09	0.1393
2.6840E+01	8.96593E-09	0.1387
2.6860E+01	7.92241E-09	0.1447
2.6880E+01	6.24911E-09	0.1584
2.6900E+01	5.20419E-09	0.1740
2.6920E+01	4.93933E-09	0.1811
2.6940E+01	4.05336E-09	0.1947
2.6960E+01	3.63144E-09	0.2055
2.6980E+01	3.08657E-09	0.2342
2.7000E+01	2.19368E-09	0.2743
2.7020E+01	1.90625E-09	0.2905
2.7040E+01	2.19483E-09	0.2778
2.7060E+01	1.95504E-09	0.3045
2.7080E+01	1.88486E-09	0.3090
2.7100E+01	1.70963E-09	0.3204
2.7120E+01	1.90220E-09	0.3057
2.7140E+01	1.64678E-09	0.3213
2.7160E+01	1.66427E-09	0.3189
2.7180E+01	1.13263E-09	0.3833
2.7200E+01	1.05186E-09	0.4094
2.7220E+01	9.66451E-10	0.4328
2.7240E+01	6.96666E-10	0.4506
2.7260E+01	5.77909E-10	0.5179
2.7280E+01	4.91188E-10	0.5656
2.7300E+01	5.00999E-10	0.5205
2.7320E+01	6.05460E-10	0.5223
2.7340E+01	7.14927E-10	0.4714
2.7360E+01	5.23251E-10	0.4943
2.7380E+01	3.33001E-10	0.6142
2.7400E+01	2.12050E-10	0.6166
2.7420E+01	1.62768E-10	0.7495
2.7440E+01	1.55696E-10	0.7748
2.7460E+01	1.43738E-10	0.7841
2.7480E+01	2.94137E-11	0.3041
2.7500E+01	2.86856E-11	0.3110
2.7520E+01	2.82353E-11	0.3156
2.7540E+01	2.59751E-11	0.3229
2.7560E+01	2.31959E-11	0.3494
2.7580E+01	2.36948E-11	0.3433
2.7600E+01	2.29953E-11	0.3524
2.7620E+01	2.23695E-11	0.3611
2.7640E+01	2.19217E-11	0.3664
2.7660E+01	2.15336E-11	0.3723

2.7680E+01	1.50542E-11	0.2751
2.7700E+01	2.24299E-11	0.4002
2.7720E+01	2.26363E-11	0.4232
2.7740E+01	2.25410E-11	0.4240
2.7760E+01	2.13097E-11	0.4367
2.7780E+01	1.82360E-11	0.4972
2.7800E+01	1.72074E-11	0.5256
2.7820E+01	1.71668E-11	0.5267
2.7840E+01	1.71719E-11	0.5266
2.7860E+01	1.55763E-11	0.5705
2.7880E+01	1.53927E-11	0.5772
2.7900E+01	1.50760E-11	0.5889
2.7920E+01	1.49225E-11	0.5949
2.7940E+01	1.48038E-11	0.5996
2.7960E+01	1.45989E-11	0.6079
2.7980E+01	1.45963E-11	0.6080
2.8000E+01	1.47953E-11	0.5999
2.8020E+01	1.49428E-11	0.5943
2.8040E+01	1.42485E-11	0.6204
2.8060E+01	1.29950E-11	0.6735
2.8080E+01	1.30266E-11	0.6718
2.8100E+01	1.28877E-11	0.6790
2.8120E+01	1.28171E-11	0.6825
2.8140E+01	1.19584E-11	0.7285
2.8160E+01	9.39552E-12	0.7032
2.8180E+01	2.71471E-12	0.2363
2.8200E+01	2.66870E-12	0.2376
2.8220E+01	2.65514E-12	0.2388
2.8240E+01	2.59963E-12	0.2427
2.8260E+01	2.49551E-12	0.2461
2.8280E+01	2.38952E-12	0.2538
2.8300E+01	2.38534E-12	0.2542
2.8320E+01	2.36917E-12	0.2534
2.8340E+01	2.22491E-12	0.2534
2.8360E+01	2.09420E-12	0.2599
2.8380E+01	2.04536E-12	0.2643
2.8400E+01	2.04531E-12	0.2643
2.8420E+01	2.00019E-12	0.2593
2.8440E+01	1.88225E-12	0.2535
2.8460E+01	1.76354E-12	0.2505
2.8480E+01	1.62299E-12	0.2557
2.8500E+01	1.58398E-12	0.2610
2.8520E+01	1.58221E-12	0.2613
2.8540E+01	1.46400E-12	0.2652
2.8560E+01	1.32066E-12	0.2784
2.8580E+01	1.26516E-12	0.2873
2.8600E+01	1.21403E-12	0.2791
2.8620E+01	1.16507E-12	0.2759
2.8640E+01	1.07098E-12	0.2849
2.8660E+01	1.00359E-12	0.2999
2.8680E+01	1.00089E-12	0.3006
2.8700E+01	1.00089E-12	0.3006
2.8720E+01	1.09255E-12	0.2908
2.8740E+01	9.94187E-13	0.3025
2.8760E+01	9.99320E-13	0.3010
2.8780E+01	9.99828E-13	0.3008
2.8800E+01	9.98130E-13	0.3013
2.8820E+01	9.85377E-13	0.3028
2.8840E+01	8.92019E-13	0.3195
2.8860E+01	8.93867E-13	0.3188
2.8880E+01	8.93852E-13	0.3188
2.8900E+01	8.93318E-13	0.3190
2.8920E+01	8.92858E-13	0.3192
2.8940E+01	8.92858E-13	0.3192
2.8960E+01	8.92858E-13	0.3192
2.8980E+01	8.92858E-13	0.3192
2.9000E+01	8.92858E-13	0.3192
2.9020E+01	8.94065E-13	0.3013
2.9040E+01	7.86438E-13	0.3137
2.9060E+01	7.89756E-13	0.3125
2.9080E+01	7.92511E-13	0.3113

2.9100E+01	7.82341E-13	0.3151
2.9120E+01	7.81859E-13	0.3153
2.9140E+01	7.81859E-13	0.3153
2.9160E+01	7.68694E-13	0.3147
2.9180E+01	7.66346E-13	0.3147
2.9200E+01	7.66346E-13	0.3147
2.9220E+01	7.86809E-13	0.3076
2.9240E+01	8.19437E-13	0.3014
2.9260E+01	8.19437E-13	0.3014
2.9280E+01	8.19437E-13	0.3014
2.9300E+01	8.20338E-13	0.3010
2.9320E+01	8.20880E-13	0.3008
2.9340E+01	8.20724E-13	0.3008
2.9360E+01	8.07475E-13	0.3012
2.9380E+01	8.59297E-13	0.2893
2.9400E+01	8.03935E-13	0.3013
2.9420E+01	7.97566E-13	0.3009
2.9440E+01	8.59631E-13	0.2914
2.9460E+01	8.53131E-13	0.2933
2.9480E+01	8.53131E-13	0.2933
2.9500E+01	8.53131E-13	0.2933
2.9520E+01	8.19724E-13	0.2992
2.9540E+01	7.99998E-13	0.3056
2.9560E+01	7.99998E-13	0.3056
2.9580E+01	7.99148E-13	0.3057
2.9600E+01	7.95173E-13	0.3060
2.9620E+01	7.39064E-13	0.3199
2.9640E+01	7.33571E-13	0.3218
2.9660E+01	7.21156E-13	0.3242
2.9680E+01	7.10681E-13	0.3265
2.9700E+01	7.10681E-13	0.3265
2.9720E+01	7.12543E-13	0.3257
2.9740E+01	7.12646E-13	0.3257
2.9760E+01	7.12646E-13	0.3257
2.9780E+01	7.14612E-13	0.3248
2.9800E+01	7.13329E-13	0.3253
2.9820E+01	7.09793E-13	0.3268
2.9840E+01	7.08823E-13	0.3272
2.9860E+01	7.02350E-13	0.3295
2.9880E+01	6.87272E-13	0.3360
2.9900E+01	6.87272E-13	0.3360
2.9920E+01	6.93120E-13	0.3333
2.9940E+01	6.80033E-13	0.3375
2.9960E+01	6.58513E-13	0.3470
2.9980E+01	6.58174E-13	0.3472
3.0000E+01	6.57856E-13	0.3473
total	2.21840E-06	0.0258

```

*****
*****
dump no.      2 on file runtpe      nps =    2000000    coll =      1403612    ctm =      3.93
nrn =      128648480

```

4 warning messages so far.

run terminated when 20000000 particle histories were done.

computer time = 3.93 minutes

```

mcnpx      version 2.5e  Mon Feb 23 09:00:00 MST 2004      04/19/05 11:58:02      probid
= 04/19/05 11:55:32

```



```

66-      C * Importance Function *
67-      C *****
68-      imp:n 1 4r 0
69-      C +-----+
70-      C |
71-      C |                               Data Card
72-      C |
73-      C +-----+
74-      C *****
75-      C * Source Definition *
76-      C * +-----+ *
77-      C * | 4.4 keV Gaussian Neutron Source | *
78-      C * | Perpendicular Beam             | *
79-      C * | Radius = 7.62 cm               | *
80-      C * | Center = 0.0, 0.0, 0.0        | *
81-      C * | Direction = +Y                 | *
82-      C * +-----+ *
83-      C *****
84-      sdef par=1 erg=d1 sur=3 rad=d2 vec=0 1 0 dir=1 pos=0.0 0.0 0.0
85-      sp1 -4 -0.0044 -2
86-      si2 0 7.6199
87-      sp2 0 1
88-      C +-----+
89-      C |
90-      C |                               Material Card
91-      C |
92-      C +-----+
93-      C *****
94-      C * Plastic Scintillator (Mass Density = 1.032 gm/cc) *
95-      C *****
96-      m1 1001 1.0 6012 1.0
97-      C *****
98-      C * Natural Lead (Mass Density = 11.350 gm/cc) *
99-      C *****
100-     m2 82000 -1.0
101-     C +-----+
102-     C |
103-     C |                               Tally Card
104-     C |
105-     C +-----+
106-     C *****
107-     C * Energy Deposition Tally (Type 6) *
108-     C *****
109-     f6:n 2
110-     C 0.2 ns time binning
111-     t6 20.0 499i 30.0
112-     fq6 t s
113-     C +-----+
114-     C |
115-     C |                               Control Card
116-     C |
117-     C +-----+
118-     C *****
119-     C * Number of Source Particles *
120-     C *****
121-     nps 2000000
122-     C *****
123-     C * Output Options *
124-     C *****
125-     print -30

```

probability distribution 1 for source variable erg
energy function 4: gaussian (fusion) spectrum

$$f(e) = c \cdot \exp(-((e-b)/a)**2)$$

fusion temperature	fusion width(a)	fusion energy(b)	fusion constant(c)	fusion fwhm
4.4000E-03	1.0421E-01	2.4637E+00	5.4138E+00	1.7353E-01

the mean of source distribution 1 is 2.4637E+00

warning. source variable rad is sampled uniformly.

probability distribution 2 for source variable rad
unbiased histogram distribution

source entry	source value	cumulative probability	probability of bin
1	0.00000E+00	0.000000E+00	0.000000E+00
2	7.61990E+00	1.000000E+00	1.000000E+00

the mean of source distribution 2 is 3.8100E+00

print table 126

average weight (relative)	tracks average cell track (cm)	population	collisions entering	collisions * weight (per history)	number weighted energy	flux weighted energy	track
1.0000E+00	1 21628985	20000000	0	0.0000E+00	2.4618E+00	2.4632E+00	
1.0000E+00	2 7657245	7657230	533409	2.6670E-02	2.1331E+00	2.3909E+00	
9.9999E-01	3 4.9058E+00	7968964	0	0.0000E+00	2.4204E+00	2.4553E+00	
9.9995E-01	4 7968967	20000000	6866886	3.4333E-01	2.3672E+00	2.4075E+00	
9.9998E-01	5 20007911	17982042	0	0.0000E+00	2.4296E+00	2.4507E+00	
	total 75342150	73608236	7400295	3.7000E-01			

ltally 6 nps = 20000000
tally type 6 track length estimate of heating. units mev/gram
particle(s): neutron

masses
cell: 2
1.49425E+01

cell 2

time		
2.4000E+01	0.00000E+00	0.0000
2.4020E+01	0.00000E+00	0.0000
2.4040E+01	2.80772E-12	1.0000
2.4060E+01	2.16655E-10	1.0000
2.4080E+01	0.00000E+00	0.0000
2.4100E+01	0.00000E+00	0.0000
2.4120E+01	4.84628E-11	1.0000
2.4140E+01	1.68902E-10	1.0000
2.4160E+01	4.35262E-10	0.7071
2.4180E+01	2.81462E-10	0.8077
2.4200E+01	1.53887E-10	1.0000
2.4220E+01	7.84510E-10	0.4849
2.4240E+01	5.76051E-10	0.5079
2.4260E+01	1.89825E-09	0.2953
2.4280E+01	2.15014E-09	0.2761
2.4300E+01	2.12945E-09	0.2738
2.4320E+01	2.19278E-09	0.2576
2.4340E+01	5.18573E-09	0.1787
2.4360E+01	5.62736E-09	0.1657
2.4380E+01	5.67207E-09	0.1695
2.4400E+01	6.52654E-09	0.1562
2.4420E+01	7.73877E-09	0.1414
2.4440E+01	1.20999E-08	0.1165
2.4460E+01	1.27598E-08	0.1106
2.4480E+01	1.78304E-08	0.0953

2.4500E+01	2.45432E-08	0.0811
2.4520E+01	2.96538E-08	0.0733
2.4540E+01	4.01751E-08	0.0641
2.4560E+01	4.34600E-08	0.0604
2.4580E+01	5.30671E-08	0.0537
2.4600E+01	7.25397E-08	0.0470
2.4620E+01	8.21762E-08	0.0435
2.4640E+01	1.19310E-07	0.0366
2.4660E+01	1.37146E-07	0.0336
2.4680E+01	1.65258E-07	0.0307
2.4700E+01	2.04121E-07	0.0278
2.4720E+01	2.28327E-07	0.0261
2.4740E+01	2.89326E-07	0.0233
2.4760E+01	3.44528E-07	0.0213
2.4780E+01	4.06141E-07	0.0196
2.4800E+01	4.67850E-07	0.0182
2.4820E+01	5.68623E-07	0.0165
2.4840E+01	6.72293E-07	0.0151
2.4860E+01	7.79069E-07	0.0141
2.4880E+01	8.89414E-07	0.0132
2.4900E+01	1.07179E-06	0.0120
2.4920E+01	1.24203E-06	0.0111
2.4940E+01	1.41900E-06	0.0104
2.4960E+01	1.63378E-06	0.0097
2.4980E+01	1.85829E-06	0.0091
2.5000E+01	2.10201E-06	0.0085
2.5020E+01	2.44872E-06	0.0079
2.5040E+01	2.78466E-06	0.0074
2.5060E+01	3.14084E-06	0.0070
2.5080E+01	3.50652E-06	0.0066
2.5100E+01	3.94817E-06	0.0062
2.5120E+01	4.35599E-06	0.0059
2.5140E+01	4.92668E-06	0.0055
2.5160E+01	5.50994E-06	0.0052
2.5180E+01	6.21248E-06	0.0049
2.5200E+01	7.00748E-06	0.0046
2.5220E+01	7.76568E-06	0.0044
2.5240E+01	8.54707E-06	0.0042
2.5260E+01	9.29791E-06	0.0040
2.5280E+01	1.01334E-05	0.0038
2.5300E+01	1.09493E-05	0.0037
2.5320E+01	1.18622E-05	0.0035
2.5340E+01	1.28536E-05	0.0034
2.5360E+01	1.37893E-05	0.0033
2.5380E+01	1.46487E-05	0.0032
2.5400E+01	1.54507E-05	0.0031
2.5420E+01	1.62919E-05	0.0030
2.5440E+01	1.70138E-05	0.0029
2.5460E+01	1.81026E-05	0.0029
2.5480E+01	1.92609E-05	0.0028
2.5500E+01	2.04253E-05	0.0027
2.5520E+01	2.14459E-05	0.0026
2.5540E+01	2.25875E-05	0.0025
2.5560E+01	2.35376E-05	0.0025
2.5580E+01	2.42593E-05	0.0024
2.5600E+01	2.49249E-05	0.0024
2.5620E+01	2.56685E-05	0.0024
2.5640E+01	2.64349E-05	0.0023
2.5660E+01	2.69104E-05	0.0023
2.5680E+01	2.75795E-05	0.0023
2.5700E+01	2.84796E-05	0.0023
2.5720E+01	2.93668E-05	0.0022
2.5740E+01	3.02826E-05	0.0022
2.5760E+01	3.09096E-05	0.0022
2.5780E+01	3.09320E-05	0.0022
2.5800E+01	3.10313E-05	0.0022
2.5820E+01	3.10975E-05	0.0021
2.5840E+01	3.12986E-05	0.0021
2.5860E+01	3.15540E-05	0.0021
2.5880E+01	3.15888E-05	0.0021
2.5900E+01	3.11993E-05	0.0021

2.5920E+01	3.05971E-05	0.0022
2.5940E+01	3.00500E-05	0.0022
2.5960E+01	2.94012E-05	0.0022
2.5980E+01	2.85752E-05	0.0022
2.6000E+01	2.80307E-05	0.0022
2.6020E+01	2.75643E-05	0.0023
2.6040E+01	2.68994E-05	0.0023
2.6060E+01	2.61881E-05	0.0023
2.6080E+01	2.53193E-05	0.0024
2.6100E+01	2.43265E-05	0.0024
2.6120E+01	2.33538E-05	0.0025
2.6140E+01	2.25776E-05	0.0025
2.6160E+01	2.17301E-05	0.0025
2.6180E+01	2.09811E-05	0.0026
2.6200E+01	2.00773E-05	0.0026
2.6220E+01	1.91368E-05	0.0027
2.6240E+01	1.83004E-05	0.0028
2.6260E+01	1.73280E-05	0.0028
2.6280E+01	1.64403E-05	0.0029
2.6300E+01	1.56523E-05	0.0030
2.6320E+01	1.49774E-05	0.0031
2.6340E+01	1.43342E-05	0.0031
2.6360E+01	1.34770E-05	0.0032
2.6380E+01	1.24564E-05	0.0033
2.6400E+01	1.16173E-05	0.0035
2.6420E+01	1.07538E-05	0.0036
2.6440E+01	9.99638E-06	0.0037
2.6460E+01	9.24952E-06	0.0039
2.6480E+01	8.57503E-06	0.0040
2.6500E+01	7.88013E-06	0.0042
2.6520E+01	7.15648E-06	0.0044
2.6540E+01	6.58731E-06	0.0046
2.6560E+01	6.08950E-06	0.0048
2.6580E+01	5.61171E-06	0.0050
2.6600E+01	5.19325E-06	0.0052
2.6620E+01	4.67998E-06	0.0054
2.6640E+01	4.24350E-06	0.0057
2.6660E+01	3.81187E-06	0.0060
2.6680E+01	3.47776E-06	0.0063
2.6700E+01	3.15934E-06	0.0066
2.6720E+01	2.87206E-06	0.0069
2.6740E+01	2.59466E-06	0.0073
2.6760E+01	2.30623E-06	0.0077
2.6780E+01	2.07809E-06	0.0081
2.6800E+01	1.89404E-06	0.0085
2.6820E+01	1.70420E-06	0.0090
2.6840E+01	1.51456E-06	0.0095
2.6860E+01	1.35810E-06	0.0100
2.6880E+01	1.20445E-06	0.0106
2.6900E+01	1.09089E-06	0.0112
2.6920E+01	9.59824E-07	0.0119
2.6940E+01	8.57482E-07	0.0126
2.6960E+01	7.64103E-07	0.0134
2.6980E+01	6.68330E-07	0.0143
2.7000E+01	5.77456E-07	0.0153
2.7020E+01	5.27585E-07	0.0161
2.7040E+01	4.66719E-07	0.0170
2.7060E+01	4.08997E-07	0.0181
2.7080E+01	3.45852E-07	0.0198
2.7100E+01	3.00115E-07	0.0212
2.7120E+01	2.59201E-07	0.0228
2.7140E+01	2.30610E-07	0.0244
2.7160E+01	1.99475E-07	0.0259
2.7180E+01	1.75806E-07	0.0274
2.7200E+01	1.49630E-07	0.0296
2.7220E+01	1.27555E-07	0.0321
2.7240E+01	1.17569E-07	0.0335
2.7260E+01	9.99545E-08	0.0364
2.7280E+01	8.81271E-08	0.0388
2.7300E+01	6.97083E-08	0.0427
2.7320E+01	6.46807E-08	0.0445

2.7340E+01	6.05171E-08	0.0462
2.7360E+01	4.81740E-08	0.0518
2.7380E+01	3.79157E-08	0.0577
2.7400E+01	3.30688E-08	0.0620
2.7420E+01	2.97568E-08	0.0655
2.7440E+01	2.56052E-08	0.0704
2.7460E+01	2.25800E-08	0.0757
2.7480E+01	1.52152E-08	0.0887
2.7500E+01	1.53062E-08	0.0875
2.7520E+01	1.50103E-08	0.0898
2.7540E+01	1.33940E-08	0.0973
2.7560E+01	9.57788E-09	0.1128
2.7580E+01	8.89777E-09	0.1180
2.7600E+01	5.29810E-09	0.1381
2.7620E+01	5.16590E-09	0.1459
2.7640E+01	4.96166E-09	0.1453
2.7660E+01	4.63014E-09	0.1565
2.7680E+01	3.24147E-09	0.1766
2.7700E+01	3.09109E-09	0.1791
2.7720E+01	3.68970E-09	0.1741
2.7740E+01	2.33393E-09	0.1878
2.7760E+01	2.71620E-09	0.1986
2.7780E+01	2.04230E-09	0.2212
2.7800E+01	1.50432E-09	0.2515
2.7820E+01	1.58396E-09	0.2510
2.7840E+01	2.03660E-09	0.2381
2.7860E+01	1.58245E-09	0.2607
2.7880E+01	1.46187E-09	0.2591
2.7900E+01	1.28469E-09	0.2527
2.7920E+01	1.20558E-09	0.2541
2.7940E+01	9.02226E-10	0.2745
2.7960E+01	6.85434E-10	0.2382
2.7980E+01	7.43777E-10	0.3087
2.8000E+01	6.62898E-10	0.3357
2.8020E+01	6.41792E-10	0.3467
2.8040E+01	5.08055E-10	0.3130
2.8060E+01	4.94893E-10	0.2628
2.8080E+01	5.08773E-10	0.2767
2.8100E+01	5.73513E-10	0.2579
2.8120E+01	4.59671E-10	0.2946
2.8140E+01	4.40261E-10	0.2706
2.8160E+01	5.41925E-10	0.2773
2.8180E+01	4.19332E-10	0.2911
2.8200E+01	2.44777E-10	0.3222
2.8220E+01	2.45328E-10	0.3129
2.8240E+01	3.36487E-10	0.3207
2.8260E+01	3.84087E-10	0.3101
2.8280E+01	3.71092E-10	0.3123
2.8300E+01	2.83499E-10	0.2690
2.8320E+01	3.18460E-10	0.2604
2.8340E+01	3.60041E-10	0.2560
2.8360E+01	4.11797E-10	0.2995
2.8380E+01	3.47232E-10	0.3292
2.8400E+01	2.25253E-10	0.3127
2.8420E+01	1.99563E-10	0.2857
2.8440E+01	2.40470E-10	0.2869
2.8460E+01	3.82221E-10	0.3432
2.8480E+01	3.10556E-10	0.3424
2.8500E+01	1.81456E-10	0.5173
2.8520E+01	1.05658E-10	0.3881
2.8540E+01	1.57665E-10	0.3579
2.8560E+01	1.76990E-10	0.3365
2.8580E+01	1.61200E-10	0.3673
2.8600E+01	2.24991E-10	0.6111
2.8620E+01	1.71685E-10	0.4541
2.8640E+01	1.59178E-10	0.4248
2.8660E+01	1.20915E-10	0.4262
2.8680E+01	1.30781E-10	0.3310
2.8700E+01	2.05444E-10	0.3593
2.8720E+01	2.30847E-10	0.2975
2.8740E+01	1.69268E-10	0.3021

2.8760E+01	2.79693E-10	0.3813
2.8780E+01	2.45757E-10	0.3603
2.8800E+01	2.28256E-10	0.3955
2.8820E+01	1.90294E-10	0.5140
2.8840E+01	8.15449E-11	0.3757
2.8860E+01	1.00629E-10	0.4541
2.8880E+01	1.31264E-10	0.3854
2.8900E+01	1.21028E-10	0.3791
2.8920E+01	1.03812E-10	0.4041
2.8940E+01	5.00220E-11	0.4953
2.8960E+01	3.53284E-11	0.7037
2.8980E+01	3.98805E-11	0.6337
2.9000E+01	1.19149E-10	0.3251
2.9020E+01	1.90021E-10	0.3317
2.9040E+01	1.78990E-10	0.3190
2.9060E+01	1.03020E-10	0.3264
2.9080E+01	6.66900E-11	0.4496
2.9100E+01	5.97477E-11	0.4873
2.9120E+01	2.81512E-11	0.4945
2.9140E+01	3.30962E-11	0.5673
2.9160E+01	4.44260E-11	0.6357
2.9180E+01	1.31848E-11	0.3686
2.9200E+01	1.22091E-11	0.3571
2.9220E+01	3.87498E-11	0.6054
2.9240E+01	5.55308E-11	0.4668
2.9260E+01	7.73899E-11	0.3823
2.9280E+01	6.99963E-11	0.4037
2.9300E+01	7.56819E-11	0.4341
2.9320E+01	7.11892E-11	0.4328
2.9340E+01	4.92465E-11	0.4911
2.9360E+01	8.70989E-11	0.3968
2.9380E+01	9.12300E-11	0.3879
2.9400E+01	7.58132E-11	0.3899
2.9420E+01	8.06041E-11	0.3914
2.9440E+01	7.71741E-11	0.4662
2.9460E+01	5.46616E-11	0.4880
2.9480E+01	3.21995E-11	0.4623
2.9500E+01	3.10002E-11	0.5206
2.9520E+01	5.21861E-11	0.5145
2.9540E+01	6.41123E-11	0.5114
2.9560E+01	4.84661E-11	0.5203
2.9580E+01	2.27660E-11	0.7596
2.9600E+01	4.07611E-11	0.5390
2.9620E+01	3.59808E-11	0.6038
2.9640E+01	4.23931E-11	0.5327
2.9660E+01	1.99380E-11	0.6101
2.9680E+01	1.50825E-11	0.7403
2.9700E+01	6.88906E-12	0.4605
2.9720E+01	3.77091E-12	0.2057
2.9740E+01	3.58500E-12	0.2117
2.9760E+01	1.44499E-11	0.7562
2.9780E+01	4.07748E-11	0.5775
2.9800E+01	5.03485E-11	0.5606
2.9820E+01	3.46740E-11	0.4563
2.9840E+01	2.92408E-11	0.5195
2.9860E+01	1.64503E-11	0.6176
2.9880E+01	1.19419E-11	0.7440
2.9900E+01	9.08612E-12	0.6776
2.9920E+01	1.23994E-11	0.7779
2.9940E+01	1.23523E-11	0.7809
2.9960E+01	1.48928E-11	0.6704
2.9980E+01	1.43718E-11	0.7240
3.0000E+01	9.92933E-12	0.5933
total	1.48869E-03	0.0003

dump no. 2 on file runtpe nps = 2000000 coll = 7400295 ctm = 5.64
nrn = 170971989

6 warning messages so far.

run terminated when 20000000 particle histories were done.

computer time = 5.66 minutes

mcnp version 2.5e Mon Feb 23 09:00:00 MST 2004
= 04/20/05 12:32:27

04/20/05 12:36:03 probid

MCNPX Output File – 5” Pb Cylinder (10” and ½” Cylinder Files Similar)

```

1-      Scintillator Broadening Deck
2-      C
3-      C PROBLEM DESCRIPTION
4-      C   One-eighth inch thick scintillator at a distance of 5.6 meters
5-      C   from the source. This represents the OMEGA geometry.
6-      C   This run includes one-half inch lead directly behind the
7-      C   scintillator and one-half inch of lead 8 inches in front
8-      C   of the scintillator. This model includes a five inch
9-      C   thick lead cylinder from the source to the back lead.
10-     C   The cylinder is 5 inches above the one-half inch lead
11-     C   radius.
12-     C   See page 67 of MS thesis notebook.
13-     C
14-     C 3456789012345678901234567890123456789012345678901234567890123456789012
15-     C      1          2          3          4          5          6          7
16-     C
17-     C +-----+
18-     C |                                           |
19-     C |                                           |
20-     C |                                           |
21-     C +-----+
22-     C *****
23-     C * Source Void *
24-     C *****
25-     C 1  0          -2  3 -7
26-     C *****
27-     C * Scintillator *
28-     C *****
29-     C 2  1 -1.032  -1  4 -5
30-     C *****
31-     C * Scintillator Void *
32-     C *****
33-     C 3  0          -2  1 -5 4
34-     C *****
35-     C * Lead *
36-     C *****
37-     C 4  2 -11.350  -2  5 -8
38-     C 5  2 -11.350  -2  7 -6
39-     C 6  2 -11.350  -10 9 -8 3
40-     C *****
41-     C * Voids *
42-     C *****
43-     C 7  0          -2  6 -4
44-     C 8  0          -9  2 -8 3
45-     C *****
46-     C * Particle Death *
47-     C *****
48-     C 999 0          10:-3:8
49-
50-     C +-----+
51-     C |                                           |
52-     C |                                           |
53-     C |                                           |
54-     C +-----+
55-     C *****
56-     C * Global Surfaces *
57-     C *****
58-     C 1  cy  3.8100
59-     C 2  cy  7.6200
60-     C 3  py  0.0000
61-     C *****
62-     C * Scintillator Planes *
63-     C *****
64-     C 4  py 560.0000
65-     C 5  py 560.3175
66-     C *****

```

```

67-      C * Lead Planes *
68-      C *****
69-      6 py 539.6800
70-      7 py 538.4100
71-      8 py 561.5875
72-      C *****
73-      C * Lead Cylinder *
74-      C *****
75-      9 cy 20.3200
76-      10 cy 33.0200
77-
78-      C *****
79-      C * Importance Function *
80-      C *****
81-      imp:n 1 7r 0
82-      C +-----+
83-      C |
84-      C |                               Data Card
85-      C |
86-      C +-----+
87-      C *****
88-      C * Source Definition *
89-      C * +-----+ *
90-      C * | 4.4 keV Gaussian Neutron Source | *
91-      C * | Perpendicular Beam | *
92-      C * | Radius = 33.02 cm | *
93-      C * | Center = 0.0, 0.0, 0.0 | *
94-      C * | Direction = +Y | *
95-      C * +-----+ *
96-      C *****
97-      sdef par=1 erg=d1 sur=3 rad=d2 vec=0 1 0 dir=1 pos=0.0 0.0 0.0
98-      spl -4 -0.0044 -2
99-      si2 0 33.0200
100-     sp2 0 1
101-     C +-----+
102-     C |
103-     C |                               Material Card
104-     C |
105-     C +-----+
106-     C *****
107-     C * Plastic Scintillator (Mass Density = 1.032 gm/cc) *
108-     C *****
109-     m1 1001 1.0 6012 1.0
110-     C *****
111-     C * Natural Lead (Mass Density = 11.350 gm/cc) *
112-     C *****
113-     m2 82000 -1.0
114-     C +-----+
115-     C |
116-     C |                               Tally Card
117-     C |
118-     C +-----+
119-     C *****
120-     C * Energy Deposition Tally (Type 6) *
121-     C *****
122-     f6:n 2
123-     C 0.2 ns time binning
124-     t6 20.0 499i 30.0
125-     fq6 t s
126-     C +-----+
127-     C |
128-     C |                               Control Card
129-     C |
130-     C +-----+
131-     C *****
132-     C * Number of Source Particles *
133-     C *****
134-     nps 20000000
135-     C *****
136-     C * Output Options *
137-     C *****

```

138- print -30

probability distribution 1 for source variable erg
energy function 4: gaussian (fusion) spectrum

$$f(e)=c*\exp(-((e-b)/a)**2)$$

fusion temperature	fusion width(a)	fusion energy(b)	fusion constant(c)	fusion fwhm
4.4000E-03	1.0421E-01	2.4637E+00	5.4138E+00	1.7353E-01

the mean of source distribution 1 is 2.4637E+00

warning. source variable rad is sampled uniformly.

probability distribution 2 for source variable rad
unbiased histogram distribution

source entry	source value	cumulative probability	probability of bin
1	0.00000E+00	0.000000E+00	0.000000E+00
2	3.30200E+01	1.000000E+00	1.000000E+00

the mean of source distribution 2 is 1.6510E+01

print table 126

average weight (relative)	tracks average cell track mfp (cm)	population	collisions	collisions * weight (per history)	number weighted energy	flux weighted energy	track
1	1 6365486	5523397	0	0.0000E+00	2.4467E+00	2.4568E+00	
9.9998E-01	0.0000E+00						
2	2 1923322	1791792	150086	7.5037E-03	2.0033E+00	2.3362E+00	
9.9995E-01	4.8344E+00						
3	3 2021469	1890614	0	0.0000E+00	2.2846E+00	2.3932E+00	
9.9992E-01	0.0000E+00						
4	4 3602837	3588084	1251064	6.2548E-02	2.1742E+00	2.3540E+00	
9.9992E-01	4.4292E+00						
5	5 4673828	4617900	1607115	8.0350E-02	2.3425E+00	2.3980E+00	
9.9992E-01	4.4016E+00						
6	6 12338518	8739950	58386578	2.9129E+00	1.4108E+00	1.7966E+00	
9.9781E-01	4.8599E+00						
7	7 4533774	4179651	0	0.0000E+00	2.3759E+00	2.4301E+00	
9.9995E-01	0.0000E+00						
8	8 14943420	11356863	0	0.0000E+00	2.4027E+00	2.4377E+00	
9.9992E-01	0.0000E+00						
total	50402654	41688251	61394843	3.0633E+00			

ltally 6 nps = 20000000
tally type 6 track length estimate of heating. units mev/gram
particle(s): neutron

masses
cell: 2
1.49425E+01

cell	time		
2	2.4000E+01	0.00000E+00	0.0000
	2.4020E+01	0.00000E+00	0.0000
	2.4040E+01	2.80772E-12	1.0000
	2.4060E+01	2.16655E-10	1.0000
	2.4080E+01	0.00000E+00	0.0000

2.4100E+01	0.00000E+00	0.0000
2.4120E+01	0.00000E+00	0.0000
2.4140E+01	0.00000E+00	0.0000
2.4160E+01	2.17675E-10	1.0000
2.4180E+01	0.00000E+00	0.0000
2.4200E+01	0.00000E+00	0.0000
2.4220E+01	1.96034E-10	1.0000
2.4240E+01	1.50028E-11	1.0000
2.4260E+01	5.74404E-10	0.5348
2.4280E+01	6.83792E-10	0.4869
2.4300E+01	4.68436E-10	0.6012
2.4320E+01	6.42569E-10	0.5181
2.4340E+01	9.26477E-10	0.4029
2.4360E+01	1.59698E-09	0.3256
2.4380E+01	8.44395E-10	0.4371
2.4400E+01	1.52456E-09	0.3274
2.4420E+01	2.14844E-09	0.2678
2.4440E+01	3.90325E-09	0.2101
2.4460E+01	3.02282E-09	0.2214
2.4480E+01	5.00249E-09	0.1871
2.4500E+01	5.82306E-09	0.1643
2.4520E+01	7.18614E-09	0.1472
2.4540E+01	8.23941E-09	0.1427
2.4560E+01	1.22599E-08	0.1189
2.4580E+01	1.29685E-08	0.1085
2.4600E+01	1.89321E-08	0.0923
2.4620E+01	1.99329E-08	0.0897
2.4640E+01	2.87778E-08	0.0744
2.4660E+01	3.41781E-08	0.0667
2.4680E+01	3.63280E-08	0.0651
2.4700E+01	4.86644E-08	0.0577
2.4720E+01	5.49968E-08	0.0536
2.4740E+01	7.20604E-08	0.0474
2.4760E+01	8.26720E-08	0.0440
2.4780E+01	1.02791E-07	0.0395
2.4800E+01	1.19192E-07	0.0365
2.4820E+01	1.38816E-07	0.0338
2.4840E+01	1.61267E-07	0.0310
2.4860E+01	1.96319E-07	0.0283
2.4880E+01	2.23453E-07	0.0266
2.4900E+01	2.61553E-07	0.0245
2.4920E+01	3.07466E-07	0.0226
2.4940E+01	3.48051E-07	0.0212
2.4960E+01	3.94569E-07	0.0198
2.4980E+01	4.64404E-07	0.0184
2.5000E+01	5.30117E-07	0.0171
2.5020E+01	6.23622E-07	0.0158
2.5040E+01	7.03877E-07	0.0149
2.5060E+01	7.76290E-07	0.0141
2.5080E+01	8.77342E-07	0.0133
2.5100E+01	9.71144E-07	0.0126
2.5120E+01	1.08516E-06	0.0119
2.5140E+01	1.21600E-06	0.0113
2.5160E+01	1.34524E-06	0.0107
2.5180E+01	1.54909E-06	0.0100
2.5200E+01	1.77033E-06	0.0093
2.5220E+01	1.94051E-06	0.0089
2.5240E+01	2.11136E-06	0.0085
2.5260E+01	2.30516E-06	0.0082
2.5280E+01	2.57013E-06	0.0077
2.5300E+01	2.76184E-06	0.0074
2.5320E+01	2.98068E-06	0.0072
2.5340E+01	3.25688E-06	0.0069
2.5360E+01	3.45776E-06	0.0066
2.5380E+01	3.68676E-06	0.0064
2.5400E+01	3.92464E-06	0.0062
2.5420E+01	4.17470E-06	0.0060
2.5440E+01	4.34163E-06	0.0059
2.5460E+01	4.60085E-06	0.0057
2.5480E+01	4.85855E-06	0.0056
2.5500E+01	5.20473E-06	0.0054

2.5520E+01	5.44985E-06	0.0053
2.5540E+01	5.75429E-06	0.0051
2.5560E+01	6.04481E-06	0.0050
2.5580E+01	6.29067E-06	0.0049
2.5600E+01	6.45413E-06	0.0048
2.5620E+01	6.72746E-06	0.0047
2.5640E+01	6.88668E-06	0.0047
2.5660E+01	6.99231E-06	0.0046
2.5680E+01	7.18284E-06	0.0046
2.5700E+01	7.42669E-06	0.0045
2.5720E+01	7.62703E-06	0.0044
2.5740E+01	7.86885E-06	0.0044
2.5760E+01	8.07968E-06	0.0043
2.5780E+01	8.12345E-06	0.0043
2.5800E+01	8.16919E-06	0.0043
2.5820E+01	8.18282E-06	0.0043
2.5840E+01	8.22379E-06	0.0043
2.5860E+01	8.27069E-06	0.0043
2.5880E+01	8.30754E-06	0.0042
2.5900E+01	8.29148E-06	0.0042
2.5920E+01	8.13024E-06	0.0043
2.5940E+01	7.96792E-06	0.0043
2.5960E+01	7.87611E-06	0.0044
2.5980E+01	7.66283E-06	0.0044
2.6000E+01	7.49744E-06	0.0045
2.6020E+01	7.38430E-06	0.0045
2.6040E+01	7.30381E-06	0.0045
2.6060E+01	7.11977E-06	0.0046
2.6080E+01	6.87816E-06	0.0047
2.6100E+01	6.65321E-06	0.0047
2.6120E+01	6.47142E-06	0.0048
2.6140E+01	6.26672E-06	0.0049
2.6160E+01	6.02460E-06	0.0050
2.6180E+01	5.81408E-06	0.0051
2.6200E+01	5.55950E-06	0.0052
2.6220E+01	5.36504E-06	0.0053
2.6240E+01	5.13237E-06	0.0054
2.6260E+01	4.93528E-06	0.0055
2.6280E+01	4.63520E-06	0.0057
2.6300E+01	4.46517E-06	0.0058
2.6320E+01	4.27583E-06	0.0059
2.6340E+01	4.08071E-06	0.0060
2.6360E+01	3.87295E-06	0.0062
2.6380E+01	3.60279E-06	0.0064
2.6400E+01	3.35332E-06	0.0067
2.6420E+01	3.11904E-06	0.0069
2.6440E+01	2.89881E-06	0.0072
2.6460E+01	2.67584E-06	0.0074
2.6480E+01	2.47644E-06	0.0077
2.6500E+01	2.32509E-06	0.0080
2.6520E+01	2.13672E-06	0.0083
2.6540E+01	1.98850E-06	0.0086
2.6560E+01	1.82145E-06	0.0090
2.6580E+01	1.68067E-06	0.0094
2.6600E+01	1.56409E-06	0.0097
2.6620E+01	1.43630E-06	0.0102
2.6640E+01	1.28622E-06	0.0107
2.6660E+01	1.20579E-06	0.0111
2.6680E+01	1.10067E-06	0.0116
2.6700E+01	9.96780E-07	0.0122
2.6720E+01	8.99580E-07	0.0129
2.6740E+01	8.22398E-07	0.0134
2.6760E+01	7.39047E-07	0.0141
2.6780E+01	6.79370E-07	0.0148
2.6800E+01	6.20190E-07	0.0155
2.6820E+01	5.55903E-07	0.0163
2.6840E+01	5.00183E-07	0.0172
2.6860E+01	4.62676E-07	0.0179
2.6880E+01	4.13648E-07	0.0189
2.6900E+01	3.60175E-07	0.0202
2.6920E+01	3.25516E-07	0.0212

2.6940E+01	3.02504E-07	0.0222
2.6960E+01	2.60919E-07	0.0238
2.6980E+01	2.41722E-07	0.0248
2.7000E+01	2.00103E-07	0.0270
2.7020E+01	1.91649E-07	0.0279
2.7040E+01	1.70395E-07	0.0294
2.7060E+01	1.48141E-07	0.0313
2.7080E+01	1.37766E-07	0.0328
2.7100E+01	1.17620E-07	0.0355
2.7120E+01	1.01094E-07	0.0384
2.7140E+01	8.81488E-08	0.0406
2.7160E+01	8.00345E-08	0.0427
2.7180E+01	6.69006E-08	0.0463
2.7200E+01	5.85217E-08	0.0493
2.7220E+01	5.50233E-08	0.0515
2.7240E+01	4.87584E-08	0.0549
2.7260E+01	4.53954E-08	0.0568
2.7280E+01	4.12350E-08	0.0606
2.7300E+01	3.52292E-08	0.0657
2.7320E+01	3.56124E-08	0.0654
2.7340E+01	3.15703E-08	0.0690
2.7360E+01	2.58150E-08	0.0755
2.7380E+01	2.33255E-08	0.0794
2.7400E+01	1.98343E-08	0.0888
2.7420E+01	1.67271E-08	0.0949
2.7440E+01	1.59169E-08	0.0973
2.7460E+01	1.46541E-08	0.1031
2.7480E+01	1.32743E-08	0.1067
2.7500E+01	1.31267E-08	0.1045
2.7520E+01	1.10010E-08	0.1109
2.7540E+01	1.09186E-08	0.1207
2.7560E+01	9.24596E-09	0.1251
2.7580E+01	9.91876E-09	0.1272
2.7600E+01	8.05507E-09	0.1284
2.7620E+01	1.09798E-08	0.1201
2.7640E+01	9.45773E-09	0.1290
2.7660E+01	9.33403E-09	0.1329
2.7680E+01	8.61410E-09	0.1389
2.7700E+01	9.52464E-09	0.1332
2.7720E+01	9.00279E-09	0.1341
2.7740E+01	7.32441E-09	0.1474
2.7760E+01	7.95747E-09	0.1441
2.7780E+01	7.89506E-09	0.1444
2.7800E+01	7.83157E-09	0.1463
2.7820E+01	8.18333E-09	0.1454
2.7840E+01	9.57448E-09	0.1392
2.7860E+01	7.57232E-09	0.1519
2.7880E+01	6.81092E-09	0.1538
2.7900E+01	8.05584E-09	0.1511
2.7920E+01	7.78535E-09	0.1495
2.7940E+01	6.25203E-09	0.1527
2.7960E+01	7.17647E-09	0.1547
2.7980E+01	6.76837E-09	0.1629
2.8000E+01	6.72410E-09	0.1557
2.8020E+01	7.76113E-09	0.1485
2.8040E+01	8.01277E-09	0.1393
2.8060E+01	7.68910E-09	0.1496
2.8080E+01	7.65358E-09	0.1509
2.8100E+01	7.68949E-09	0.1460
2.8120E+01	6.42418E-09	0.1603
2.8140E+01	6.62070E-09	0.1600
2.8160E+01	6.56973E-09	0.1620
2.8180E+01	7.01892E-09	0.1482
2.8200E+01	8.71864E-09	0.1436
2.8220E+01	7.77338E-09	0.1469
2.8240E+01	8.08766E-09	0.1511
2.8260E+01	8.06109E-09	0.1449
2.8280E+01	8.65165E-09	0.1426
2.8300E+01	7.52695E-09	0.1544
2.8320E+01	6.27920E-09	0.1576
2.8340E+01	6.94963E-09	0.1539

2.8360E+01	9.02695E-09	0.1450
2.8380E+01	7.72967E-09	0.1516
2.8400E+01	6.39789E-09	0.1603
2.8420E+01	7.36475E-09	0.1531
2.8440E+01	5.88187E-09	0.1716
2.8460E+01	7.07549E-09	0.1608
2.8480E+01	7.26357E-09	0.1572
2.8500E+01	7.38503E-09	0.1550
2.8520E+01	7.51895E-09	0.1536
2.8540E+01	6.80072E-09	0.1518
2.8560E+01	5.59884E-09	0.1689
2.8580E+01	6.44270E-09	0.1602
2.8600E+01	7.02431E-09	0.1572
2.8620E+01	7.17811E-09	0.1538
2.8640E+01	6.93801E-09	0.1560
2.8660E+01	5.76850E-09	0.1658
2.8680E+01	5.39281E-09	0.1681
2.8700E+01	6.78261E-09	0.1542
2.8720E+01	4.89349E-09	0.1747
2.8740E+01	4.69155E-09	0.1819
2.8760E+01	6.10259E-09	0.1653
2.8780E+01	5.76076E-09	0.1634
2.8800E+01	4.83892E-09	0.1819
2.8820E+01	5.78146E-09	0.1673
2.8840E+01	6.31865E-09	0.1543
2.8860E+01	7.02894E-09	0.1510
2.8880E+01	6.36988E-09	0.1558
2.8900E+01	6.77156E-09	0.1549
2.8920E+01	6.11197E-09	0.1595
2.8940E+01	5.44147E-09	0.1725
2.8960E+01	3.99471E-09	0.1872
2.8980E+01	5.37411E-09	0.1706
2.9000E+01	6.37229E-09	0.1563
2.9020E+01	7.33765E-09	0.1441
2.9040E+01	6.07779E-09	0.1578
2.9060E+01	4.43229E-09	0.1779
2.9080E+01	4.16724E-09	0.1781
2.9100E+01	4.65940E-09	0.1802
2.9120E+01	5.51830E-09	0.1671
2.9140E+01	5.27212E-09	0.1707
2.9160E+01	4.54284E-09	0.1733
2.9180E+01	4.36522E-09	0.1819
2.9200E+01	4.62135E-09	0.1911
2.9220E+01	3.33605E-09	0.2021
2.9240E+01	3.90516E-09	0.1977
2.9260E+01	4.54276E-09	0.1780
2.9280E+01	5.65279E-09	0.1703
2.9300E+01	5.11562E-09	0.1745
2.9320E+01	4.47440E-09	0.1796
2.9340E+01	4.46581E-09	0.1754
2.9360E+01	4.86604E-09	0.1690
2.9380E+01	5.83140E-09	0.1561
2.9400E+01	5.11896E-09	0.1669
2.9420E+01	4.85029E-09	0.1729
2.9440E+01	3.56967E-09	0.1898
2.9460E+01	2.90431E-09	0.2040
2.9480E+01	4.57041E-09	0.1776
2.9500E+01	3.86198E-09	0.1900
2.9520E+01	3.60257E-09	0.2057
2.9540E+01	3.43319E-09	0.2076
2.9560E+01	4.18246E-09	0.1881
2.9580E+01	3.79964E-09	0.2039
2.9600E+01	3.17913E-09	0.2099
2.9620E+01	3.31730E-09	0.1969
2.9640E+01	2.93845E-09	0.2210
2.9660E+01	2.93349E-09	0.2246
2.9680E+01	3.48814E-09	0.2004
2.9700E+01	3.67361E-09	0.1959
2.9720E+01	3.94894E-09	0.1821
2.9740E+01	3.96223E-09	0.1731
2.9760E+01	3.49686E-09	0.1880

2.9780E+01	4.34154E-09	0.1717
2.9800E+01	3.66391E-09	0.1916
2.9820E+01	5.08240E-09	0.1745
2.9840E+01	4.80718E-09	0.1777
2.9860E+01	4.15123E-09	0.1794
2.9880E+01	3.29391E-09	0.2098
2.9900E+01	3.39020E-09	0.2077
2.9920E+01	3.43348E-09	0.2032
2.9940E+01	1.98926E-09	0.2220
2.9960E+01	2.89013E-09	0.2278
2.9980E+01	3.13517E-09	0.2170
3.0000E+01	3.13854E-09	0.2172
total	3.99939E-04	0.0009

dump no. 2 on file runtpe nps = 20000000 coll = 61394843 ctm = 7.46
nrn = 521016999

4 warning messages so far.

run terminated when 20000000 particle histories were done.

computer time = 7.47 minutes

mcnpx version 2.5e Mon Feb 23 09:00:00 MST 2004 04/15/05 14:58:32 probid
= 04/15/05 14:53:49


```

67-      sp2 0 1
68-      C +-----+
69-      C |
70-      C |                      Material Card
71-      C |
72-      C +-----+
73-      C *****
74-      C * Plastic Scintillator (Mass Density = 1.032 gm/cc) *
75-      C *****
76-      m1 1001 1.0 6012 1.0
77-      C +-----+
78-      C |
79-      C |                      Tally Card
80-      C |
81-      C +-----+
82-      C *****
83-      C * Energy Deposition Tally (Type 6) *
84-      C *****
85-      f6:n 2
86-      C 0.2 ns time binning
87-      t6 0.0 4999i 100.0
88-      fq6 t s
89-      C +-----+
90-      C |
91-      C |                      Control Card
92-      C |
93-      C +-----+
94-      C *****
95-      C * Number of Source Particles *
96-      C *****
97-      nps 20000000
98-      C *****
99-      C * Output Options *
100-     C *****
101-     print -30

```

probability distribution 1 for source variable erg
energy function 4: gaussian (fusion) spectrum

$$f(e)=c*\exp(-((e-b)/a)**2)$$

fusion temperature	fusion width(a)	fusion energy(b)	fusion constant(c)	fusion fwhm
9.0000E-04	4.7041E-02	2.4541E+00	1.1994E+01	7.8328E-02

the mean of source distribution 1 is 2.4541E+00

warning. source variable rad is sampled uniformly.

probability distribution 2 for source variable rad
unbiased histogram distribution

source entry	source value	cumulative probability	probability of bin
1	0.00000E+00	0.000000E+00	0.000000E+00
2	3.80990E+00	1.000000E+00	1.000000E+00

the mean of source distribution 2 is 1.9049E+00

print table 126

average	tracks average cell entering	population	collisions	collisions * weight	number weighted	flux weighted	track
weight (relative)	track mfp (cm)			(per history)	energy	energy	

1	1	20889562	20000000	0	0.0000E+00	2.4366E+00	2.4536E+00
1.0000E+00		0.0000E+00					
2	2	20000000	20000000	6757425	3.3786E-01	8.0288E-01	2.2172E+00
9.9999E-01		4.6693E+00					

total		40889562	40000000	6757425	3.3786E-01		
-------	--	----------	----------	---------	------------	--	--

ltally 6 nps = 20000000
 tally type 6 track length estimate of heating. units mev/gram
 particle(s): neutron

masses
 cell: 2
 5.97700E+01

cell 2
 time

2.4000E+01	0.00000E+00	0.0000
2.4020E+01	0.00000E+00	0.0000
2.4040E+01	0.00000E+00	0.0000
2.4060E+01	0.00000E+00	0.0000
2.4080E+01	0.00000E+00	0.0000
2.4100E+01	0.00000E+00	0.0000
2.4120E+01	0.00000E+00	0.0000
2.4140E+01	4.90431E-11	0.6478
2.4160E+01	2.10490E-10	0.5774
2.4180E+01	3.14156E-10	0.4269
2.4200E+01	8.70767E-10	0.2554
2.4220E+01	1.66234E-09	0.1908
2.4240E+01	2.87916E-09	0.1435
2.4260E+01	4.84290E-09	0.1084
2.4280E+01	8.61434E-09	0.0812
2.4300E+01	1.55015E-08	0.0618
2.4320E+01	2.60275E-08	0.0472
2.4340E+01	4.37474E-08	0.0366
2.4360E+01	7.02150E-08	0.0288
2.4380E+01	1.14707E-07	0.0225
2.4400E+01	1.84054E-07	0.0178
2.4420E+01	2.94483E-07	0.0140
2.4440E+01	4.65129E-07	0.0112
2.4460E+01	7.13821E-07	0.0090
2.4480E+01	1.06566E-06	0.0074
2.4500E+01	1.57425E-06	0.0061
2.4520E+01	2.29435E-06	0.0050
2.4540E+01	3.28773E-06	0.0042
2.4560E+01	4.64282E-06	0.0035
2.4580E+01	6.44388E-06	0.0030
2.4600E+01	8.79086E-06	0.0026
2.4620E+01	1.18323E-05	0.0022
2.4640E+01	1.56404E-05	0.0019
2.4660E+01	2.03732E-05	0.0017
2.4680E+01	2.60687E-05	0.0015
2.4700E+01	3.29157E-05	0.0013
2.4720E+01	4.09470E-05	0.0012
2.4740E+01	5.01497E-05	0.0010
2.4760E+01	6.05156E-05	0.0009
2.4780E+01	7.17921E-05	0.0009
2.4800E+01	8.39111E-05	0.0008
2.4820E+01	9.67607E-05	0.0007
2.4840E+01	1.10005E-04	0.0007
2.4860E+01	1.23188E-04	0.0006
2.4880E+01	1.35872E-04	0.0006
2.4900E+01	1.47691E-04	0.0006
2.4920E+01	1.58313E-04	0.0006
2.4940E+01	1.67374E-04	0.0005
2.4960E+01	1.74410E-04	0.0005
2.4980E+01	1.79298E-04	0.0005
2.5000E+01	1.81756E-04	0.0005
2.5020E+01	1.81761E-04	0.0005
2.5040E+01	1.79233E-04	0.0005
2.5060E+01	1.74433E-04	0.0005

2.5080E+01	1.67475E-04	0.0005
2.5100E+01	1.58593E-04	0.0005
2.5120E+01	1.48265E-04	0.0006
2.5140E+01	1.36855E-04	0.0006
2.5160E+01	1.24882E-04	0.0006
2.5180E+01	1.12468E-04	0.0007
2.5200E+01	1.00052E-04	0.0007
2.5220E+01	8.78349E-05	0.0007
2.5240E+01	7.61714E-05	0.0008
2.5260E+01	6.53184E-05	0.0009
2.5280E+01	5.53015E-05	0.0009
2.5300E+01	4.63592E-05	0.0010
2.5320E+01	3.84153E-05	0.0011
2.5340E+01	3.15178E-05	0.0013
2.5360E+01	2.55482E-05	0.0014
2.5380E+01	2.04710E-05	0.0015
2.5400E+01	1.62539E-05	0.0017
2.5420E+01	1.27794E-05	0.0019
2.5440E+01	1.00011E-05	0.0022
2.5460E+01	7.75313E-06	0.0025
2.5480E+01	5.96512E-06	0.0028
2.5500E+01	4.56824E-06	0.0031
2.5520E+01	3.48552E-06	0.0035
2.5540E+01	2.65018E-06	0.0040
2.5560E+01	2.00023E-06	0.0045
2.5580E+01	1.51992E-06	0.0050
2.5600E+01	1.15943E-06	0.0055
2.5620E+01	8.94896E-07	0.0061
2.5640E+01	6.94072E-07	0.0066
2.5660E+01	5.40500E-07	0.0070
2.5680E+01	4.27138E-07	0.0075
2.5700E+01	3.41978E-07	0.0078
2.5720E+01	2.77626E-07	0.0081
2.5740E+01	2.28745E-07	0.0082
2.5760E+01	1.91322E-07	0.0082
2.5780E+01	1.62474E-07	0.0081
2.5800E+01	1.41199E-07	0.0082
2.5820E+01	1.22318E-07	0.0081
2.5840E+01	1.07213E-07	0.0080
2.5860E+01	9.46490E-08	0.0077
2.5880E+01	8.43955E-08	0.0077
2.5900E+01	7.54595E-08	0.0076
2.5920E+01	6.72377E-08	0.0072
2.5940E+01	6.04789E-08	0.0070
2.5960E+01	5.48979E-08	0.0070
2.5980E+01	4.99479E-08	0.0072
2.6000E+01	4.57202E-08	0.0073
2.6020E+01	4.16799E-08	0.0071
2.6040E+01	3.81827E-08	0.0071
2.6060E+01	3.49700E-08	0.0072
2.6080E+01	3.22708E-08	0.0073
2.6100E+01	2.97949E-08	0.0074
2.6120E+01	2.74123E-08	0.0074
2.6140E+01	2.53791E-08	0.0075
2.6160E+01	2.35895E-08	0.0076
2.6180E+01	2.19305E-08	0.0077
2.6200E+01	2.02907E-08	0.0077
2.6220E+01	1.88395E-08	0.0078
2.6240E+01	1.75347E-08	0.0079
2.6260E+01	1.63844E-08	0.0080
2.6280E+01	1.53112E-08	0.0081
2.6300E+01	1.43240E-08	0.0083
2.6320E+01	1.34644E-08	0.0084
2.6340E+01	1.26666E-08	0.0085
2.6360E+01	1.18919E-08	0.0086
2.6380E+01	1.11707E-08	0.0086
2.6400E+01	1.05077E-08	0.0086
2.6420E+01	9.85853E-09	0.0086
2.6440E+01	9.27406E-09	0.0086
2.6460E+01	8.76111E-09	0.0088
2.6480E+01	8.26732E-09	0.0088

2.6500E+01	7.78661E-09	0.0089
2.6520E+01	7.34350E-09	0.0089
2.6540E+01	6.93344E-09	0.0090
2.6560E+01	6.54726E-09	0.0091
2.6580E+01	6.19979E-09	0.0091
2.6600E+01	5.86278E-09	0.0092
2.6620E+01	5.54602E-09	0.0093
2.6640E+01	5.24972E-09	0.0093
2.6660E+01	4.97913E-09	0.0094
2.6680E+01	4.72351E-09	0.0094
2.6700E+01	4.48681E-09	0.0094
2.6720E+01	4.26665E-09	0.0094
2.6740E+01	4.06489E-09	0.0095
2.6760E+01	3.88054E-09	0.0096
2.6780E+01	3.70115E-09	0.0096
2.6800E+01	3.52725E-09	0.0097
2.6820E+01	3.36963E-09	0.0098
2.6840E+01	3.22318E-09	0.0098
2.6860E+01	3.07764E-09	0.0099
2.6880E+01	2.93807E-09	0.0100
2.6900E+01	2.80968E-09	0.0100
2.6920E+01	2.67820E-09	0.0100
2.6940E+01	2.54971E-09	0.0099
2.6960E+01	2.43580E-09	0.0099
2.6980E+01	2.33921E-09	0.0100
2.7000E+01	2.24708E-09	0.0101
2.7020E+01	2.15409E-09	0.0102
2.7040E+01	2.06697E-09	0.0102
2.7060E+01	1.97685E-09	0.0100
2.7080E+01	1.89845E-09	0.0101
2.7100E+01	1.81819E-09	0.0102
2.7120E+01	1.74426E-09	0.0102
2.7140E+01	1.68101E-09	0.0103
2.7160E+01	1.62166E-09	0.0102
2.7180E+01	1.56072E-09	0.0103
2.7200E+01	1.50686E-09	0.0104
2.7220E+01	1.44864E-09	0.0103
2.7240E+01	1.39231E-09	0.0103
2.7260E+01	1.33595E-09	0.0102
2.7280E+01	1.28501E-09	0.0103
2.7300E+01	1.23969E-09	0.0103
2.7320E+01	1.19727E-09	0.0104
2.7340E+01	1.15609E-09	0.0105
2.7360E+01	1.11803E-09	0.0105
2.7380E+01	1.07821E-09	0.0106
2.7400E+01	1.03964E-09	0.0106
2.7420E+01	1.00488E-09	0.0107
2.7440E+01	9.71240E-10	0.0108
2.7460E+01	9.39500E-10	0.0108
2.7480E+01	9.07128E-10	0.0109
2.7500E+01	8.79465E-10	0.0110
2.7520E+01	8.50927E-10	0.0110
2.7540E+01	8.24824E-10	0.0111
2.7560E+01	7.98516E-10	0.0112
2.7580E+01	7.71961E-10	0.0112
2.7600E+01	7.48612E-10	0.0112
2.7620E+01	7.25933E-10	0.0112
2.7640E+01	7.03161E-10	0.0113
2.7660E+01	6.81592E-10	0.0114
2.7680E+01	6.61342E-10	0.0114
2.7700E+01	6.42067E-10	0.0114
2.7720E+01	6.22549E-10	0.0115
2.7740E+01	6.04518E-10	0.0115
2.7760E+01	5.86912E-10	0.0114
2.7780E+01	5.69794E-10	0.0115
2.7800E+01	5.52392E-10	0.0115
2.7820E+01	5.36703E-10	0.0115
2.7840E+01	5.22495E-10	0.0116
2.7860E+01	5.09676E-10	0.0117
2.7880E+01	4.95284E-10	0.0117
2.7900E+01	4.80430E-10	0.0118

2.7920E+01	4.67705E-10	0.0118
2.7940E+01	4.55423E-10	0.0118
2.7960E+01	4.42136E-10	0.0119
2.7980E+01	4.28731E-10	0.0118
2.8000E+01	4.15628E-10	0.0116
2.8020E+01	4.03687E-10	0.0116
2.8040E+01	3.92113E-10	0.0117
2.8060E+01	3.81184E-10	0.0117
2.8080E+01	3.71692E-10	0.0118
2.8100E+01	3.62218E-10	0.0118
2.8120E+01	3.53101E-10	0.0118
2.8140E+01	3.43953E-10	0.0118
2.8160E+01	3.34783E-10	0.0119
2.8180E+01	3.25424E-10	0.0118
2.8200E+01	3.17083E-10	0.0118
2.8220E+01	3.08816E-10	0.0118
2.8240E+01	3.01092E-10	0.0117
2.8260E+01	2.93254E-10	0.0117
2.8280E+01	2.86444E-10	0.0117
2.8300E+01	2.79508E-10	0.0117
2.8320E+01	2.73564E-10	0.0118
2.8340E+01	2.67700E-10	0.0118
2.8360E+01	2.61097E-10	0.0119
2.8380E+01	2.55240E-10	0.0119
2.8400E+01	2.49434E-10	0.0120
2.8420E+01	2.43794E-10	0.0120
2.8440E+01	2.38584E-10	0.0121
2.8460E+01	2.32569E-10	0.0122
2.8480E+01	2.27737E-10	0.0122
2.8500E+01	2.22421E-10	0.0122
2.8520E+01	2.16743E-10	0.0122
2.8540E+01	2.11651E-10	0.0122
2.8560E+01	2.06356E-10	0.0123
2.8580E+01	2.01768E-10	0.0123
2.8600E+01	1.98092E-10	0.0123
2.8620E+01	1.93989E-10	0.0124
2.8640E+01	1.90256E-10	0.0124
2.8660E+01	1.86323E-10	0.0125
2.8680E+01	1.82213E-10	0.0125
2.8700E+01	1.78259E-10	0.0126
2.8720E+01	1.75087E-10	0.0126
2.8740E+01	1.70939E-10	0.0126
2.8760E+01	1.66855E-10	0.0126
2.8780E+01	1.63287E-10	0.0126
2.8800E+01	1.59785E-10	0.0127
2.8820E+01	1.56197E-10	0.0127
2.8840E+01	1.52706E-10	0.0128
2.8860E+01	1.49976E-10	0.0128
2.8880E+01	1.47113E-10	0.0129
2.8900E+01	1.43987E-10	0.0130
2.8920E+01	1.41156E-10	0.0130
2.8940E+01	1.37883E-10	0.0129
2.8960E+01	1.35063E-10	0.0129
2.8980E+01	1.32221E-10	0.0129
2.9000E+01	1.29817E-10	0.0130
2.9020E+01	1.27358E-10	0.0130
2.9040E+01	1.25258E-10	0.0131
2.9060E+01	1.22827E-10	0.0131
2.9080E+01	1.20380E-10	0.0131
2.9100E+01	1.18035E-10	0.0130
2.9120E+01	1.16274E-10	0.0131
2.9140E+01	1.14309E-10	0.0131
2.9160E+01	1.12234E-10	0.0132
2.9180E+01	1.10084E-10	0.0131
2.9200E+01	1.08225E-10	0.0132
2.9220E+01	1.06272E-10	0.0132
2.9240E+01	1.04693E-10	0.0133
2.9260E+01	1.02991E-10	0.0133
2.9280E+01	1.01346E-10	0.0134
2.9300E+01	9.96974E-11	0.0134
2.9320E+01	9.80185E-11	0.0135

2.9340E+01	9.64351E-11	0.0135
2.9360E+01	9.45673E-11	0.0135
2.9380E+01	9.28491E-11	0.0136
2.9400E+01	9.13762E-11	0.0136
2.9420E+01	8.97848E-11	0.0137
2.9440E+01	8.80057E-11	0.0135
2.9460E+01	8.60921E-11	0.0135
2.9480E+01	8.44103E-11	0.0135
2.9500E+01	8.30773E-11	0.0135
2.9520E+01	8.15359E-11	0.0136
2.9540E+01	7.99740E-11	0.0136
2.9560E+01	7.84824E-11	0.0136
2.9580E+01	7.72083E-11	0.0136
2.9600E+01	7.57366E-11	0.0136
2.9620E+01	7.44399E-11	0.0136
2.9640E+01	7.32284E-11	0.0136
2.9660E+01	7.21006E-11	0.0137
2.9680E+01	7.11005E-11	0.0137
2.9700E+01	6.97745E-11	0.0136
2.9720E+01	6.84980E-11	0.0136
2.9740E+01	6.74373E-11	0.0136
2.9760E+01	6.63937E-11	0.0136
2.9780E+01	6.54751E-11	0.0136
2.9800E+01	6.45217E-11	0.0137
2.9820E+01	6.34309E-11	0.0137
2.9840E+01	6.24864E-11	0.0138
2.9860E+01	6.13645E-11	0.0138
2.9880E+01	6.03137E-11	0.0138
2.9900E+01	5.93858E-11	0.0139
2.9920E+01	5.84762E-11	0.0140
2.9940E+01	5.75776E-11	0.0140
2.9960E+01	5.67651E-11	0.0140
2.9980E+01	5.58118E-11	0.0140
3.0000E+01	5.47115E-11	0.0140
3.0020E+01	5.38698E-11	0.0140
3.0040E+01	5.30021E-11	0.0140
3.0060E+01	5.20870E-11	0.0141
3.0080E+01	5.11606E-11	0.0141
3.0100E+01	5.03894E-11	0.0141
3.0120E+01	4.96748E-11	0.0141
3.0140E+01	4.88667E-11	0.0142
3.0160E+01	4.81990E-11	0.0142
3.0180E+01	4.75167E-11	0.0143
3.0200E+01	4.69614E-11	0.0144
3.0220E+01	4.61305E-11	0.0144
3.0240E+01	4.54006E-11	0.0143
3.0260E+01	4.47538E-11	0.0144
3.0280E+01	4.40900E-11	0.0144
3.0300E+01	4.35372E-11	0.0145
3.0320E+01	4.28993E-11	0.0145
3.0340E+01	4.23007E-11	0.0145
3.0360E+01	4.15812E-11	0.0144
3.0380E+01	4.08285E-11	0.0144
3.0400E+01	4.02887E-11	0.0144
3.0420E+01	3.96803E-11	0.0144
3.0440E+01	3.92254E-11	0.0144
3.0460E+01	3.87211E-11	0.0145
3.0480E+01	3.81641E-11	0.0145
3.0500E+01	3.77457E-11	0.0146
3.0520E+01	3.72666E-11	0.0147
3.0540E+01	3.67559E-11	0.0147
3.0560E+01	3.62854E-11	0.0148
3.0580E+01	3.57856E-11	0.0147
3.0600E+01	3.53456E-11	0.0147
3.0620E+01	3.48198E-11	0.0147
3.0640E+01	3.43472E-11	0.0148
3.0660E+01	3.38505E-11	0.0148
3.0680E+01	3.33829E-11	0.0147
3.0700E+01	3.29660E-11	0.0148
3.0720E+01	3.25490E-11	0.0148
3.0740E+01	3.21269E-11	0.0149

3.0760E+01	3.17744E-11	0.0149
3.0780E+01	3.13956E-11	0.0149
3.0800E+01	3.09165E-11	0.0150
3.0820E+01	3.05328E-11	0.0150
3.0840E+01	3.01618E-11	0.0151
3.0860E+01	2.97626E-11	0.0151
3.0880E+01	2.93504E-11	0.0151
3.0900E+01	2.90266E-11	0.0152
3.0920E+01	2.87264E-11	0.0152
3.0940E+01	2.84017E-11	0.0153
3.0960E+01	2.79977E-11	0.0152
3.0980E+01	2.76355E-11	0.0152
3.1000E+01	2.72849E-11	0.0153
3.1020E+01	2.69635E-11	0.0154
3.1040E+01	2.66578E-11	0.0154
3.1060E+01	2.63342E-11	0.0155
3.1080E+01	2.60436E-11	0.0155
3.1100E+01	2.57501E-11	0.0156
3.1120E+01	2.54818E-11	0.0157
3.1140E+01	2.51840E-11	0.0157
3.1160E+01	2.48229E-11	0.0157
3.1180E+01	2.44884E-11	0.0157
3.1200E+01	2.42046E-11	0.0158
3.1220E+01	2.38532E-11	0.0157
3.1240E+01	2.35035E-11	0.0157
3.1260E+01	2.32004E-11	0.0156
3.1280E+01	2.28738E-11	0.0156
3.1300E+01	2.25961E-11	0.0157
3.1320E+01	2.22520E-11	0.0157
3.1340E+01	2.19599E-11	0.0157
3.1360E+01	2.16349E-11	0.0157
3.1380E+01	2.13700E-11	0.0157
3.1400E+01	2.10684E-11	0.0157
3.1420E+01	2.07907E-11	0.0157
3.1440E+01	2.05899E-11	0.0157
3.1460E+01	2.03357E-11	0.0158
3.1480E+01	2.00908E-11	0.0159
3.1500E+01	1.98199E-11	0.0159
3.1520E+01	1.96323E-11	0.0160
3.1540E+01	1.94338E-11	0.0160
3.1560E+01	1.91799E-11	0.0160
3.1580E+01	1.89362E-11	0.0160
3.1600E+01	1.87046E-11	0.0160
3.1620E+01	1.84653E-11	0.0160
3.1640E+01	1.82709E-11	0.0160
3.1660E+01	1.80963E-11	0.0161
3.1680E+01	1.79385E-11	0.0162
3.1700E+01	1.77516E-11	0.0162
3.1720E+01	1.75907E-11	0.0163
3.1740E+01	1.73972E-11	0.0164
3.1760E+01	1.71707E-11	0.0164
3.1780E+01	1.70151E-11	0.0165
3.1800E+01	1.68112E-11	0.0165
3.1820E+01	1.65971E-11	0.0165
3.1840E+01	1.63808E-11	0.0166
3.1860E+01	1.61876E-11	0.0166
3.1880E+01	1.60288E-11	0.0167
3.1900E+01	1.58692E-11	0.0167
3.1920E+01	1.57053E-11	0.0168
3.1940E+01	1.55637E-11	0.0169
3.1960E+01	1.54179E-11	0.0170
3.1980E+01	1.52343E-11	0.0170
3.2000E+01	1.50490E-11	0.0170
3.2020E+01	1.48424E-11	0.0169
3.2040E+01	1.46809E-11	0.0170
3.2060E+01	1.45293E-11	0.0170
3.2080E+01	1.43508E-11	0.0170
3.2100E+01	1.42203E-11	0.0171
3.2120E+01	1.40806E-11	0.0172
3.2140E+01	1.39427E-11	0.0172
3.2160E+01	1.38229E-11	0.0173

3.2180E+01	1.36925E-11	0.0174
3.2200E+01	1.35706E-11	0.0175
3.2220E+01	1.34534E-11	0.0175
3.2240E+01	1.33287E-11	0.0176
3.2260E+01	1.31883E-11	0.0176
3.2280E+01	1.30083E-11	0.0175
3.2300E+01	1.28432E-11	0.0175
3.2320E+01	1.26656E-11	0.0173
3.2340E+01	1.25070E-11	0.0174
3.2360E+01	1.23546E-11	0.0174
3.2380E+01	1.22167E-11	0.0174
3.2400E+01	1.20375E-11	0.0173
3.2420E+01	1.18912E-11	0.0174
3.2440E+01	1.17650E-11	0.0175
3.2460E+01	1.16676E-11	0.0175
3.2480E+01	1.15720E-11	0.0176
3.2500E+01	1.14656E-11	0.0177
3.2520E+01	1.13564E-11	0.0177
3.2540E+01	1.12365E-11	0.0174
3.2560E+01	1.11512E-11	0.0174
3.2580E+01	1.10264E-11	0.0173
3.2600E+01	1.09482E-11	0.0173
3.2620E+01	1.08338E-11	0.0174
3.2640E+01	1.07352E-11	0.0174
3.2660E+01	1.06416E-11	0.0175
3.2680E+01	1.05392E-11	0.0174
3.2700E+01	1.04321E-11	0.0173
3.2720E+01	1.03249E-11	0.0173
3.2740E+01	1.02068E-11	0.0167
3.2760E+01	1.00755E-11	0.0165
3.2780E+01	9.96559E-12	0.0166
3.2800E+01	9.88008E-12	0.0166
3.2820E+01	9.77655E-12	0.0166
3.2840E+01	9.68007E-12	0.0166
3.2860E+01	9.54530E-12	0.0166
3.2880E+01	9.44783E-12	0.0166
3.2900E+01	9.36405E-12	0.0167
3.2920E+01	9.27322E-12	0.0167
3.2940E+01	9.19122E-12	0.0167
3.2960E+01	9.08738E-12	0.0167
3.2980E+01	8.99490E-12	0.0167
3.3000E+01	8.91750E-12	0.0168
total	3.92327E-03	0.0001

dump no. 2 on file runtpe nps = 2000000 coll = 6757425 ctm = 5.88
nrn = 197129716

4 warning messages so far.

run terminated when 20000000 particle histories were done.

computer time = 5.88 minutes

mcnp version 2.5e Mon Feb 23 09:00:00 MST 2004 10/03/05 15:15:31 probid
= 10/03/05 15:12:27


```

67-      sp2 0 1
68-      C +-----+
69-      C |
70-      C |                      Material Card
71-      C |
72-      C +-----+
73-      C *****
74-      C * Plastic Scintillator (Mass Density = 1.032 gm/cc) *
75-      C *****
76-      m1 1001 1.0 6012 1.0
77-      C +-----+
78-      C |
79-      C |                      Tally Card
80-      C |
81-      C +-----+
82-      C *****
83-      C * Energy Deposition Tally (Type 6) *
84-      C *****
85-      f6:n 2
86-      C 0.2 ns time binning
87-      t6 0.0 4999i 100.0
88-      fq6 t s
89-      C +-----+
90-      C |
91-      C |                      Control Card
92-      C |
93-      C +-----+
94-      C *****
95-      C * Number of Source Particles *
96-      C *****
97-      nps 20000000
98-      C *****
99-      C * Output Options *
100-     C *****
101-     print -30

```

probability distribution 1 for source variable erg
energy function 4: gaussian (fusion) spectrum

$$f(e)=c*\exp(-((e-b)/a)**2)$$

fusion temperature	fusion width(a)	fusion energy(b)	fusion constant(c)	fusion fwhm
3.3000E-03	9.0204E-02	2.4611E+00	6.2546E+00	1.5020E-01

the mean of source distribution 1 is 2.4611E+00

warning. source variable rad is sampled uniformly.

probability distribution 2 for source variable rad
unbiased histogram distribution

source entry	source value	cumulative probability	probability of bin
1	0.00000E+00	0.000000E+00	0.000000E+00
2	3.80990E+00	1.000000E+00	1.000000E+00

the mean of source distribution 2 is 1.9049E+00

print table 126

average weight (relative)	tracks average cell track (cm)	population entering mfp	collisions	collisions * weight (per history)	number weighted energy	flux weighted energy	track
---------------------------	--------------------------------	-------------------------	------------	-----------------------------------	------------------------	----------------------	-------

1	1	20240902	20000000	0	0.0000E+00	2.4596E+00	2.4609E+00
1.0000E+00		0.0000E+00					
2	2	20000000	20000000	1392591	6.9629E-02	2.1359E+00	2.3895E+00
1.0000E+00		4.9082E+00					
total		40240902	40000000	1392591	6.9629E-02		

ltally 6 nps = 20000000
tally type 6 track length estimate of heating. units mev/gram
particle(s): neutron

masses
cell: 2
1.49425E+01

cell 2
time

2.3400E+01	0.000000E+00	0.0000
2.3420E+01	4.47430E-10	0.6175
2.3440E+01	1.85419E-10	0.7823
2.3460E+01	0.000000E+00	0.0000
2.3480E+01	3.45874E-10	0.6652
2.3500E+01	1.10128E-09	0.3713
2.3520E+01	1.25510E-09	0.3519
2.3540E+01	1.48247E-09	0.3295
2.3560E+01	2.26563E-09	0.2724
2.3580E+01	1.98158E-09	0.2738
2.3600E+01	3.76310E-09	0.2147
2.3620E+01	5.69690E-09	0.1697
2.3640E+01	7.42839E-09	0.1469
2.3660E+01	1.08771E-08	0.1208
2.3680E+01	1.43838E-08	0.1050
2.3700E+01	1.73251E-08	0.0957
2.3720E+01	2.30602E-08	0.0830
2.3740E+01	3.44312E-08	0.0684
2.3760E+01	4.36968E-08	0.0606
2.3780E+01	5.06466E-08	0.0555
2.3800E+01	7.10937E-08	0.0470
2.3820E+01	9.36854E-08	0.0407
2.3840E+01	1.20324E-07	0.0359
2.3860E+01	1.57930E-07	0.0315
2.3880E+01	2.00869E-07	0.0278
2.3900E+01	2.61685E-07	0.0242
2.3920E+01	3.47522E-07	0.0211
2.3940E+01	4.27908E-07	0.0189
2.3960E+01	5.32483E-07	0.0170
2.3980E+01	6.66048E-07	0.0152
2.4000E+01	8.06195E-07	0.0138
2.4020E+01	1.00548E-06	0.0123
2.4040E+01	1.25596E-06	0.0110
2.4060E+01	1.53329E-06	0.0100
2.4080E+01	1.86418E-06	0.0091
2.4100E+01	2.25772E-06	0.0082
2.4120E+01	2.69126E-06	0.0075
2.4140E+01	3.27715E-06	0.0068
2.4160E+01	3.88938E-06	0.0062
2.4180E+01	4.62983E-06	0.0057
2.4200E+01	5.39544E-06	0.0053
2.4220E+01	6.35385E-06	0.0049
2.4240E+01	7.45917E-06	0.0045
2.4260E+01	8.73348E-06	0.0042
2.4280E+01	1.00224E-05	0.0039
2.4300E+01	1.15319E-05	0.0036
2.4320E+01	1.31531E-05	0.0034
2.4340E+01	1.51051E-05	0.0031
2.4360E+01	1.71295E-05	0.0029
2.4380E+01	1.92580E-05	0.0028
2.4400E+01	2.16519E-05	0.0026
2.4420E+01	2.43529E-05	0.0025
2.4440E+01	2.70820E-05	0.0023
2.4460E+01	3.00242E-05	0.0022

2.4480E+01	3.31094E-05	0.0021
2.4500E+01	3.64248E-05	0.0020
2.4520E+01	3.98042E-05	0.0019
2.4540E+01	4.32927E-05	0.0018
2.4560E+01	4.67341E-05	0.0018
2.4580E+01	5.04879E-05	0.0017
2.4600E+01	5.42555E-05	0.0016
2.4620E+01	5.81663E-05	0.0016
2.4640E+01	6.20146E-05	0.0015
2.4660E+01	6.57618E-05	0.0015
2.4680E+01	6.92152E-05	0.0014
2.4700E+01	7.27288E-05	0.0014
2.4720E+01	7.63164E-05	0.0014
2.4740E+01	7.93769E-05	0.0013
2.4760E+01	8.25011E-05	0.0013
2.4780E+01	8.52528E-05	0.0013
2.4800E+01	8.77150E-05	0.0013
2.4820E+01	9.00817E-05	0.0013
2.4840E+01	9.20470E-05	0.0012
2.4860E+01	9.36894E-05	0.0012
2.4880E+01	9.46849E-05	0.0012
2.4900E+01	9.55676E-05	0.0012
2.4920E+01	9.62766E-05	0.0012
2.4940E+01	9.64580E-05	0.0012
2.4960E+01	9.61340E-05	0.0012
2.4980E+01	9.54363E-05	0.0012
2.5000E+01	9.45189E-05	0.0012
2.5020E+01	9.30126E-05	0.0012
2.5040E+01	9.14583E-05	0.0012
2.5060E+01	8.97302E-05	0.0012
2.5080E+01	8.75298E-05	0.0013
2.5100E+01	8.48036E-05	0.0013
2.5120E+01	8.20954E-05	0.0013
2.5140E+01	7.90997E-05	0.0013
2.5160E+01	7.59552E-05	0.0014
2.5180E+01	7.28436E-05	0.0014
2.5200E+01	6.95611E-05	0.0014
2.5220E+01	6.61304E-05	0.0014
2.5240E+01	6.25965E-05	0.0015
2.5260E+01	5.92899E-05	0.0015
2.5280E+01	5.57244E-05	0.0016
2.5300E+01	5.23559E-05	0.0016
2.5320E+01	4.89465E-05	0.0017
2.5340E+01	4.55320E-05	0.0017
2.5360E+01	4.23540E-05	0.0018
2.5380E+01	3.91282E-05	0.0019
2.5400E+01	3.60868E-05	0.0020
2.5420E+01	3.30961E-05	0.0020
2.5440E+01	3.03619E-05	0.0021
2.5460E+01	2.77147E-05	0.0022
2.5480E+01	2.54020E-05	0.0023
2.5500E+01	2.28751E-05	0.0025
2.5520E+01	2.06273E-05	0.0026
2.5540E+01	1.87583E-05	0.0027
2.5560E+01	1.68878E-05	0.0029
2.5580E+01	1.51759E-05	0.0030
2.5600E+01	1.35455E-05	0.0032
2.5620E+01	1.20470E-05	0.0034
2.5640E+01	1.06697E-05	0.0036
2.5660E+01	9.47212E-06	0.0038
2.5680E+01	8.39291E-06	0.0041
2.5700E+01	7.35701E-06	0.0043
2.5720E+01	6.43021E-06	0.0046
2.5740E+01	5.64438E-06	0.0049
2.5760E+01	4.92260E-06	0.0053
2.5780E+01	4.28436E-06	0.0057
2.5800E+01	3.71521E-06	0.0061
2.5820E+01	3.24414E-06	0.0065
2.5840E+01	2.77182E-06	0.0070
2.5860E+01	2.40044E-06	0.0075
2.5880E+01	2.04962E-06	0.0082

2.5900E+01	1.73499E-06	0.0089
2.5920E+01	1.50836E-06	0.0095
2.5940E+01	1.30395E-06	0.0102
2.5960E+01	1.07922E-06	0.0112
2.5980E+01	9.17704E-07	0.0122
2.6000E+01	7.70316E-07	0.0132
2.6020E+01	6.52711E-07	0.0143
2.6040E+01	5.51316E-07	0.0156
2.6060E+01	4.47257E-07	0.0173
2.6080E+01	3.69655E-07	0.0191
2.6100E+01	3.16227E-07	0.0206
2.6120E+01	2.69380E-07	0.0223
2.6140E+01	2.16763E-07	0.0246
2.6160E+01	1.89402E-07	0.0264
2.6180E+01	1.57391E-07	0.0290
2.6200E+01	1.24289E-07	0.0327
2.6220E+01	1.03654E-07	0.0359
2.6240E+01	8.67533E-08	0.0393
2.6260E+01	7.19756E-08	0.0425
2.6280E+01	5.81316E-08	0.0475
2.6300E+01	4.51542E-08	0.0537
2.6320E+01	3.98714E-08	0.0577
2.6340E+01	3.01919E-08	0.0657
2.6360E+01	2.53673E-08	0.0707
2.6380E+01	1.92610E-08	0.0802
2.6400E+01	1.33253E-08	0.0947
2.6420E+01	1.42289E-08	0.0948
2.6440E+01	9.93020E-09	0.1127
2.6460E+01	6.40344E-09	0.1319
2.6480E+01	7.73074E-09	0.1255
2.6500E+01	5.04216E-09	0.1416
2.6520E+01	4.89306E-09	0.1581
2.6540E+01	3.72653E-09	0.1780
2.6560E+01	3.39775E-09	0.1840
2.6580E+01	4.19659E-09	0.1766
2.6600E+01	2.64761E-09	0.2092
2.6620E+01	1.58707E-09	0.2402
2.6640E+01	1.42117E-09	0.2547
2.6660E+01	7.21519E-10	0.3064
2.6680E+01	4.87045E-10	0.2361
2.6700E+01	1.17662E-09	0.2904
2.6720E+01	7.68243E-10	0.2828
2.6740E+01	4.71507E-10	0.2917
2.6760E+01	4.51733E-10	0.3408
2.6780E+01	4.43575E-10	0.3546
2.6800E+01	2.50459E-10	0.0848
2.6820E+01	2.32026E-10	0.0873
2.6840E+01	2.11501E-10	0.0768
2.6860E+01	1.91484E-10	0.0683
2.6880E+01	1.76810E-10	0.0600
2.6900E+01	1.64318E-10	0.0568
2.6920E+01	2.79104E-10	0.4429
2.6940E+01	2.02973E-10	0.2709
2.6960E+01	1.42283E-10	0.0586
2.6980E+01	1.34800E-10	0.0571
2.7000E+01	1.29643E-10	0.0577
2.7020E+01	1.26125E-10	0.0587
2.7040E+01	1.22062E-10	0.0592
2.7060E+01	1.17137E-10	0.0597
2.7080E+01	1.10264E-10	0.0606
2.7100E+01	1.04224E-10	0.0609
2.7120E+01	1.00549E-10	0.0619
2.7140E+01	9.79878E-11	0.0630
2.7160E+01	9.46526E-11	0.0639
2.7180E+01	9.02148E-11	0.0650
2.7200E+01	8.66578E-11	0.0663
2.7220E+01	8.37987E-11	0.0669
2.7240E+01	8.12195E-11	0.0679
2.7260E+01	7.84908E-11	0.0693
2.7280E+01	7.50050E-11	0.0712
2.7300E+01	7.29314E-11	0.0723

2.7320E+01	7.02554E-11	0.0735
2.7340E+01	6.78488E-11	0.0754
2.7360E+01	6.52290E-11	0.0765
2.7380E+01	6.33379E-11	0.0781
2.7400E+01	6.08616E-11	0.0739
2.7420E+01	5.79288E-11	0.0692
2.7440E+01	5.60947E-11	0.0694
2.7460E+01	5.44338E-11	0.0704
2.7480E+01	5.19506E-11	0.0711
2.7500E+01	4.99586E-11	0.0725
2.7520E+01	4.73703E-11	0.0742
2.7540E+01	4.52421E-11	0.0753
2.7560E+01	4.33167E-11	0.0755
2.7580E+01	4.09721E-11	0.0718
2.7600E+01	4.04425E-11	0.0724
2.7620E+01	3.98445E-11	0.0732
2.7640E+01	3.86916E-11	0.0734
2.7660E+01	3.72980E-11	0.0735
2.7680E+01	3.66597E-11	0.0739
2.7700E+01	3.39417E-11	0.0699
2.7720E+01	3.20776E-11	0.0701
2.7740E+01	3.08091E-11	0.0712
2.7760E+01	2.98769E-11	0.0723
2.7780E+01	2.91579E-11	0.0733
2.7800E+01	2.81653E-11	0.0742
2.7820E+01	2.72379E-11	0.0749
2.7840E+01	2.66264E-11	0.0758
2.7860E+01	2.57130E-11	0.0770
2.7880E+01	2.47353E-11	0.0789
2.7900E+01	2.41418E-11	0.0800
2.7920E+01	2.30249E-11	0.0796
2.7940E+01	2.22157E-11	0.0801
2.7960E+01	2.17599E-11	0.0798
2.7980E+01	2.01630E-11	0.0782
2.8000E+01	1.94789E-11	0.0790
2.8020E+01	1.90559E-11	0.0795
2.8040E+01	1.87965E-11	0.0804
2.8060E+01	1.85582E-11	0.0807
2.8080E+01	1.80584E-11	0.0813
2.8100E+01	1.71026E-11	0.0817
2.8120E+01	1.64997E-11	0.0835
2.8140E+01	1.63111E-11	0.0836
2.8160E+01	1.61990E-11	0.0841
2.8180E+01	1.56386E-11	0.0856
2.8200E+01	1.51808E-11	0.0842
2.8220E+01	1.46098E-11	0.0840
2.8240E+01	1.36263E-11	0.0784
2.8260E+01	1.33725E-11	0.0794
2.8280E+01	1.31881E-11	0.0801
2.8300E+01	1.29708E-11	0.0808
2.8320E+01	1.27266E-11	0.0811
2.8340E+01	1.23226E-11	0.0824
2.8360E+01	1.22258E-11	0.0829
2.8380E+01	1.20358E-11	0.0837
2.8400E+01	1.18884E-11	0.0845
2.8420E+01	1.16093E-11	0.0855
2.8440E+01	1.14427E-11	0.0866
2.8460E+01	1.12570E-11	0.0871
2.8480E+01	1.10572E-11	0.0872
2.8500E+01	1.06685E-11	0.0886
2.8520E+01	1.03888E-11	0.0894
2.8540E+01	1.00634E-11	0.0909
2.8560E+01	9.89770E-12	0.0916
2.8580E+01	9.65972E-12	0.0926
2.8600E+01	9.42756E-12	0.0941
2.8620E+01	9.30609E-12	0.0950
2.8640E+01	9.03025E-12	0.0966
2.8660E+01	8.91430E-12	0.0976
2.8680E+01	8.77979E-12	0.0983
2.8700E+01	8.58366E-12	0.0997
2.8720E+01	8.35040E-12	0.1006

2.8740E+01	7.89218E-12	0.1010
2.8760E+01	7.60751E-12	0.1027
2.8780E+01	7.30453E-12	0.0993
2.8800E+01	6.97098E-12	0.0937
2.8820E+01	6.92261E-12	0.0942
2.8840E+01	6.78794E-12	0.0948
2.8860E+01	6.49723E-12	0.0953
2.8880E+01	6.43789E-12	0.0961
2.8900E+01	6.33452E-12	0.0972
2.8920E+01	6.05124E-12	0.0940
2.8940E+01	5.75076E-12	0.0951
2.8960E+01	5.58264E-12	0.0953
2.8980E+01	5.42201E-12	0.0953
2.9000E+01	5.12024E-12	0.0938
2.9020E+01	5.08826E-12	0.0942
2.9040E+01	4.94210E-12	0.0923
2.9060E+01	4.85564E-12	0.0933
2.9080E+01	4.83487E-12	0.0936
2.9100E+01	4.77126E-12	0.0940
2.9120E+01	4.57796E-12	0.0938
2.9140E+01	4.49912E-12	0.0947
2.9160E+01	4.46469E-12	0.0951
2.9180E+01	4.43917E-12	0.0955
2.9200E+01	4.32666E-12	0.0953
2.9220E+01	4.21574E-12	0.0949
2.9240E+01	4.11750E-12	0.0961
2.9260E+01	4.02801E-12	0.0958
2.9280E+01	3.95627E-12	0.0966
2.9300E+01	3.87359E-12	0.0972
2.9320E+01	3.78522E-12	0.0929
2.9340E+01	3.57477E-12	0.0863
2.9360E+01	3.53030E-12	0.0871
2.9380E+01	3.49073E-12	0.0879
2.9400E+01	3.41316E-12	0.0884
2.9420E+01	3.39057E-12	0.0885
2.9440E+01	3.31455E-12	0.0889
2.9460E+01	3.17392E-12	0.0881
2.9480E+01	3.13748E-12	0.0888
2.9500E+01	3.10531E-12	0.0892
2.9520E+01	2.99177E-12	0.0912
2.9540E+01	2.96066E-12	0.0915
2.9560E+01	2.88923E-12	0.0913
2.9580E+01	2.88354E-12	0.0914
2.9600E+01	2.85448E-12	0.0921
2.9620E+01	2.84654E-12	0.0923
2.9640E+01	2.81051E-12	0.0929
2.9660E+01	2.76539E-12	0.0922
2.9680E+01	2.66639E-12	0.0928
2.9700E+01	2.63984E-12	0.0935
2.9720E+01	2.63766E-12	0.0936
2.9740E+01	2.62200E-12	0.0940
2.9760E+01	2.61043E-12	0.0944
2.9780E+01	2.58698E-12	0.0949
2.9800E+01	2.50909E-12	0.0964
2.9820E+01	2.47376E-12	0.0970
2.9840E+01	2.43740E-12	0.0976
2.9860E+01	2.41878E-12	0.0978
2.9880E+01	2.37956E-12	0.0987
2.9900E+01	2.36473E-12	0.0993
2.9920E+01	2.35745E-12	0.0995
2.9940E+01	2.30499E-12	0.0999
2.9960E+01	2.25881E-12	0.1001
2.9980E+01	2.17116E-12	0.1009
3.0000E+01	2.13780E-12	0.1020
3.0020E+01	2.13243E-12	0.1023
3.0040E+01	2.11437E-12	0.1019
3.0060E+01	2.05596E-12	0.1029
3.0080E+01	2.02000E-12	0.1040
3.0100E+01	2.00517E-12	0.1046
3.0120E+01	2.00059E-12	0.1049
3.0140E+01	1.99611E-12	0.1051

3.0160E+01	1.99298E-12	0.1052
3.0180E+01	1.98833E-12	0.1053
3.0200E+01	1.96960E-12	0.1058
3.0220E+01	1.95355E-12	0.1066
3.0240E+01	1.90539E-12	0.1079
3.0260E+01	1.88278E-12	0.1090
3.0280E+01	1.87400E-12	0.1093
3.0300E+01	1.85268E-12	0.1103
3.0320E+01	1.84044E-12	0.1109
3.0340E+01	1.83615E-12	0.1112
3.0360E+01	1.83173E-12	0.1114
3.0380E+01	1.82648E-12	0.1117
3.0400E+01	1.81296E-12	0.1123
3.0420E+01	1.79147E-12	0.1134
3.0440E+01	1.78247E-12	0.1138
3.0460E+01	1.76299E-12	0.1146
3.0480E+01	1.75717E-12	0.1149
3.0500E+01	1.73543E-12	0.1160
3.0520E+01	1.71668E-12	0.1171
3.0540E+01	1.70204E-12	0.1178
3.0560E+01	1.68251E-12	0.1189
3.0580E+01	1.66578E-12	0.1199
3.0600E+01	1.64864E-12	0.1206
3.0620E+01	1.63898E-12	0.1212
3.0640E+01	1.63063E-12	0.1217
3.0660E+01	1.61235E-12	0.1223
3.0680E+01	1.57721E-12	0.1238
3.0700E+01	1.53984E-12	0.1223
3.0720E+01	1.46495E-12	0.1169
3.0740E+01	1.43547E-12	0.1166
3.0760E+01	1.42715E-12	0.1170
3.0780E+01	1.41071E-12	0.1179
3.0800E+01	1.35280E-12	0.1187
3.0820E+01	1.33149E-12	0.1178
3.0840E+01	1.30911E-12	0.1179
3.0860E+01	1.29448E-12	0.1187
3.0880E+01	1.27660E-12	0.1199
3.0900E+01	1.27079E-12	0.1203
3.0920E+01	1.25776E-12	0.1204
3.0940E+01	1.23593E-12	0.1209
3.0960E+01	1.23302E-12	0.1212
3.0980E+01	1.22430E-12	0.1218
3.1000E+01	1.21046E-12	0.1220
3.1020E+01	1.16074E-12	0.1194
3.1040E+01	1.12639E-12	0.1214
3.1060E+01	1.11300E-12	0.1226
3.1080E+01	1.10565E-12	0.1232
3.1100E+01	1.09915E-12	0.1238
3.1120E+01	1.07612E-12	0.1241
3.1140E+01	1.04581E-12	0.1250
3.1160E+01	1.04539E-12	0.1250
3.1180E+01	1.01375E-12	0.1236
3.1200E+01	1.00192E-12	0.1248
3.1220E+01	9.60085E-13	0.1238
3.1240E+01	9.48334E-13	0.1250
3.1260E+01	9.45329E-13	0.1253
3.1280E+01	9.42335E-13	0.1257
3.1300E+01	8.92374E-13	0.1234
3.1320E+01	8.65416E-13	0.1250
3.1340E+01	8.54917E-13	0.1258
3.1360E+01	8.43727E-13	0.1272
3.1380E+01	8.32365E-13	0.1283
3.1400E+01	8.10293E-13	0.1295
3.1420E+01	8.09236E-13	0.1297
3.1440E+01	8.07004E-13	0.1300
3.1460E+01	8.05668E-13	0.1302
3.1480E+01	8.05021E-13	0.1303
3.1500E+01	8.04359E-13	0.1304
3.1520E+01	7.97330E-13	0.1313
3.1540E+01	7.94078E-13	0.1318
3.1560E+01	7.84844E-13	0.1330

3.1580E+01	7.83149E-13	0.1333
3.1600E+01	7.82003E-13	0.1334
3.1620E+01	7.75443E-13	0.1343
3.1640E+01	7.60758E-13	0.1358
3.1660E+01	7.59157E-13	0.1360
3.1680E+01	7.51602E-13	0.1369
3.1700E+01	7.48544E-13	0.1374
3.1720E+01	7.40450E-13	0.1383
3.1740E+01	7.36742E-13	0.1389
3.1760E+01	7.25803E-13	0.1406
3.1780E+01	7.16991E-13	0.1420
3.1800E+01	7.13995E-13	0.1425
3.1820E+01	7.10188E-13	0.1428
3.1840E+01	7.06165E-13	0.1435
3.1860E+01	7.03319E-13	0.1440
3.1880E+01	6.98933E-13	0.1448
3.1900E+01	6.97663E-13	0.1451
3.1920E+01	6.52858E-13	0.1365
3.1940E+01	6.36452E-13	0.1365
3.1960E+01	6.21392E-13	0.1377
3.1980E+01	5.94508E-13	0.1422
3.2000E+01	5.91397E-13	0.1429
3.2020E+01	5.88921E-13	0.1430
3.2040E+01	5.86256E-13	0.1431
3.2060E+01	5.76284E-13	0.1392
3.2080E+01	5.46651E-13	0.1369
3.2100E+01	5.41349E-13	0.1380
3.2120E+01	5.39068E-13	0.1385
3.2140E+01	5.34556E-13	0.1394
3.2160E+01	5.32354E-13	0.1398
3.2180E+01	5.30609E-13	0.1402
3.2200E+01	5.27145E-13	0.1410
3.2220E+01	5.25871E-13	0.1413
3.2240E+01	5.25447E-13	0.1414
3.2260E+01	5.24260E-13	0.1416
3.2280E+01	5.18812E-13	0.1428
3.2300E+01	5.18357E-13	0.1429
3.2320E+01	5.15194E-13	0.1437
3.2340E+01	5.11751E-13	0.1446
3.2360E+01	5.10477E-13	0.1449
3.2380E+01	5.07734E-13	0.1456
3.2400E+01	5.05847E-13	0.1460
3.2420E+01	5.04593E-13	0.1464
3.2440E+01	5.03926E-13	0.1466
3.2460E+01	5.03590E-13	0.1467
3.2480E+01	5.02272E-13	0.1469
3.2500E+01	4.98118E-13	0.1480
3.2520E+01	4.93304E-13	0.1493
3.2540E+01	4.93006E-13	0.1494
3.2560E+01	4.92876E-13	0.1494
3.2580E+01	4.92737E-13	0.1494
3.2600E+01	4.91206E-13	0.1499
3.2620E+01	4.88636E-13	0.1506
3.2640E+01	4.87577E-13	0.1510
3.2660E+01	4.87553E-13	0.1510
3.2680E+01	4.81458E-13	0.1521
3.2700E+01	4.76004E-13	0.1534
3.2720E+01	4.67797E-13	0.1553
3.2740E+01	4.66331E-13	0.1558
3.2760E+01	4.57996E-13	0.1579
3.2780E+01	4.56106E-13	0.1585
3.2800E+01	4.55913E-13	0.1585
3.2820E+01	4.55030E-13	0.1588
3.2840E+01	4.54382E-13	0.1590
3.2860E+01	4.53370E-13	0.1594
3.2880E+01	4.52858E-13	0.1596
3.2900E+01	4.52127E-13	0.1598
3.2920E+01	4.32786E-13	0.1585
3.2940E+01	4.27995E-13	0.1599
3.2960E+01	4.20649E-13	0.1550
3.2980E+01	3.90951E-13	0.1472

3.3000E+01 3.88635E-13 0.1481
total 3.88487E-03 0.0001

dump no. 2 on file runtpe nps = 20000000 coll = 1392591 ctm = 4.56
nrn = 128492764

4 warning messages so far.

run terminated when 20000000 particle histories were done.

computer time = 4.56 minutes

mcpnx version 2.5e Mon Feb 23 09:00:00 MST 2004 10/03/05 14:18:24 probid
= 10/03/05 14:15:58

APPENDIX F

BROAD Logic and FORTRAN Code

Gaussian Time Convolution

The energy deposition tally used in MCNPX has been configured to match the time binning that was used at OMEGA. The OMEGA time binning is 0.2 ns. The MCNPX data is output in a histogram format. One must add a “response” function to the MCNPX output to match the physics of the problem. Every event that occurs in the detectors happens with a Gaussian shape. For every event, the actual response of the detector will follow

$$f(t) = e^{-\frac{1}{2} \frac{(t-t_0)^2}{\sigma^2}},$$

where t_0 is the mean time value and σ is the width factor. The width factor is related to the full width at half maximum by

$$\sigma = \frac{FWHM}{2\sqrt{-2 \ln(0.5)}}.$$

To correctly account for the Gaussian nature of the problem, the MCNPX data must have a Gaussian function folded in. The only economic method to account for the spread is to write a small FORTRAN code that will easily read in the MCNPX data and perform the Gaussian fold. The program will be referred to as BROAD. The following are steps for the code’s execution.

- 1) Read MCNPX output and determine where the tally data is located
- 2) Store time, energy deposition and relative error data into corresponding arrays
- 3) Normalize energy deposition by determining the maximum value of the energy deposition and convert MCNPX tally time unit into nanoseconds
- 4) Integrate the MCNPX data to determine the total area underneath the curve
- 5) For a given folding factor, calculate the Gaussian for each time bin

- 6) Find the multiplicative factor needed for each bin to conserve each bin's area
- 7) Calculate each new bin's Gaussian that conserves the bin area
- 8) Sum all Gaussian points over all time to conserve the total integral
- 9) Integrate new Gaussian to make sure that the integral of the original MCNPX data matches the newly spread data integral
- 10) Normalize the new spread data for easy comparison to other data
- 11) Print normalized data to ASCII text file

A copy of the FORTRAN90 source code is included in this appendix.

Data Read

To determine the location of the data within the MCNPX output, the code searches the output for a specific line that indicates the beginning of the data. The data is preceded with a line that contains eight blank characters followed by the word "time". When BROAD searches the MCNPX output file and locates the preceding phrase, it notes the line number of the output file in an integer variable. The energy deposition data will begin one line after " time". To determine the end of the data, BROAD again searches for a specific phrase in the output file. The data will always be trailed by six spaces followed by "total". BROAD searches for the line that includes " total" and stores the line number in an integer variable. The data begins one line after the start variable and one line before the end variable. There are limitations to this method of parsing. The most detrimental is if there is more than one time tally in the output file. BROAD has been written specifically for this thesis and it is assumed that all the output files will conform to the same formatting. Specifically, there is only one tally per output file.

Data Storage

After the data has been parsed, it is written to a “scratch” file that is only used for ease of programming. This “scratch” file is removed after the program is finished running. The tally output by MCNPX is formatted in a specific way. The MCNPX output is formatted using the format ‘(3X,1P1E11.4,2X,1P1E12.5,0P1F7.4)’. BROAD used this format to read in the energy deposition and relative error for each time bin.

Data Normalization and Time Conversion

To easily compare experimental data to computational data, all data should be normalized. The easiest method of normalization is to find the maximum value and divide all the values by the maximum value.

$$N(i) = \frac{E(i)}{E_{\max}}$$

All versions of MCNP use time units of shakes. A shake is defined as 10 nanoseconds. Each time value was converted to nanoseconds by simply multiplying by 10.

MCNPX Data Integration

The total number of particles must be preserved. One way to determine if particles are conserved is to compute the integral (total area) of the curve. OMEGA’s detection system is setup for a 0.2 ns time resolution. This binning was conserved in MCNPX, so to integrate the curve, BROAD simply multiplies the energy deposition value for each time bin by the bin width of 0.2 ns. BROAD then sums each time bin to determine the total area.

Point Gaussian Determination

For each time bin, BROAD converts the histogram to a Gaussian curve. Using the Gaussian width factor based on the FWHM that is to be “folded” in, BROAD calculates the time bin specific Gaussian function with

$$G(t) = e^{-\frac{1}{2} \frac{(t-t_0)^2}{\sigma^2}}$$

Point Gaussian Coefficient for Equal Bin Area

Again, the bin area must be conserved if one is to fold in a Gaussian function properly.

For each time bin, a Gaussian multiplicative constant is determined by

$$C = \frac{1}{\sum_i G(t) * \frac{0.2}{A_{bin}}}$$

where A_{bin} is the MCNPX bin area for the specific time bin.

Point Gaussian Equal Area Determination

Finally, to determine the bin specific Gaussian function that will conserve the bin area, the equation

$$G(t) = C * e^{-\frac{1}{2} \frac{(t-t_0)^2}{\sigma^2}}$$

is used.

Total Gaussian Sum and Total Area Determination

To conserve total particles in the curve, each time bin's contribution for each Gaussian function is summed. Each point Gaussian time bin is multiplied by 0.2 and summed to determine the total area under the curve. The following is the DO loop that executes the calculation.

```
DO i=1, (enddata) - (startdata+1)
    gauss(i) = exp(- (0.5) * ((time(i) - time(j)) ** 2 / (sigma ** 2)))
    gausssum = gausssum + gauss(i)
END DO

! Find the constant multiplier to conserve each bins area
c = 1 / (gausssum * (0.2/binarea))

! Compute new Gaussian with equal area as the original bin
```

```

DO i=1, (enddata) - (startdata+1)
    gaussnew(i) = c * exp(-(0.5)*((time(i)-time(j))**2/(sigma**2)))
    newsum = newsum + gaussnew(i)
    ! Keep a running tab to sum each new Gaussian
    broad(i) = broad(i) + gaussnew(i)
END DO
END DO

! Calculate the area under the curve of the new broadened data
DO i=1, (enddata) - (startdata+1)
    area1 = area1 + (broad(i) * 0.2)
END DO

```

The total area is printed to the screen with the original MCNPX data area to show the user equality among the curves.

Gaussian Normalization

Again, the newly broadened data is normalized to easily compare to other data. The normalization is simply the bin value divided by the maximum value.

$$N(t) = \frac{G(t)}{G_{\max}}$$

ASCII File Output

Finally, BROAD writes the new Gaussian as a function of time to broad.txt. The “scratch” file is removed and all remaining open files are closed.

BROAD FORTRAN Code

```
PROGRAM Broaden

IMPLICIT NONE

! This program will read in mcnpx tally data
! and broaden each bin by a user-defined
! width. The newly broadened spectrum will be
! printed out to broad.txt

! This program assumes 0.2-ns time resolution

REAL      :: time(10000), edep(10000), relerr(10000)
INTEGER   :: i, j, icount, startdata, enddata
CHARACTER*80 :: line, filename
CHARACTER(132) :: linearray(10000), tempstring
REAL      :: c, binarea, gauss(10000), gausssum, sigma, fwhm
REAL      :: timemax, edepmax, gaussnew(10000), newsum
REAL      :: broad(10000), broadmax, area0, area1

! Open mcnpx data file

PRINT *, "Enter MCNPx Output File name:"
READ *, filename

icount = 0

OPEN(UNIT=12, FILE=filename, STATUS="old")

1000 READ(12,3000,END=2000) line

3000 FORMAT(A)
```

```

icount = icount + 1

GO TO 1000

! 2000 WRITE(*,3100) icount

! 3100 FORMAT(1X,"Input contains ",I6," lines.")

2000 REWIND(12)

DO i=1,icount
    READ(12,'(A)') linearray(i)
END DO

DO i=1,icount
    IF(linearray(i) == "      time") THEN
        startdata = i
        ! PRINT *, startdata
    END IF
    tempstring = linearray(i)
    IF(tempstring(1:11) == "      total") THEN
        enddata = i
        ! PRINT *, enddata
    END if
END DO

REWIND(12)

OPEN(UNIT=11,STATUS="scratch")

DO i=startdata+1,enddata-1
    WRITE(11,'(A)') linearray(i)
END DO

REWIND(11)

timemax = 0

edepmax = 0

```

```

DO i=1, (enddata) - (startdata+1)
    READ(11, '(3X,1P1E11.4,2X,1P1E12.5,0P1F7.4)') time(i), edep(i), relerr(i)
END DO

CLOSE(11)

! Find max energy deposition to normalize the data
DO i=1, (enddata) - (startdata+1)
    IF(edep(i) > edepmax) THEN
        timemax = time(i) * 10.0
        edepmax = edep(i)
    END IF
END DO

! Normalize data & convert time to ns
DO i=1, (enddata) - (startdata+1)
    edep(i) = edep(i) / edepmax
    time(i) = time(i) * 10.0
END DO

! Calculate the area under the curve of
! the original mcnp data
area0 = 0
DO i=1, (enddata) - (startdata+1)
    area0 = area0 + (edep(i) * 0.2)
END DO

PRINT *, "MCNPx Data Area ", area0

! fwhm must be changed in the f90 code to
! change the broadening function
PRINT *, "Enter broadening time"

```

```

READ *, fwhm

! fwhm = 1.0

! Calculate sigma for the Gaussian
sigma = fwhm / (2*sqrt(-2*log(0.5)))

! Find data normalized Gaussian
DO j=1, (enddata) - (startdata+1)
! Find the mcnp bin area
binarea = 0.2 * edep(j)
newsum = 0.0
gausssum = 0.0
! Calculate the Gaussian
DO i=1, (enddata) - (startdata+1)
    gauss(i) = exp(-(0.5)*((time(i)-time(j))**2)/(sigma**2))
    gausssum = gausssum + gauss(i)
END DO
! Find the constant multiplier to conserve each bins area
c = 1/ (gausssum * (0.2/binarea))
! Compute new Gaussian with equal area as the original bin
DO i=1, (enddata) - (startdata+1)
    gaussnew(i) = c * exp(-(0.5)*((time(i)-time(j))**2)/(sigma**2))
    newsum = newsum + gaussnew(i)
    ! Keep a running tab to sum each new Gaussian
    broad(i) = broad(i) + gaussnew(i)
END DO
END DO

! Calculate the area under the curve of the new broadened data

```

```

DO i=1, (enddata) - (startdata+1)
    area1 = area1 + (broad(i) * 0.2)
END DO

PRINT *, "Broadened Area ", area1

OPEN (UNIT=22, FILE="broad.txt", STATUS="REPLACE")

! Renormalize the newly broadened data
DO i=1, (enddata) - (startdata+1)
    IF(broad(i) > broadmax) THEN
        broadmax = broad(i)
    END IF
END DO

DO i=1, (enddata) - (startdata+1)
    broad(i) = broad(i) / broadmax
END DO

! Print data to broad.txt
DO i=1, (enddata) - (startdata+1)
    WRITE(22, '(1P1E11.4, 2X, 1P1E12.5)') time(i), broad(i)
END DO

PRINT *, "Normalized output printed to broad.txt"

END PROGRAM Broaden

```


Distribution

- 2 University of New Mexico
Department of Chemical and Nuclear Engineering
Attn: Gary Cooper
MSC 01 1120
1 University of New Mexico
Albuquerque, NM 87131-0001
- 1 University of New Mexico
Department of Chemical and Nuclear Engineering
Attn: Robert Busch
MSC 01 1120
1 University of New Mexico
Albuquerque, NM 87131-0001
- 1 Bechtel/Nevada
Attn: Lee Ziegler
2621 Loosee Road
Las Vegas, NV 89030
- 1 University of Rochester
Laboratory for Laser Energetics
Attn: Vladimir Glebov
250 East River Road
Rochester, NY 14623
- 15 Pacific Northwest National Laboratory
Attn: Jason Starner
P.O. Box 999
M/S K8-34
Richland, WA 99352
- 1 MS 1153 P. J. McDaniel, 5441
- 1 MS 1153 L. C. Sanchez, 5441
- 1 MS 1186 T. A. Mehlhorn, 1674
- 1 MS 1186 J. R. Starner, 1674
- 1 MS 1196 G. A. Chandler, 1677
- 1 MS 1196 G. W. Cooper, 1677
- 1 MS 1196 J. K. Franklin, 1677

1	MS 1196	R. J. Leeper, 1677
1	MS 1196	A. J. Nelson, 1677
1	MS 1196	C. L. Ruiz, 1677
2	MS 9018	Central Technical Files, 8944
2	MS 0899	Technical Library, 4536